

平成 27 年度

修士論文

Mechanical Assessment of Fire Damage of the Ancient Greek Temple of Marble Stone

指導教員 花里 利一 教授

三重大学大学院工学研究科
建築学専攻
山田 眞生

MECHANICAL ASSESSMENT OF FIRE DAMAGE OF THE ANCIENT GREEK TEMPLE OF MARBLE STONE

CONTENTS

CHAPTER 1. INTRODUCTION

1.1	Abstract1-1
1.2	Background and purpose1-2
1.3	Past studies1-3
1.4	Field research at the Parthenon, Athens1-4

CHAPTER 2. LABORATORY TESTS OF MARBLE

2.1	About marble specimen2-1
2.2	Heating tests2-1
2.2.1	Method of heating tests	
I)	Measurements of water content2-5
II)	Ocular inspection2-6
III)	Measurements of weight variation2-6
2.2.2	Results and discussions	
I)	Water content of marble2-8
II)	Weight variation of marble2-8
III)	Damage of specimens2-11
IV)	Discussions2-13
2.3	Mechanical properties tests	
2.3.1	Method of compressive tests2-15
2.3.2	Marble specimen properties	
I)	Dimensions of specimens2-15
II)	Crystal direction2-15
2.3.3	Results and discussions	
I)	Compressive tests2-16
II)	Compressive strength affected by difference on crystal direction2-17
III)	Stress-strain curve2-18
IV)	Discussions2-26
2.4	Measuring the dynamic modulus of elasticity	
2.4.1	Non-destructive method2-27
2.4.2	Results and discussions2-28

CHAPTER 3. THERMAL AND CHEMICAL ANALYSES		
3.1	Outlines of thermal analyses3-1
3.1.1	Thermal gravimeter and differential thermal analysis (TG-DTA)3-1
3.1.2	X-ray diffraction test3-2
3.1.3	Election probe microanalysis (EPMA)3-2
3.1.4	Hot-wire method3-2
3.1.5	Thermal mechanical analysis3-4
3.2	Results and discussions	
3.2.1	TG-DTA3-5
3.2.2	X-ray diffraction3-6
3.2.3	EPMA3-6
3.2.4	Thermal conductivity3-7
3.2.4	Thermal expansion rate3-16
CHAPTER 4. THERMAL ANALYSES	4-1
4.1	Thermal transmitting analysis	
I)	Modeling4-1
II)	Input conditions of analysis4-2
III)	Results and discussions4-4
4.2	Thermal analysis for a marble dram	
4.2.1	Heat conduction analysis	
I)	Modeling4-7
II)	Input conditions of analysis4-8
4.2.2	Thermal stress analysis4-10
4.2.3	Results and discussions4-11
4.3	Thermal analysis for a marble multi-dram column	
4.3.1	Heat conduction analysis	
I)	Modeling4-18
II)	Input conditions of analysis4-18
4.3.2	Thermal stress analysis4-18
4.3.3	Results and discussions4-18
CHAPTER 5. Concluding Remarks		
5.1	Conclusions5-1
5.2	Further study5-2
Acknowledgment		
References		
Appendix		

CHAPTER 1. INTRODUCTION

1.1 Abstract

Historical masonry heritages buildings existing in earthquake-prone countries have been affected many times by earthquakes in their long histories. The Parthenon, Athens in Greece is one of the most famous buildings, and it well known that the Parthenon was damaged seriously by earthquakes and especially human disasters. Therefore, restoration works have been performed carefully since 1975. In addition, marble stone constructions, for example marble column, also suffered serious damage by two historical fires. However, a lot of researches, studies or monitoring results on earthquakes have been reported so far, there have been insufficient knowledge and lack of information on the mechanical characteristics of marble stones affected by high temperature caused by fires. Hence the Acropolis Restoration Office has not made the restoration plan that takes into account fire damages.

Such fire damage might reduce seismic safety of those marble constructions, as seismic activity in Greece is high in Mediterranean Sea area. As well as, it might cause serious issues to be solved for restoration of heritage marble structures. The scope of the present study is to describe the mechanical material properties of marble stones affected by high temperature and to estimate the state of suffering or the scale of the suffering with the thermal stress simulation to the marble multi-dram column. Therefore, in the present study, we conducted four heating tests, three compressive tests, and thermal analysis for the measurement of physical properties to marble specimens, and then we performed the heating simulation by ANSYS code. In addition, the international collaborative research had been established with the National Technical University of Athens (NTUA) and TSMA since 2008, the present study is a part of those studies.

In the experimental study, the cracks occurred on the marble specimens caused by the thermal shock during cooling time. Moreover, the heated specimen expanded with the passage of time by moisture absorbing, and then cracks significantly were developed. Accordingly, moisture absorption affected deterioration process of marble. In addition, the compressive strength of marble specimen began to decrease at the temperature of 300 °C and the specimen heated at over 750 °C collapsed naturally during cooling time. In the result of thermal gravimeter and differential thermal analysis, there were CaCO₃ and CaO in the specimen heated at 800 °C. On the other hand, CaCO₃ completely disappeared in the specimen heated at 1,000 °C. Moreover, it was found that the thermal conductivity and thermal expansion rate of marble have irreversibility caused by high temperature. Furthermore, we verified whether this non-destructive method could be suitable for the field survey to the actual buildings with the non-destructive test using by the resonant frequency tester. Marble stone has crystal direction, we also checked effects of each crystal direction to the modulus of elasticity and the modulus of rigidity. The marble specimen having vertical crystal direction and the compressive strength were correlated on each other, however the specimen having horizontal one didn't have the relation to the compressive strength. From the result, non-destructive method may be suitable to the actual buildings for estimation of the compressive strength as long as the crystal direction is noted.

In order to grasp hourly variation of a marble multi-dram with time history simulation of temperature of whole a multi-dram column, we performed the non-stationary heat conduction analysis and thermal stress analysis by finite element method on the computer utilizing the results presented in the previous experimental studies as the reference modeling data. In the result of thermal stress analysis by ANSYS code to a marble dram model, the compressive stress was caused along the circumferential direction of the marble dram. In addition, the tensile stress was also caused in the radial direction at the depth of about 30 cm from the surface. Moreover, from the result image of the heat distributions obtained by the heating simulation, it is found that there were the significant difference in temperature between surface and internal marble dram. Hence, there were also a difference of thermal expansion coefficients between surface and internal one while marble dram was cooled after heating. Thus, it is seen from the above result that micro cracks occurred within around this area.

1.2 Background and purpose

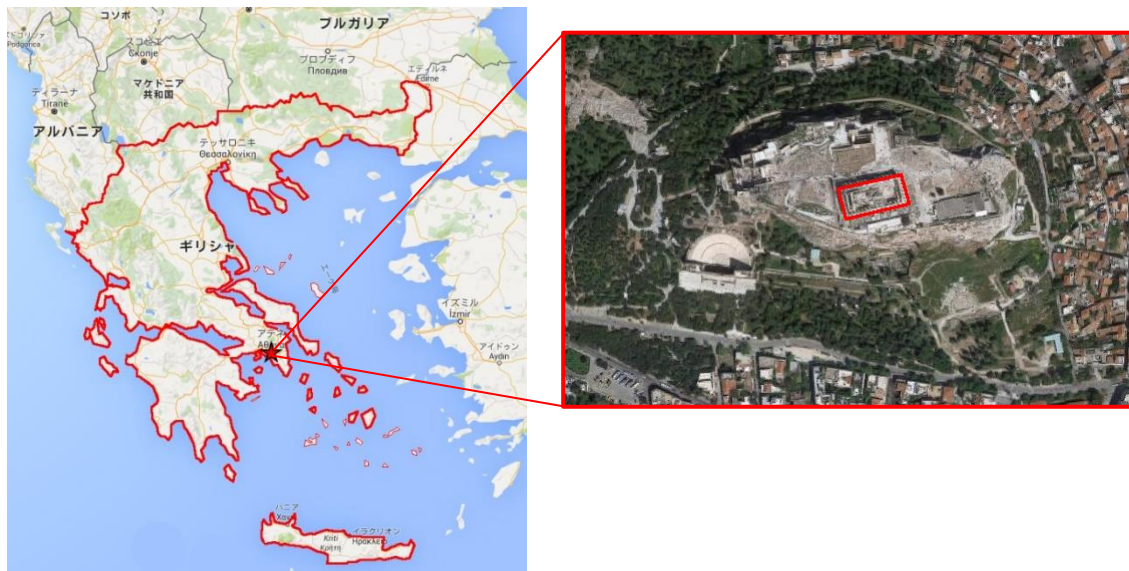


Fig.1-1: Overview map of Greece and the Parthenon

In Mediterranean Sea area, there exist a number of ancient constructions of marble. The Parthenon is representative of them. In their long history, those marble stone heritages sometimes suffered serious damage by historical fires or earthquakes. Although there were some large earthquakes during long history; about 25 centuries, The Parthenon is existence now. However, The Parthenon is awfully damaged because of the inferno by the raid of the Heruli (267), the bombardment by Venetian during the second Turkish-Venetian war (1687), and the other various man-made disasters.⁽¹⁾

1980s, Hanazato et al. evaluated the characteristics of the Parthenon Athens, and Acropolis hill.⁽²⁾ By this study, International collaborative research had been established with the National Technical University of Athens (NTUA) since 2008. However, there are insufficient knowledge and lack about the information

about the character as the mechanical material of marble stone affected by fire. Sometimes, it might cause serious issues to be solved for their restoration projects. This imposes necessity for assessment of the fire damage to structural seismic safety.

The scope of the present study is, as the fundamental research, to study the mechanical material characteristics of marble stones affected by high temperature caused by fire. Damage by historical fires should be considered for restoration.

1.3 Past studies

In 1980s, Hanazato et al. analyzed seismic response on the Parthenon and Acropolis hill.⁽²⁾ The masonry columns were firstly modeled using a lumped mass system with both translational and rotational degrees of freedom. Three types of models were used for the analysis. As results, the data of the natural periods of the Parthenon's columns were evaluated. Moreover, the liner response analysis was performed to examine the earthquake resistant capacity against the synthetic ground motions corresponding to the return period of 100 and 1000 years.⁽³⁾ The analytical results showed that the Parthenon was safe against the anticipated ground motions derived probabilistically for both return periods. However, the columns of the monuments has fundamental periods which were longer than the predominant periods of the anticipated ground motions, therefore it would be expected that the Parthenon Athens would behave as a flexible structure.

In addition, Ms. Oyaizu conducted micro tremor measurements in order to study actual behaviors and to grasp the fundamental dynamic characteristics, earthquake monitoring has been undertaken at the Parthenon and the Prambanan Temples, Indonesia.⁽⁴⁾ At the Parthenon, two small earthquakes were recorded in 2010 and the end of 2011, and four earthquakes were recorded at the Prambanan Temple as well. Seismic response analysis of both the Parthenon and the Prambanan Temples were conducted by using these earthquake records.

H. P. Mouzakis et al. reported the results that experimental investigation of the earthquake response of marble model which was 1:3 scale of the classical column.⁽⁵⁾ Also, C. Papantonopoulos et al. conducted the numerical prediction of the earthquake response of classical columns using the distinct element method.⁽⁶⁾ The analysis results of distinct element method were compared with the experimental data, and they were able to capture the main features of the response quite well. From this, it was confirmed that this method would be able to be useful for the restoration process of ancient monuments to estimate the response to expected earthquake motions.

A number of studies on the thermo-mechanical performance of rocks and stones have been conducted in rock engineering field to construct structures for storage of oils and radioactive wastes. As well as, thermal weathering of them has been studied for assessment of deterioration of rocks not only under natural climate conditions, but also under mountain fires. Fundamental data of their thermal properties were published in the scientific chronological tables in Japan. However, most of those past studies dealt with granite, andesite, tuff, sandstone or the other popular rocks. Only a few studies have been performed on mechanical properties of marble. Hence, N. Sakai described the compressive tests of marble (Akiyoshi Marble in

Japan) subjected to high temperature from the room temperature to 600 °C , showing gradual reduction of strength with temperature.⁽⁷⁾

1.4 Field research at the Parthenon, Athens

In June of 2013 and October of 2015, we made field inspections of the Parthenon Athens, Greece to understand the present restoration method and to grasp the condition of marble stones used for the Parthenon.

Fig.1-2 shows the erstwhile Parthenon's plan on the basis of recent finding. The Parthenon suffers historical damages in the past; examples include the arson by the Heruli (267) and the bombardment by the Venetian (1687). In "The Parthenon and its impact in modern times", P. Tournikiotis mentioned the state of the damage by the arson of the Heruli as follows;

The damage caused to the building by the fire was very serious. The gigantic roof beams and rafters (timber with a volume of 480 cubic meters) were consumed by fire, and must have burned for many days. Almost all the marble roof, weighing about 350 tons, crashed to the ground in fragments. The abrupt and extreme rise in temperature caused severe heat cracking on all the marble surfaces in the area where there was burning wood;⁽¹⁾

For the above writing, it is thought that the damage by the arson of the Heruli occurred in the whole building. It is common knowledge that the wooden beams and roof had been burned down in the historical fire caused by Heruli, and then they got serious damages that almost columns were broken by the bombardment by the Venetian.⁽¹⁾ (See Fig.1-3) In addition, it is said that the damages by the Venetian are biased to south-east side of the Parthenon. Moreover, The Parthenon has a minaret in the west side, and it is said that this minaret was made in the 17th century by the Turkish. Therefore, we consider the almost damage of the colonnade in the west side of the Parthenon as the fire damage caused by Heruli.

We drew a damage state map in order to grasp fire damages. (See Fig.1-4) We observed the characteristic damage that the marble specimen surface exfoliated. In addition, we expect that the crystal of marble stone influence on direction of the cracking. The columns of western side looks so similar than the failure mode of marble specimens heated at the high temperature. (See Chapter 2) Hence, we judged that almost of these damages is caused by historical fires.

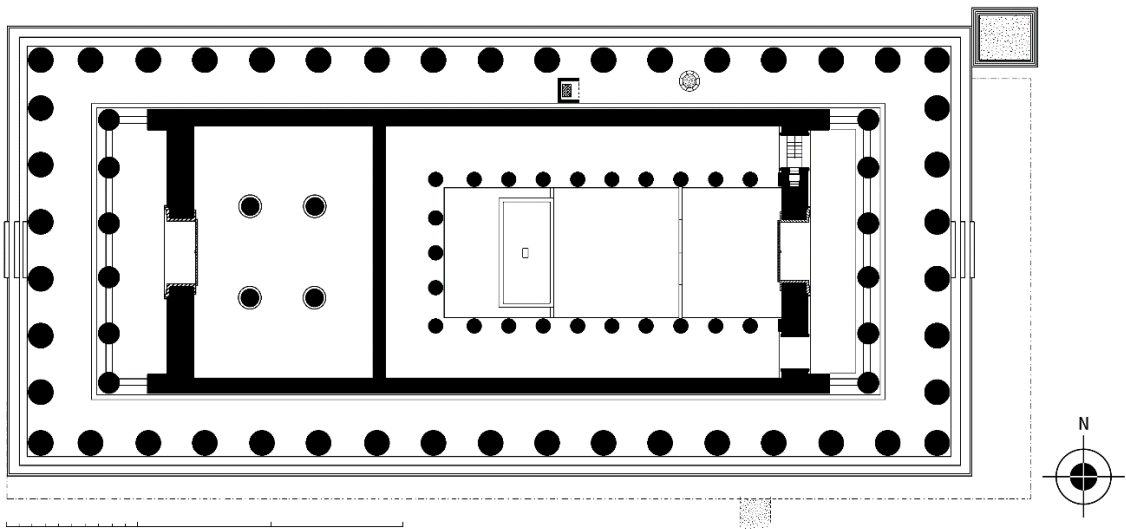


Fig.1-2: Reconstruction of the plane on the basis of recent finding (Drawing by M. Korres.)

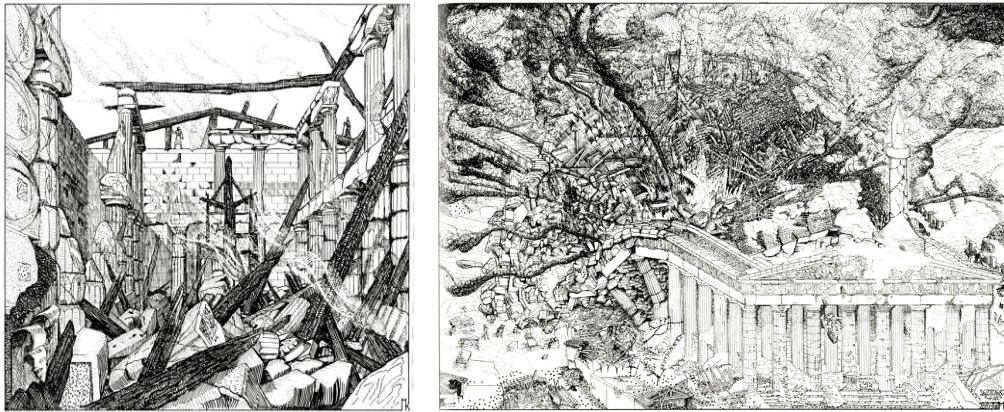


Fig.1-3: Drawings on imagination of the damages (left: 267, right: 1687) (Drawing by M. Korres.)

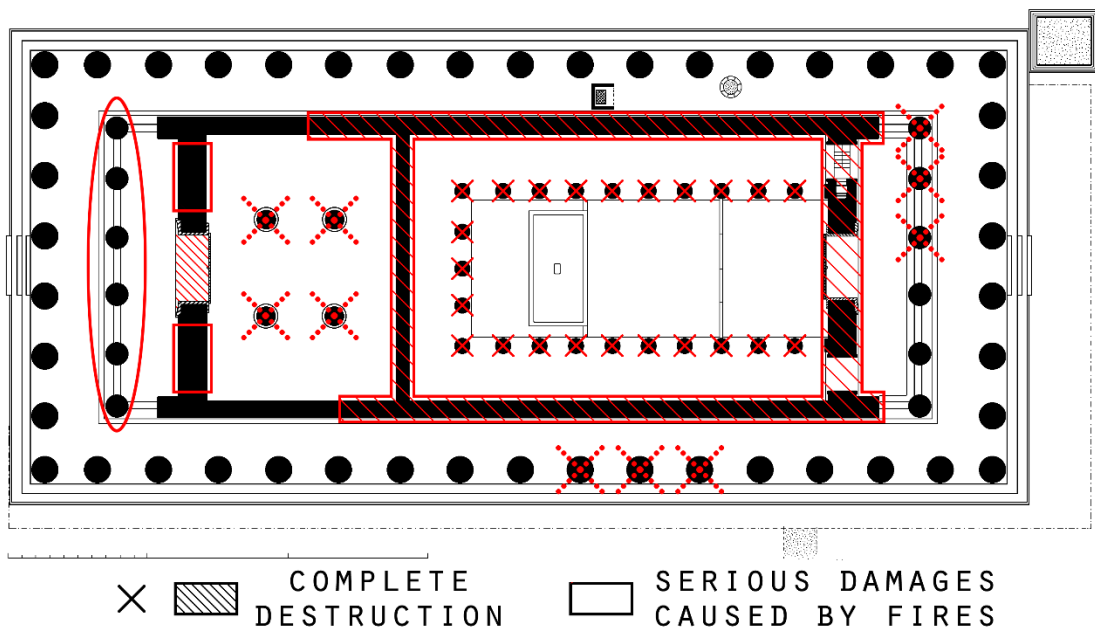


Fig.1-4: Present plan of damage area by fire

Fig.1-5 and Fig.1-6 show that the marble column and marble wall on west side might have especially large damages caused by historical fires. The surface of almost columns on west side is peeled off, and the depth of those cracks is about 20 cm from the surface. The literature⁽¹⁾ suggests that the Venetian bombed on the northeast side of the Parthenon intensively. In addition, the damages caused by bomb are not recognized from the appearances of marble columns on west side. Thus, taking into consideration the factors mentioned above, the fire caused by the arson of the Heruli was the main cause of the damages that those marble members on west side of the Parthenon have.

Moreover, the marble pediment on the top of the Parthenon had been badly foxed. (See Fig.1-7) Those discolorations of the surface of marble stone might be caused by high temperature. In addition, the border between discoloration area and un-discoloration area is straight and clear. Therefore, the upper from the un-discoloration area of the pediment is considered to be covered with wooden beams or something members in that time of fire. For this reason, those area have not been heated by direct fire. Thus, by comparing the columns with damages caused by fires on the west side and this un-discoloration marble, it is possible to envisage the damage scale caused by high temperature with considering the natural degradation. (e.g. ultraviolet rays or acid rain)

Accordingly in the present study, we decided to input the marble column on west side and the surrounding environment as the condition data and modeling base for the thermal analyses by ANSYS code. (See Chapter 3) As a side note, the columns on west side were Doric, with 16 flutes. Moreover the diameter of those columns was about 1.9 meters and the height of 13.2 meters. (A column was made up of 11 marble multi-drums and the height of one multi-drum was about 1.2 meters)⁽¹⁾



Fig.1-5: Internal column damaged by historical fires on the west side



Fig.1-6: Wall damaged by historical fires on the west side

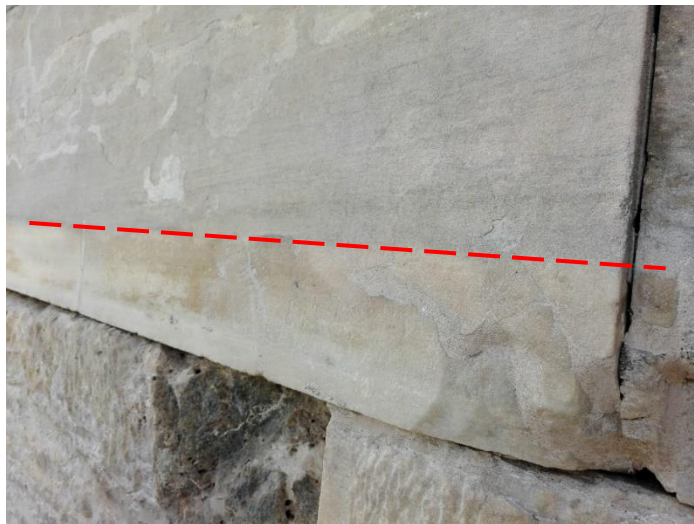


Fig.1-7: Marble pediment with discoloration on the top of the Parthenon

In regard to the way of the former restoration of the marble stone, since there were only a few studies have been performed on mechanical properties of marble, it was the sloppy method for the restoration. The normal concrete was injected into the cracks caused by high temperature on marble stone, and the iron clamps were used for the joining of the marble members. (See Fig.1-8) As the result, the adverse effects on marble stone were reported from the repairing using them, especially, the damage due to rust of iron clamps was very serious.⁽⁸⁾ The corrosion expansion of the iron caused the breakage of the marble members. However, at the present restoration, white cement is accepted for injection into cracks of marble instead of normal concrete and as adhesive marble members, moreover the almost iron clamps were replaced by the titanium clamps. (See Fig.1-9)

The restoration plan of the Parthenon is divided into 12 groups: Group 1 is the east side of the Parthenon, Group 2 is the north side, Group 3 is the south side, Group 4 is the western front of the Parthenon, Group 5

is the porch on the east side, Group 6 is the walls on east side, Group 7 is the walls on the north side, Group 8 is the walls on the south side, Group 9 is the porch on the west side, Group 10 is the walls on the west side, Group 11 is the roof and ceiling on the west side, and Group 12 is the floor.⁽⁸⁾ At present, the restoration on east side has completely been done, thereby the restoration plan of Group 4 have started. New marble stones are quarried out from the Mt. Pentelikon, and then they are cut according to the lacking parts of original marble members for the restoration of the pillar have serious damages caused by fire and bomb. (See Fig.1-10)



Fig.1-8: Former restoration using normal concrete and iron clamp



Fig.1-9: Present restoration using white cement and titanium clamp

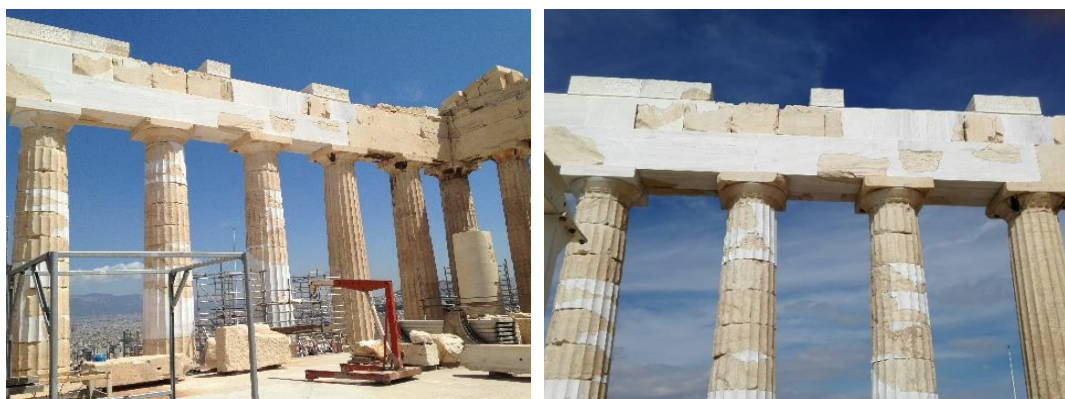


Fig.1-10: Restoration of the colonnade on the east side have completely done

CHAPTER 2. LABORATORY TESTS OF MARBLE

2.1 About marble specimen

In the present study, we conducted three tests, heating test, compressive test and elastic wave test, to the cylindrical marble specimens ($\phi 50 \times 100^H$ mm) and the prism marble specimen ($50^L \times 50^W \times 100^H$ mm or $100^L \times 100^W \times 200^H$ mm). Marble stones using these tests are called Dionyssos marble, and the quarry of these marble is the same as Pentelic marble for used in the Parthenon. This quarry is located in the suburbs of Athens, and the marble that is taken in the south side of the mountain is called Pentelic marble and the one that is taken in the north side of the mountain is called Dionyssos.

2.2 Heating test

We conducted heating tests four times, the first test was performed in Tsukuba, Japan (hereafter ‘Case-1’) and the second and third tests were performed in Mie, Japan (hereafter ‘Case-2’ and ‘Case-3’), and the final test was performed in Athens, Greece (hereafter ‘Case-4’). In addition, cylindrical marble specimens ($\phi 50 \times 100^H$ mm) were used in Case-1 and prism marble specimens ($50^L \times 50^W \times 100^H$ mm) were used in Case-2 and Case-3, and prism marble specimens ($100^L \times 100^W \times 200^H$ mm) were used in Case-4. (See Table.2-2-1)

Table.2-2-1: Implementation status of heating tests

Case number	Specimen size	Location
1	$\phi 50 \times 100^H$ mm	Tsukuba, Japan
2	$50^L \times 50^W \times 100^H$ mm	Mie, Japan
3		
4	$100^L \times 100^W \times 200^H$ mm	Athens, Greece

In Case-1, two marble specimens were set in piles of two in the oven, and then they were heated simultaneously at one time. (See Fig.2-2-1) Fig.2-2-2 shows time history at temperature as the experimental conditions. Because the high speed electric oven had little time-lag reaching to the target temperature in the chamber of the oven, the specimens were set in the oven before starting heating. Marble specimens were heated for 90 minutes until the internal temperature of the specimens reached to setting temperature (pre-heating), and then continued keeping the temperature for 30 minute, 1 hour, 2 hours or 4 hours at the temperature. Moreover a thermocouple (Type K: $\phi 3.2$ mm) was installed to one of two specimens to confirm that the internal temperature of the specimen continued keeping the temperature, and temperature in the chamber of the oven was also measured at the same time.

Fig.2-2-3 shows the oven used to conduct these heating tests in Case-2 and Case-3, 6 specimens were set on same level line and were heated in the oven. Shown in these cases, because the electric

oven had huge time-lag between starting heating and reaching setting temperature, the specimens were set in the oven after reaching to setting temperature (200 °C, 400 °C, 650 °C, 800 °C or 1,000 °C) in chamber of the oven, and heated for 210 minutes. As a side note, 90 minutes of them is for pre-heating time. (See Fig.2-2-4) After heating test, the specimens heated were left in the oven as it is whole one night. Moreover, they were moved to desiccators for controlling humidity after confirming the specimen's temperature.

In addition, these specimens in Case-2 and Case-3 were not installing thermocouples.

In Case-4, 12 specimens were set and were heated as well as Case-2 and Case-3. (See Fig.2-2-5) The two marble specimens with thermocouples were set in the central position of the oven, and we managed the temperature of internal oven and specimens by the attached thermometer. In addition, these two specimens were used repeatedly by the all conditions of the heating test in Case-4.

Fig.2-2-6 shows time history at temperature as the experimental conditions in Case-4. The temperature rising rate in this tests was set 200 °C/hour, and the specimens were heated until internal temperature of the specimens reached to the setting temperature for pre-heating. After heating tests, the specimens heated were left in the oven as it is whole one night as well as Case-2 and Case-3, and they were moved from the oven after confirming the oven temperature became less than 100 °C.

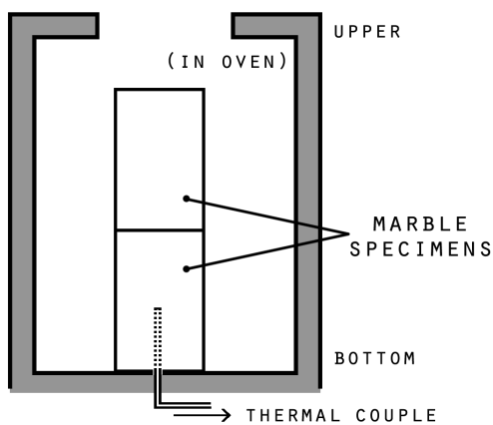


Fig.2-2-1: Test equipment and how to on Case-1

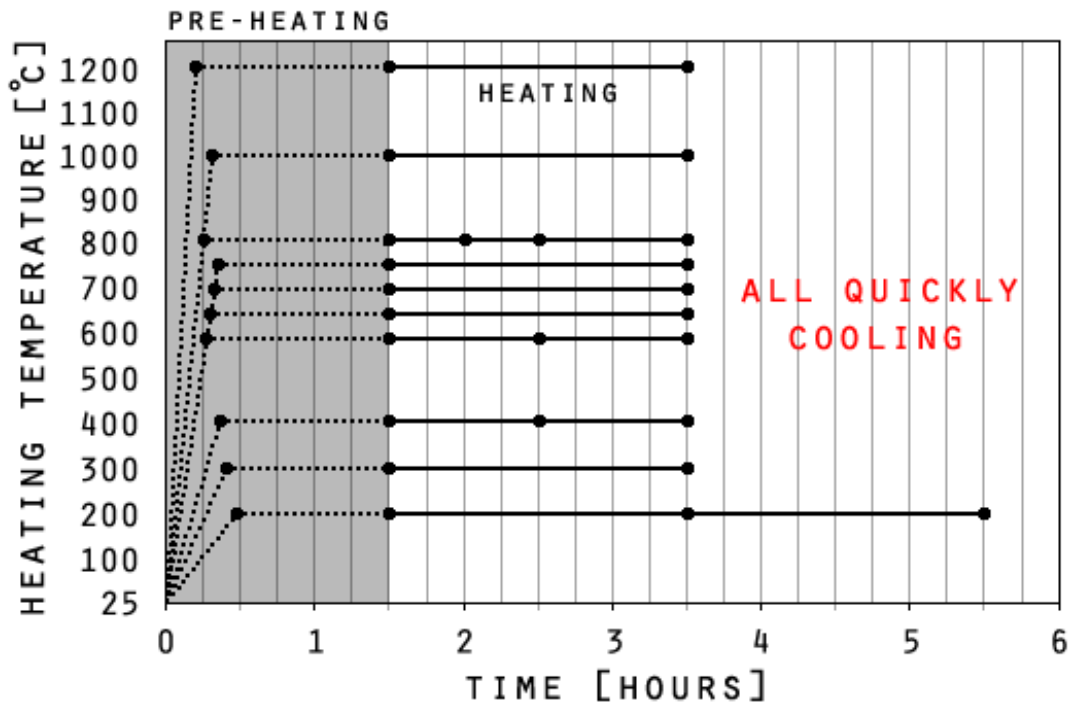


Fig.2-2-2: Experimental condition of Case-1

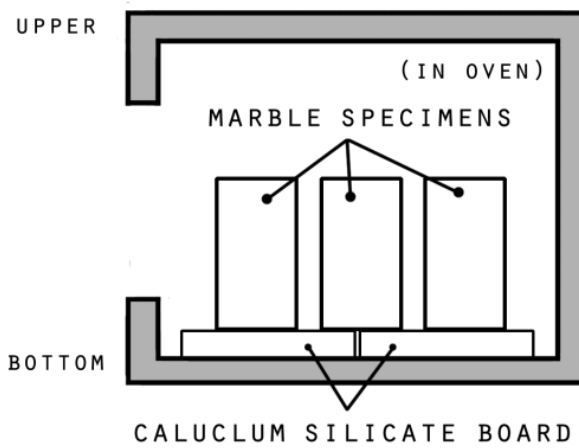


Fig.2-2-3: Test equipment on Case-2 and Case-3

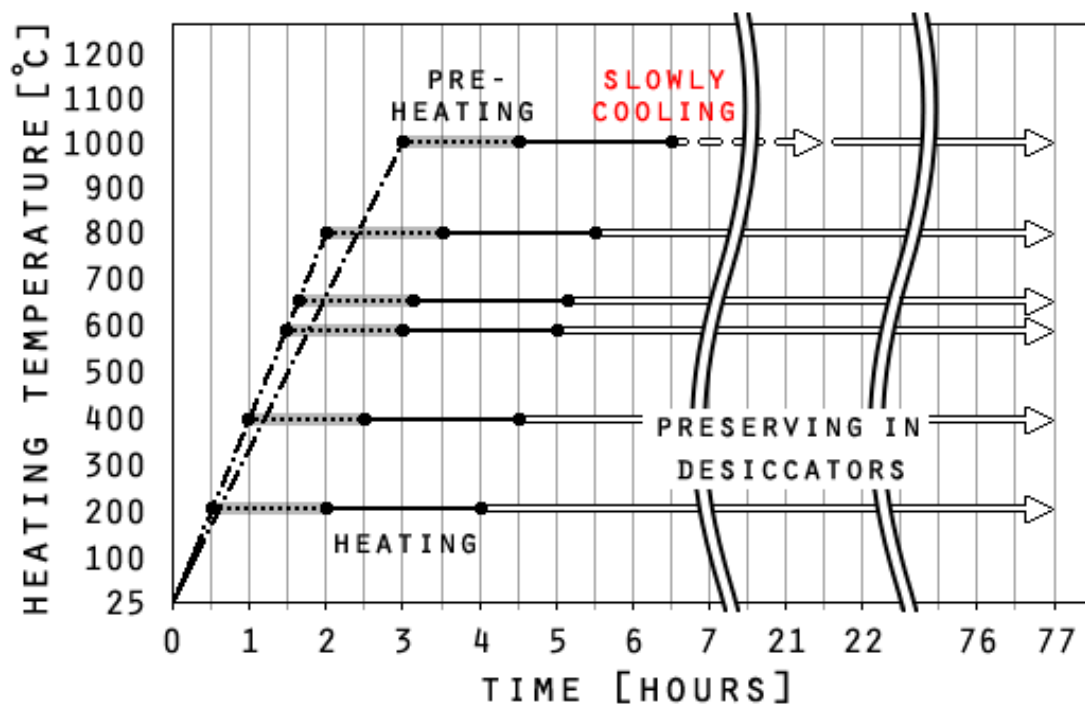


Fig.2-2-4: Experimental condition of Case-2 and Case-3

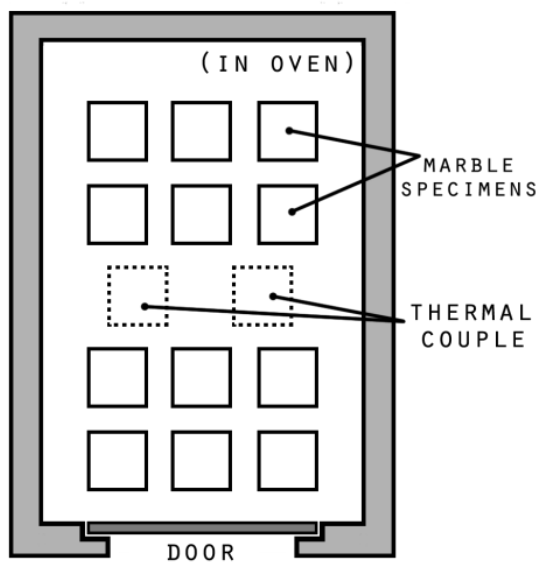


Fig.2-2-5: Test equipment on Case-4

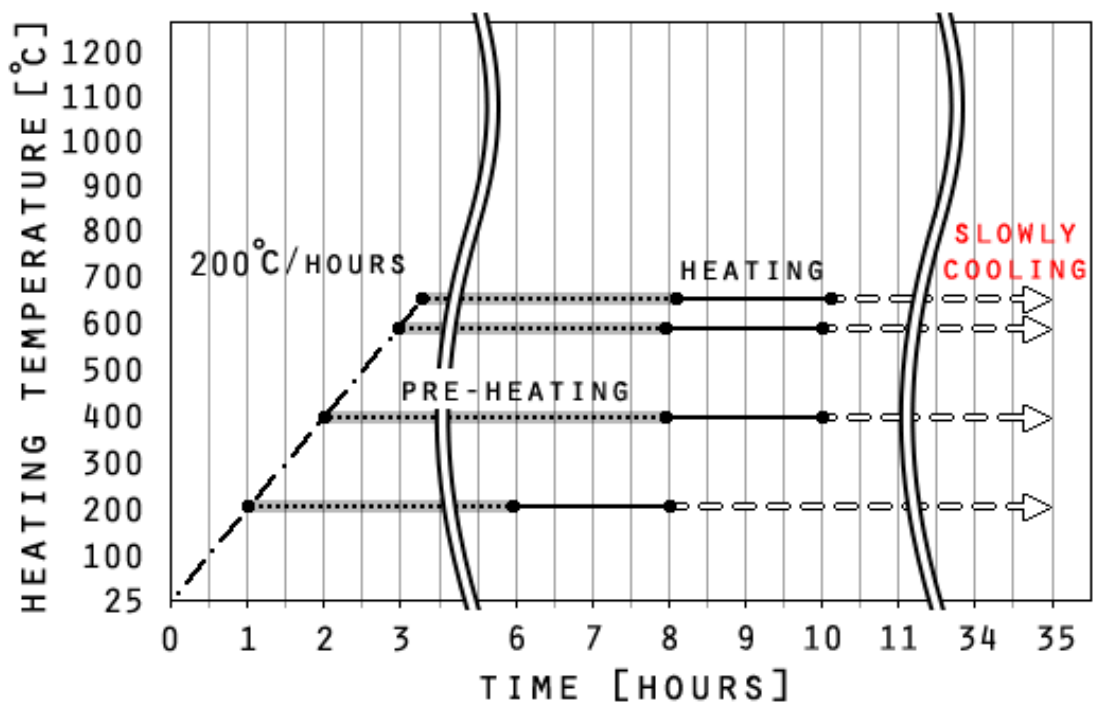


Fig.2-2-6: Experimental condition of Case-4

2.2.1 Method of heating tests

D) Measurements of water content

Marble is a metamorphic rock composed of, commonly, calcite or dolomite, and the chemical formula for marble is CaCO_3 . Eq. (1) is the chemical equation of the reaction in pyrolysis CaCO_3 . CaCO_3 is changed into CaO as CO_2 evaporates. At this time, the weight of marble stones begins to decrease. Moreover, CaO absorbs moisture in the air, and then it is changed into Ca(OH)_2 while giving off the heat of reaction. (See Eq. (2))⁽⁹⁾

Fig2-2-8 shows prospective flow of the weight decrease. Therefore, we expected that water content is useful data for understanding weight decrease because of occurring chemical reaction. A total of 3 specimens of marble stones were examined by the Forced Air Flow Oven (See Fig.2-2-7) for understanding how many weight decreased by evaporating water content. Hence, the specimens were heated at 110 °C for 24 hours, and the weight was compared



Fig.2-2-7: WFO-601SD

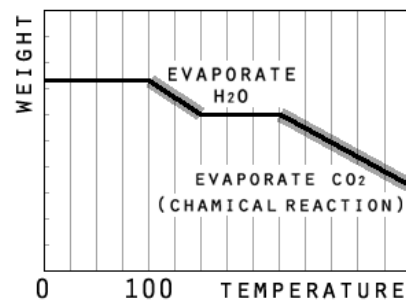
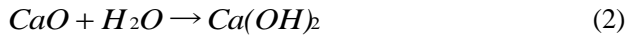
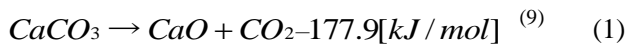


Fig.2-2-8: Image of weight decrease

before and after drying by using an electric balance.



II) Ocular inspection

Immediately after finishing heating test in Case-1, the heated marble specimens were pulled out from the oven (=quickly cooling) and the weight was measured by an electronic balance. And then, while specimens were cooled down, we took photos for recording process of deterioration by camera. On the other hand, in Case-2, after heating, marble specimens were left as it is in the closed oven for whole one night (=slowly cooling). In addition, the specimens were preserved in desiccators for 3 days.

From these different experimental conditions, we observed effects on the deterioration process of marble specimen by controlling humidity in desiccators, and then compared deterioration process of marble specimens heated at high temperature between Case-1, Case-2 and Case-4.

III) Measurements of weight variation

After heating tests in all of tests, weight of the specimen was measured by an electronic balance. Hence, while specimens were cooled down naturally in the air, photographs were periodically taken to record the change of aspect of specimens in Case-1. Fig.2-2-9 shows a setup using this test. One specimen was set with a thermocouple and the other was hung on the electronic balance. The electronic balance covered with aluminum seats for protecting against electromagnetic wave from the electric oven. Fig.2-2-10 shows the experimental temperature condition of this measurement. In the electric oven, two specimens were heated at the same time at the temperature between room temperature and 1,200 °C.

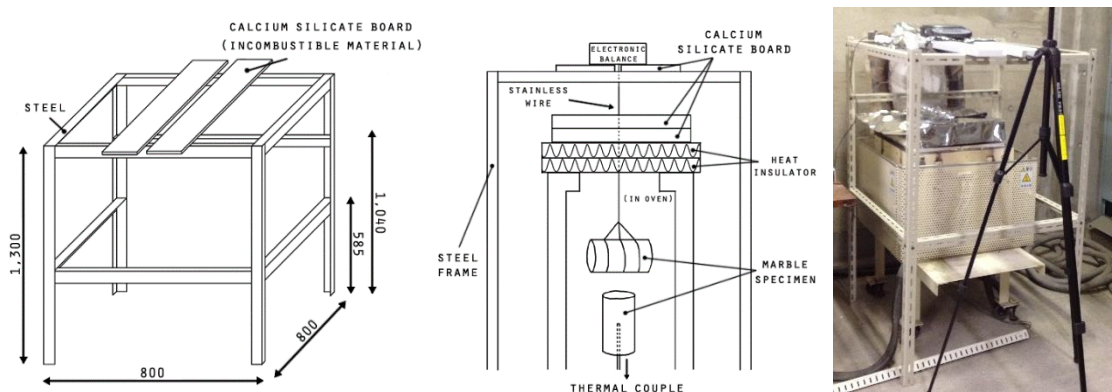


Fig.2-2-9: Experimental setup using for weight – measurement test –

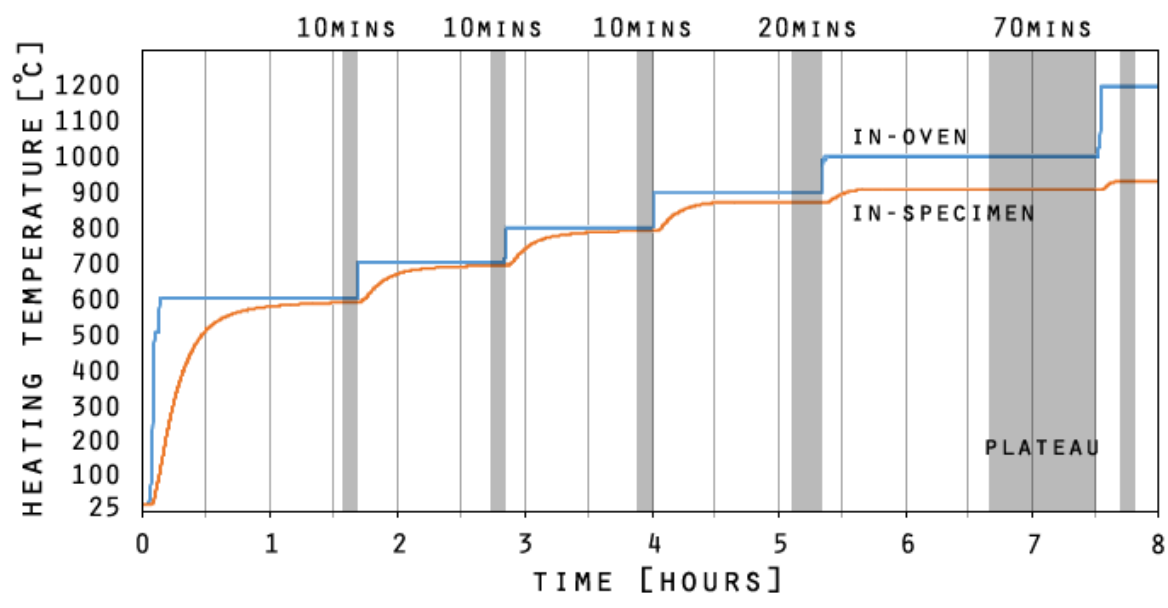


Fig.2-2-10: Experimental conditions of the weight – measurement test –

2.2.2 Results and discussions

D) Water content of marble

Table.2-2-2 shows the weight variation of specimens of marble stones caused by heating at 110 °C. Negligible density variation less than 0.2 % was found, which demonstrated no water content of the marble stones.

Table 2-2-2: Results of measurement of the water content

	Before → After	Water Content [%]
Specimen A	487.5 [g] → 487.6 [g]	0.00
Specimen B	544.3 [g] → 544.2 [g]	0.00
Specimen C	524.6 [g] → 524.5 [g]	0.00

II) Weight variation of marble

Fig.2-2-11 shows the relation between heating temperature with time and weight variation in Case-1. In this figure, “In-specimen temp.” denotes the temperature at the center of specimen. The irregular weight variation shown at 1,000 °C was caused by an experimental trouble, therefore, should be neglected. In the present heating test, reduction of weight was initiated at 750 °C. In addition, soon after having set the higher temperature from 750 °C, the weight of specimen decreased remarkably.

Fig.2-2-12 and Fig.2-2-13 show the weight variation of specimens after the heating tests at temperature between 200 °C and 1,200 °C in Case-1. Weight variation at between 200 °C and 600 °C was less than 0.2 %, indicating no density reduction was caused at the range between 200 °C and 600 °C. However, the remarkable weight variation of specimens was found after the heating at between 750 °C and 1,200 °C. The weight of specimens just after the heating at 800 °C became less than 97 % of the initial one even if there found a little difference in weight caused by the heating time. Moreover, the weight of the specimens heated at 1,000 °C and 1,200 °C was reduced to be less than 60 %.

Shown in Fig.2-2-13, the weight of the specimens heated at 800 °C was recovered during the cooling time in the air in Case-1. The weight of the specimen regained with the passage of time.

Fig.2-2-14 and Fig.2-2-15 indicate the density variation and weight variation in Case-3. Both variations of the marble specimen having vertical crystal direction were decreased more.

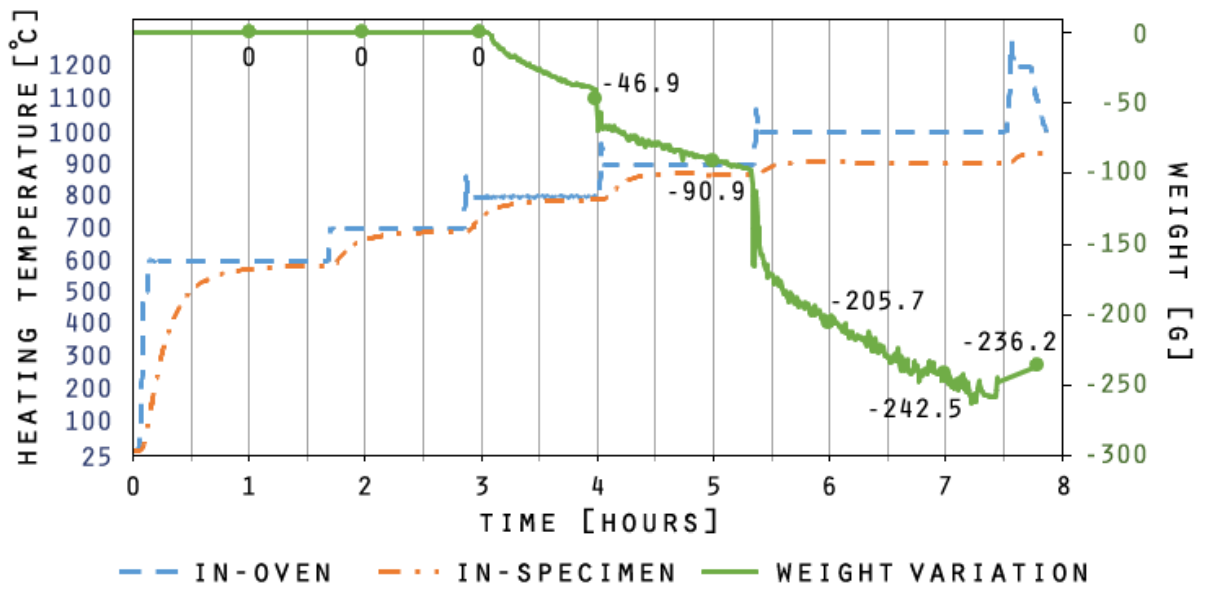


Fig.2-2-11: Weight variation with time in step heating test by raising 100 °C in Case-1

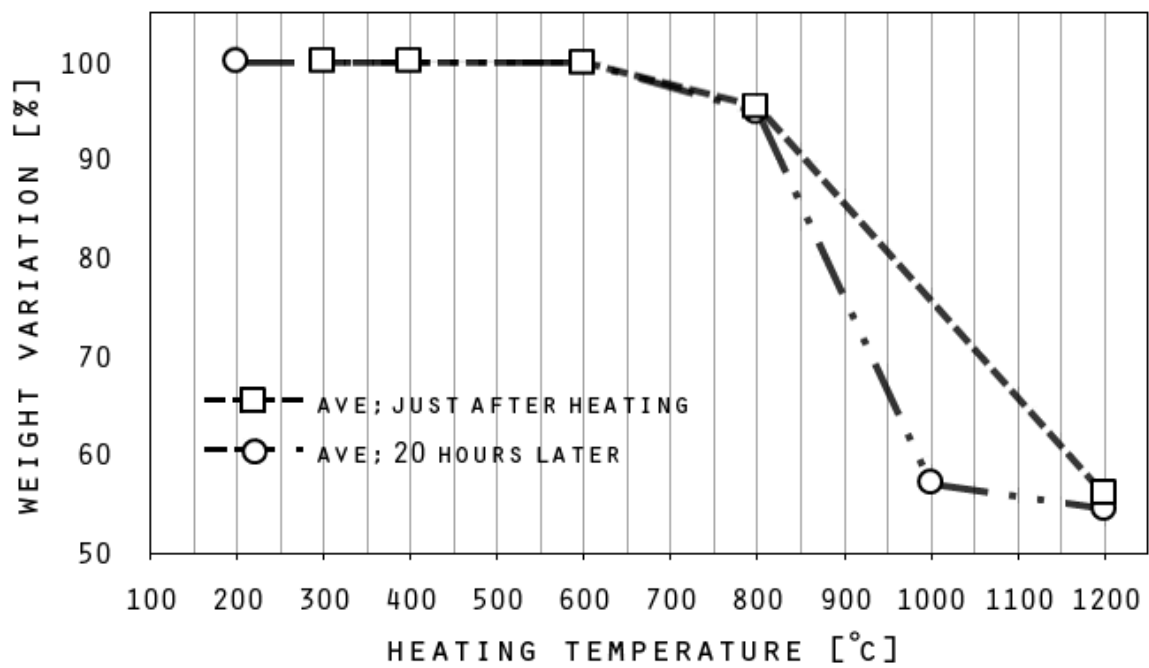


Figure 2-2-12: Relation between heating temperature and weight variation with constant temperature tests in Case-1

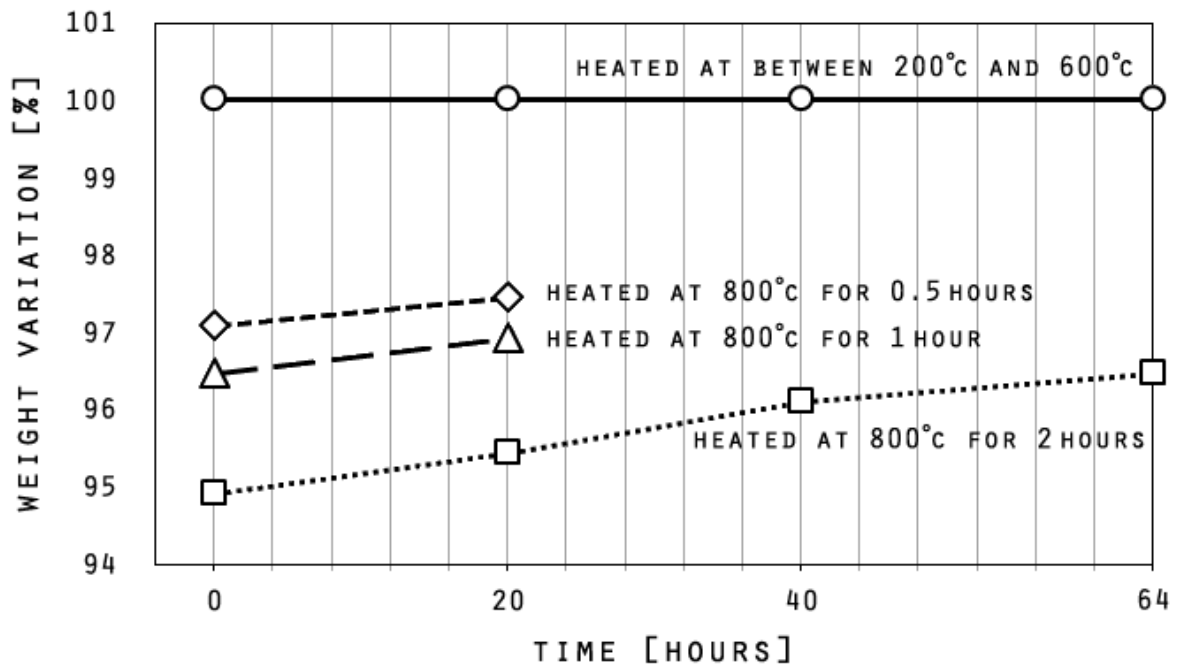


Figure 2-2-13: Relation between elapsed time after heating and weight variation in Case-1

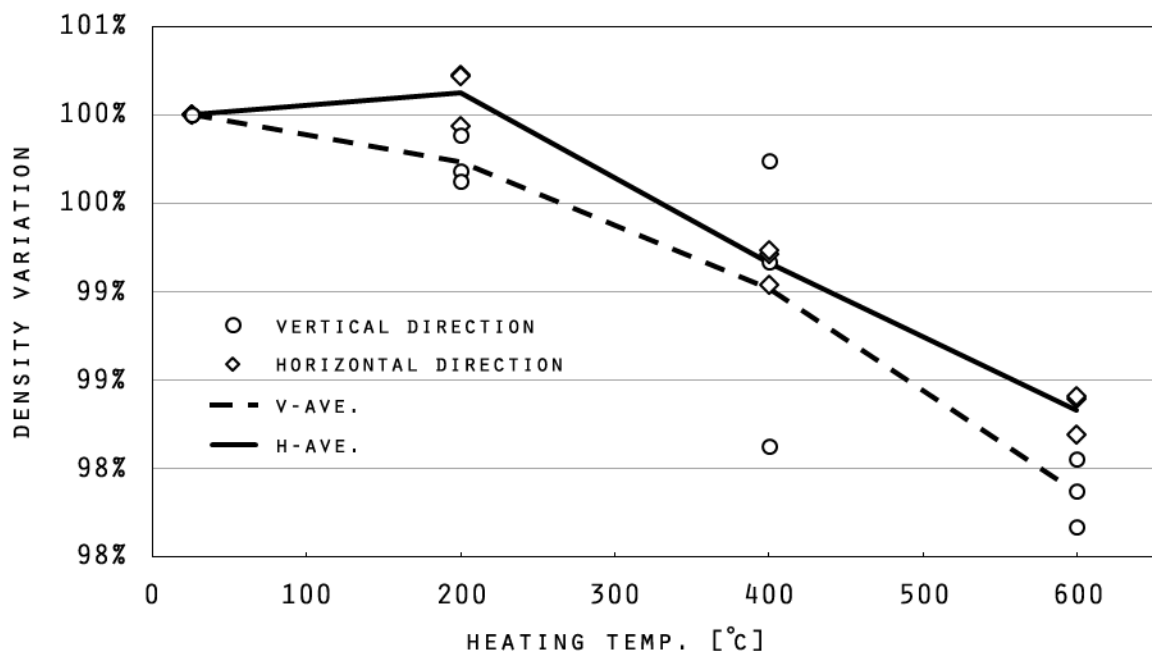


Figure 2-2-14: Relation between density variation and heating temperature in Case-3

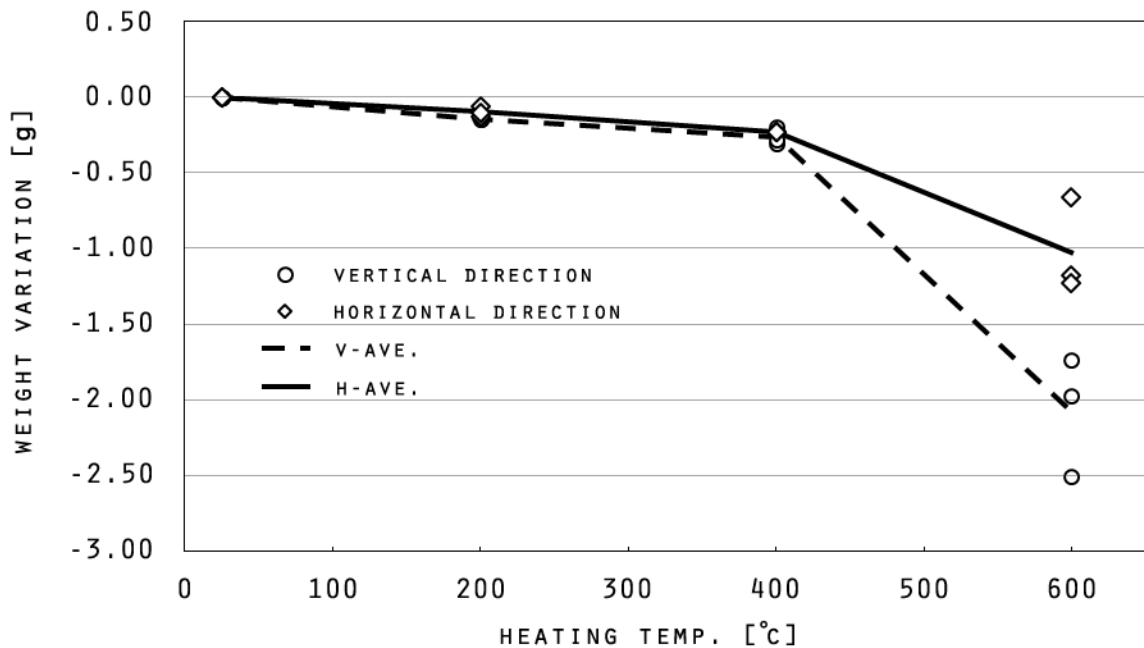


Figure 2-2-15: Relation between heating temperature and weight variation in Case-3

III) Damage of specimens by high temperature

In Case-1, deterioration of the marble specimens heated at temperature higher than 800 °C were remarkably observed. Fig.2-2-16 and Fig.2-2-17 show the specimens heated at 800 °C. At first, the specimen has some cracks in the edge of the specimen along the curve of the specimen (1 and 2) and a crack in the side of the specimen's body (3). With the passage of time, this cracks were developed (4) and eventually, the surface layer of the specimen was separated into several parts of the specimen (5). In addition, the cracks also occurred in the internal specimen as well as cracks in the edge of the specimen. Moreover, the distortion was gradually caused at the inner part of the specimen and extended to whole body with the passage of time (I). During exposing to the air, the strength of the specimen was getting lower and the thin surface layer of the specimen which thickness was 1-2 mm are cast off. Eventually the specimen reached to collapse, while cracks were developed (II and III).

Fig.2-2-18 shows Deterioration process of marble specimens heated at 800 °C or 1,000 °C in Case-2. A marble specimen heated at 800 °C has an angled crack of which length was 17 mm just after heating (A). The angled crack of the specimen were developed after heating in the desiccator for 72 hours, then the surface of the marble specimen heated at 800 °C was exfoliated and collapsed near the developed crack (B). On the other hand, a marble specimen heated at 1,000 °C had a large crack on the side of the specimen, and it didn't develop (C), hence the surface of the marble specimen heated at 1,000 °C didn't have variation near the crack (D and E). In addition, comparing number of cracks between marble specimens heated at 800 °C and these heated at 1,000 °C, the number of cracks was almost the same. Furthermore, most of cracks occurred on the side of the

specimens.

Fig.2-2-19 shows the deterioration process of marble specimens heated at 650 °C in Case-4. The size of the marble specimens using in Case-4 was bigger than them using in Case-1, Case-2 and Case-3, hence the pre-heating time needed about 3~4 times longer. Hence, the appearance deterioration of the specimen was observed more seriously, however the specimen was heated at just 650°C. After heating tests, the cracks of the tortoise shell form occurred in the bottom side of the specimen, moreover the cracks progressed with time, and then this process resulted in the delamination of surface of the specimen. (A) Besides, the marble specimens using in Case-4 were prism shapes, hence almost cracks on the specimens occurred partially around the edge of the specimen. In particular, there were serious damages around four corner parts of the specimen, and eventually the specimen collapsed with time. (B and C)

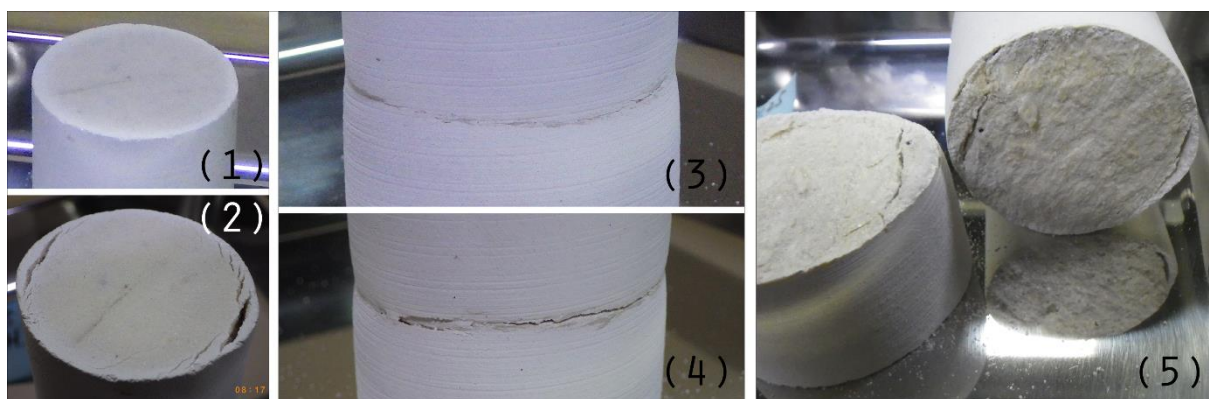


Fig.2-2-16: Deterioration process of heated marbles in Case-1

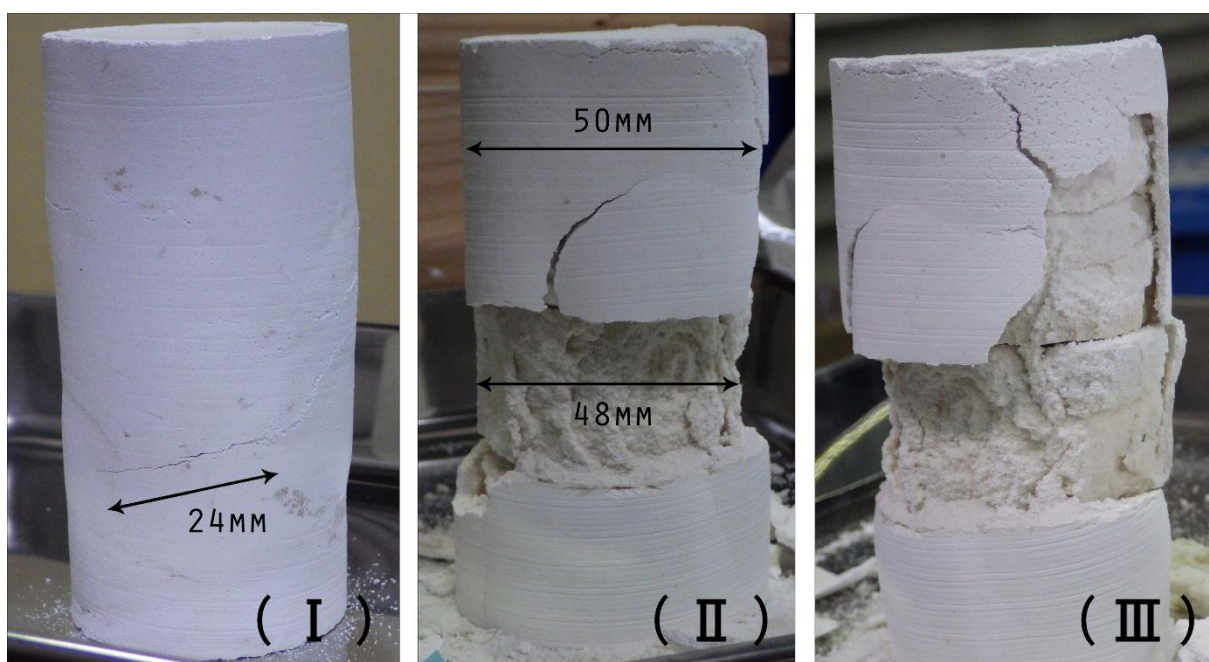


Fig.2-2-17: Deterioration process of heated marbles in Case-1

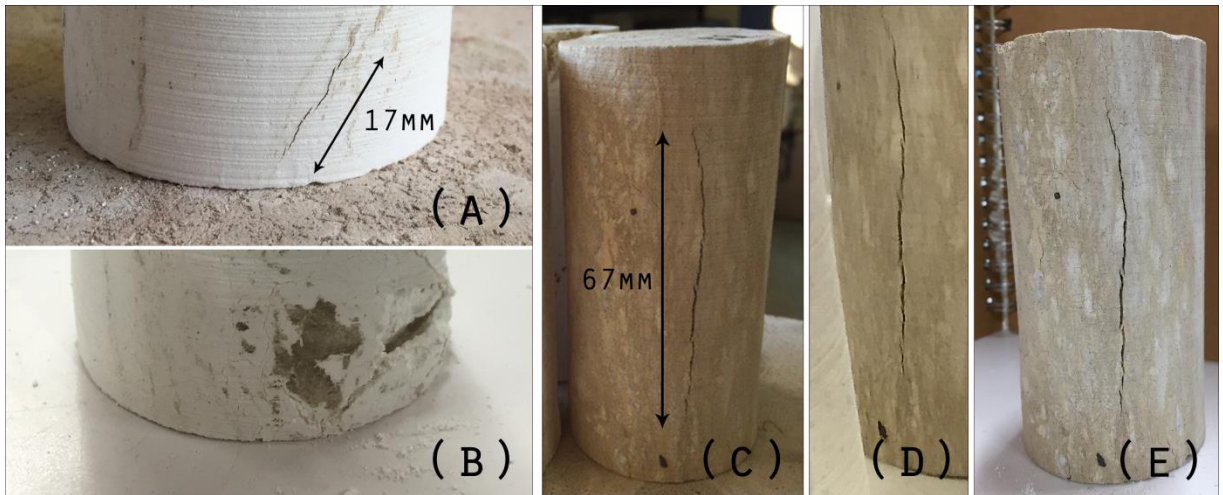


Fig.2-2-18: Deterioration process of heated marbles in Case-2

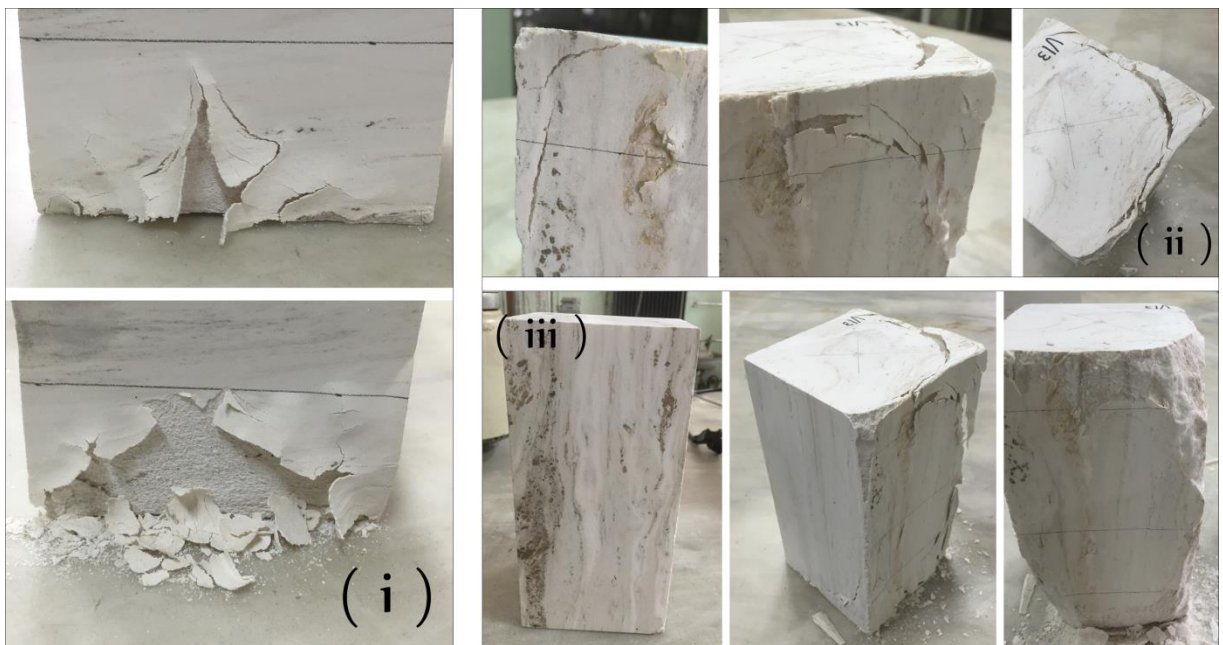


Fig.2-2-19: Deterioration process of heated marbles in Case-4

IV) Discussions

From results of measurement of content water test, the water content of marble was 0.0 % and marble contains no water. Therefore, it should be recognized that the chemical reaction of CaCO_3 and the weight reduction of the specimens occurred at the same time in heating tests at high temperatures. Based on above mentions results, Fig.2-2-11 shows chemical reaction expressed by Eq. (1) started in the specimens at 700 °C. Such reduction of the density was caused by the chemical reaction described by Eq. (1), when the specimen released CO_2 . Accordingly, moisture absorption

affected deterioration process of marble. As shown in Fig.2-2-13, weight of all of the specimens heated at 800 °C increased with the passage of time by moisture absorbing, and deterioration of the specimens significantly proceeded. (See Fig.2-2-16 and Fig.2-2-17) This phenomenon can be interpreted by exhaustion of CO₂ expressed by Eq. (2). In addition, the water content of the marble heated at 800 °C after 64 hours later from finishing heating test was bigger than the one of un-heated marble, however the water content of un-heated marble (CaCO₂) was confirmed 0 % (See 2.2.2-I). From this, CaCO₂ changed into CaO at that time.

In addition, cooling speed after end of the heating also affected occurring cracks on marble. As shown in Fig.2-2-18, there were some differences between quickly cooling and slowly cooling. The rapid temperature change gave the specimens big shock, hence occurring cracks on marble depended on the thermal shock caused by quickly cooling than heating temperature.

2.3 Mechanical properties tests

2.3.1 Method of compressive tests

It is necessary to understand that how compressive strength is reduced by heating. Furthermore, there is degree of damage of marble stones by high temperature. Thus, we conducted compressive tests of a total of 52 specimens (16 specimens in Case-1 and 12 specimens in Case-2 and 24 specimens in Case-3) of marble after the heating tests by the compressive tests. Fig.3-3-1 shows the amsler testing machine using for these tests.



Fig.2-3-1: Using machine

2.3.2 Marble specimen properties

I) Dimensions of specimens

In according to the reference ⁽¹⁰⁾, the density of the marble is between 2.6 and 2.8 (g/cm³), and that of the marble specimen using in our heating test and compression tests is 2.7 (g/cm³).

II) Crystal direction

Stones and rocks such as marble including the marble have crystal directions called 'joint'. In general, when the marble is produced, they are prepared so that crystal direction of marble is perpendicular to that of loading. (See Fig.2-3-2)

It is important to take into account the effect of the crystal direction on the compressive strength for the fundamental study of characteristic of marble. Accordingly, 18 of marble prism specimens were conducted the compression tests for confirming effects of the compressive strength caused by difference in crystal direction. Furthermore, we observed the effects of the compressive strength caused by difference between cylindrical specimens and rectangular them.

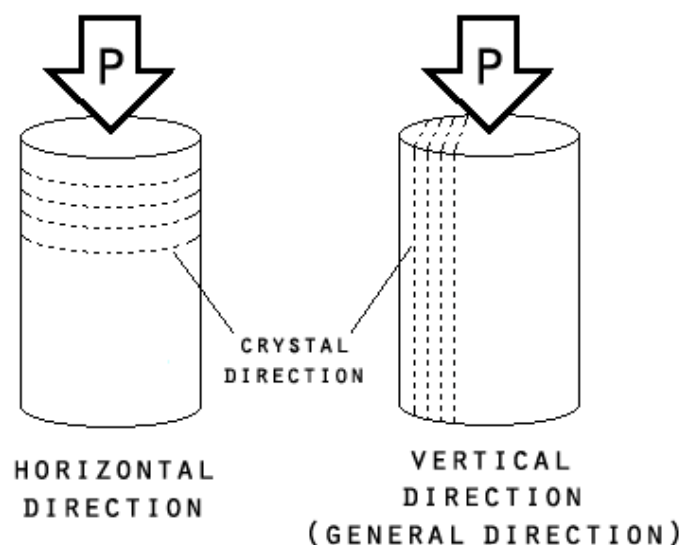


Fig.2-3-2: Crystal direction

2.3.3 Results and discussions

D) Compressive tests

Fig.2-3-3 shows the fracture mode of the specimens after the compressive tests of the un-heated specimen (A) and the specimens of heating at 400 °C (B) or 600 °C (C). Most of the heated specimens showed shear failure mode regardless of degree of temperature, shown in these photos. In addition, these marble specimen didn't be performed treatment of end.

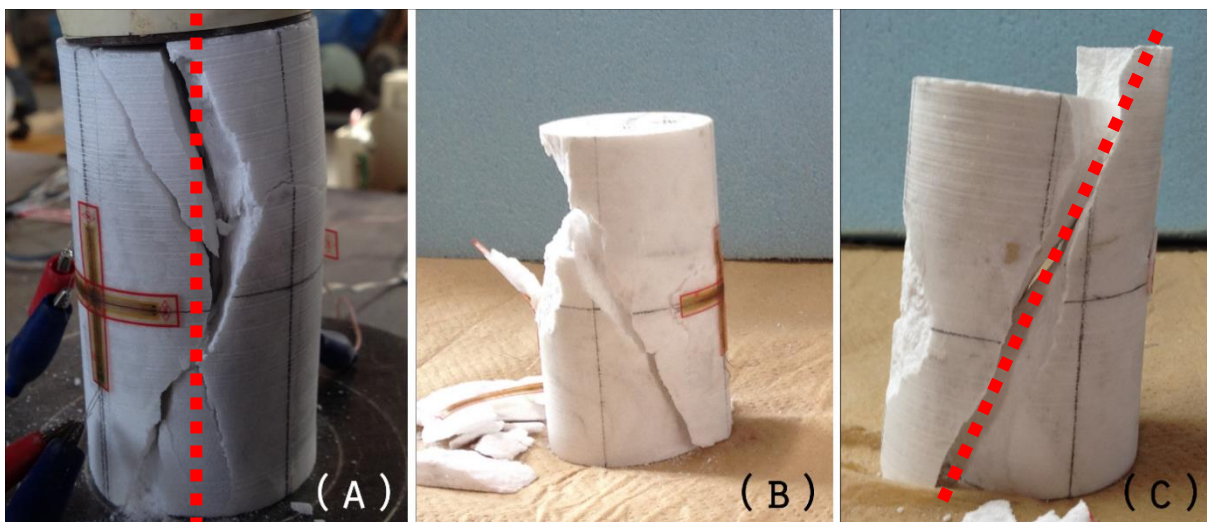


Fig.2-3-3: Failure mode of marble specimens in Case-1

Fig.2-3-4 and Fig.2-3-5 show the relation between heating temperature and strength of the marble among Case-1, Case-2 and Case-3. In addition, all of the compressive strength in Fig.2-3-4 is them of the marble specimens have vertical crystal direction. Moreover, the data of same condition of heating time (90 minutes for pre-heating and 2 hours) among Case-1, Case-2 and Case-3 was shown in this figure.

In this figure, the strength began to decrease at the temperature of 300 °C. Additionally, the specimen heated at over 750 °C didn't be conformed compressive test because the specimen heated at over 750 °C collapsed naturally while cooling (See Fig.2-2-17). Thus, the compressive strength of the specimen heated at over 750 °C was treated as 0 (N/mm²).

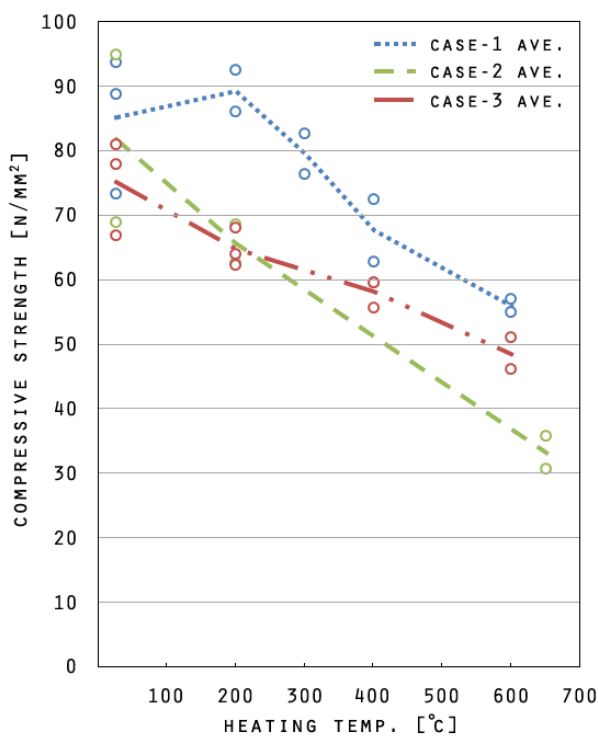


Fig.2-3-4: Compressive strength (N/mm²)

Therefore, strength was reduced remarkably at the temperature between 600 °C and 800 °C.

In addition in Case-2 and Case-3, although heated marble specimens were preserved in desiccators until just before the compressive tests, the strength of the specimens heated at under 650 °C were not affected by moisture control.

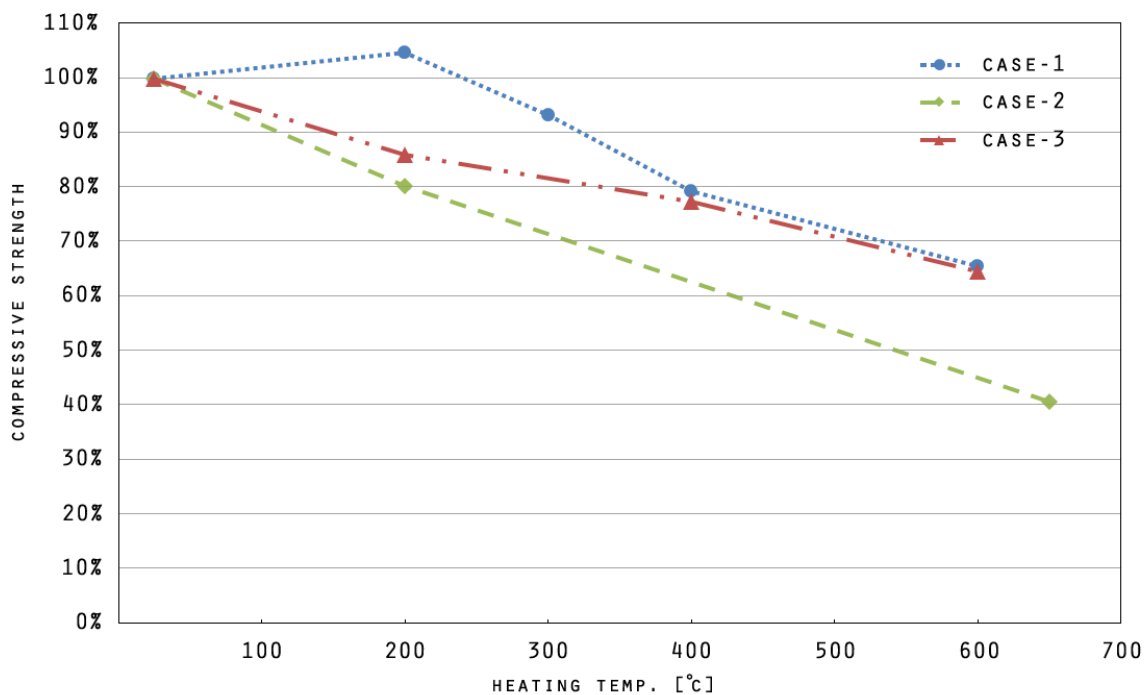


Fig.2-3-5: Compressive strength (%)

II) Compressive strength affected by difference on crystal direction

Fig.2-3-6 describes the compressive strength of each crystal direction of marble in Case-1 and Case-3. In Case-1, there was big difference between vertical direction and horizontal direction, however there was not so big difference between both directions in Case-3.

In case-1, the compressive strength of the specimens having vertical crystal direction heated at 650 °C were about 22 % stronger than that of the specimens having horizontal crystal direction heated at 650 °C. On the other hand, the specimens having horizontal crystal direction were at most 20 % stronger than that of the specimens having vertical crystal direction. In addition, compared to the un-heated specimen, the strength of the specimens heated at 650 °C was decreased by about 40 % in both cases.

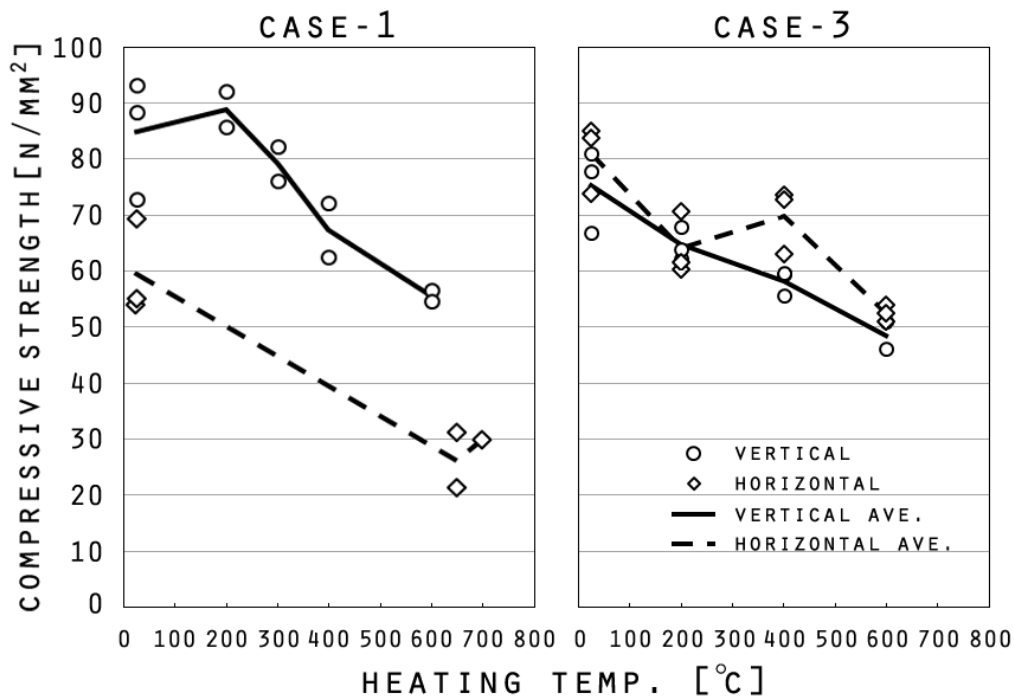


Fig.2-3-6: Effect of crystal direction upon the compressive strength in Case-1 and Case-2

III) Stress-strain curve

Fig.2-3-7 ~Fig.2-3-12 show the stress-strain curves of marble specimens in Case-1 and Fig.2-3-13 ~Fig2-3-20 show the them of marble specimens in Case-3. The stress-strain courves of un-heated specimen in both of cases have general courve, nevertheless the curves of heated specimen have the downward convex courves. Therefore, the Young's modulus of each marble specimen was started to calculate from pressing 10 kN considering the initial fitting around edge of the specimen during compression. In addition, these Young's moduus were calcularted by using the 1/3 times values of the maxium compressive strength.

Fig.2-3-21 suggests the Young's modulus of each specimens. Compared to the Young's modulus of un-heated specimen, that of the specimen heated at 650 °C was decreased by 30 %. Moreover, this graph shows the higher heating temperature is, thw lower the Young's modulus as temperature-dependent.

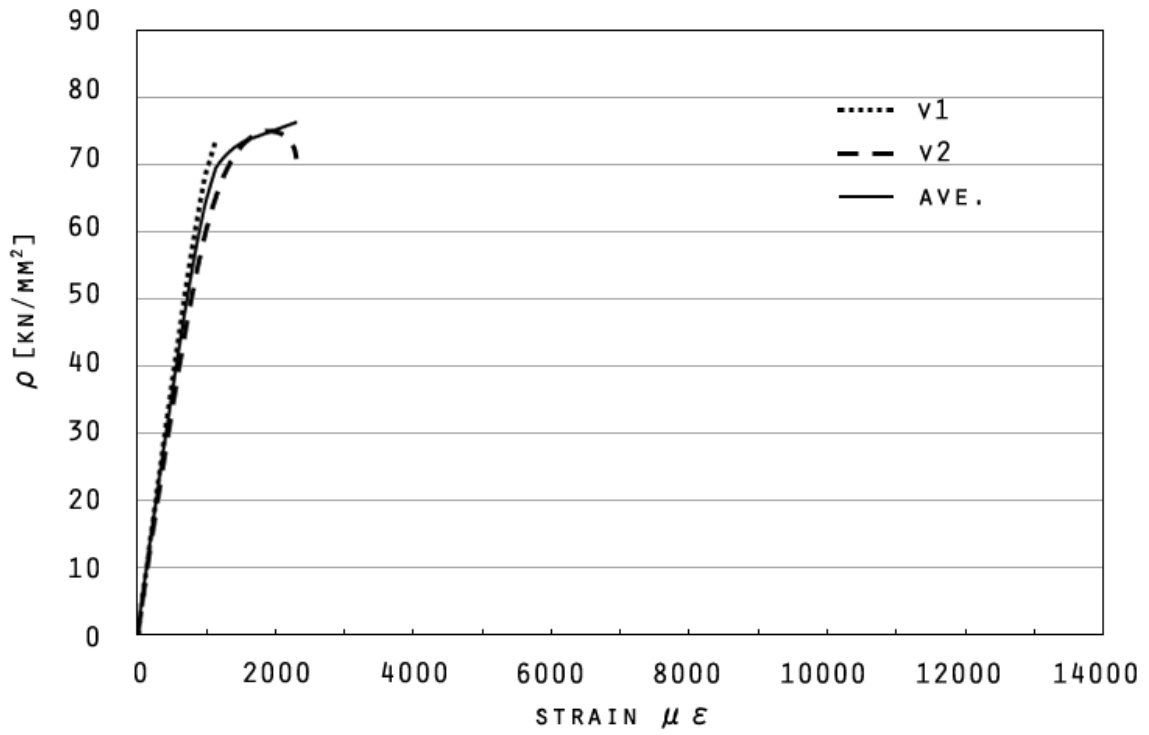


Fig.2-3-7: Stress-strain curve of un-heated marbles having vertical crystal direction in Case-1

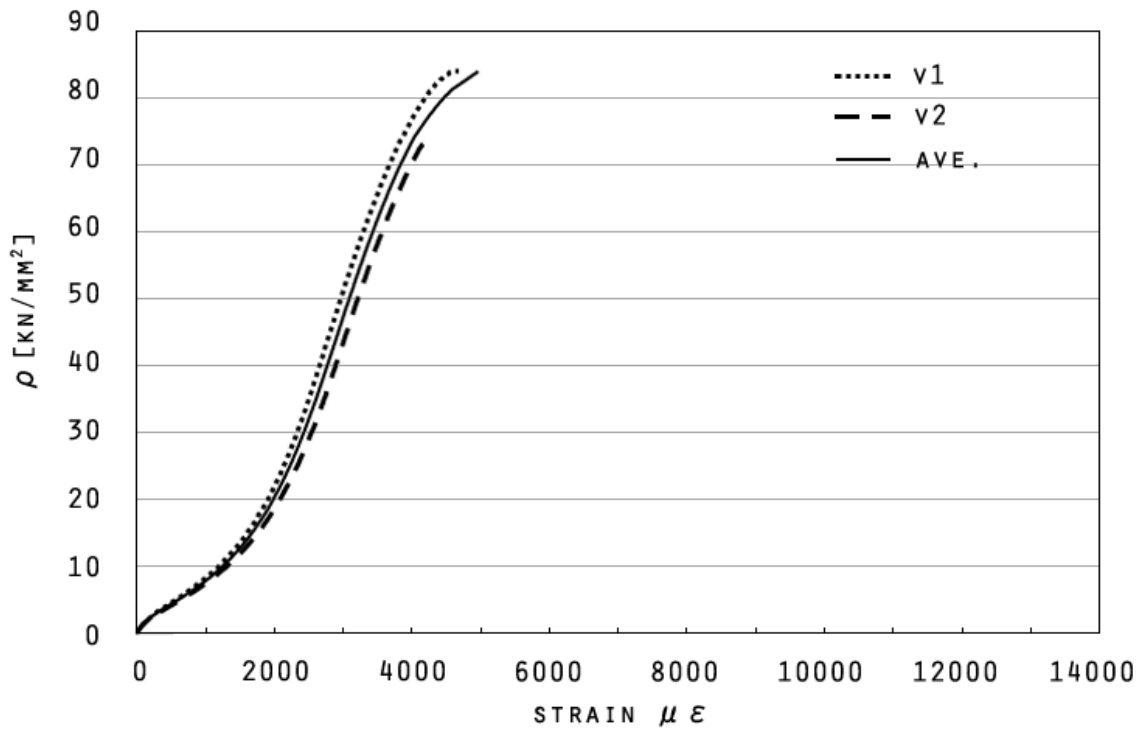


Fig.2-3-8: Stress-strain curve of marbles having vertical crystal direction heated at 300 °C for 2 hours in Case-1

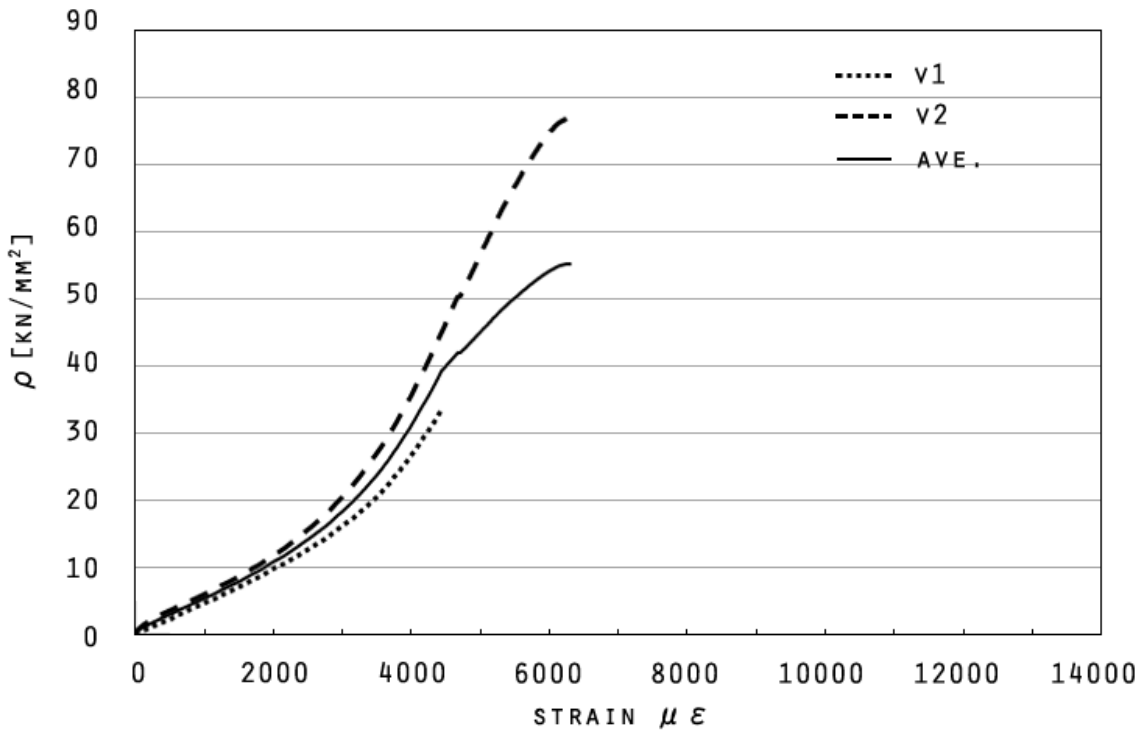


Fig.2-3-9: Stress-strain curve of marbles having vertical crystal direction heated at 400 °C for 1 hour in Case-1

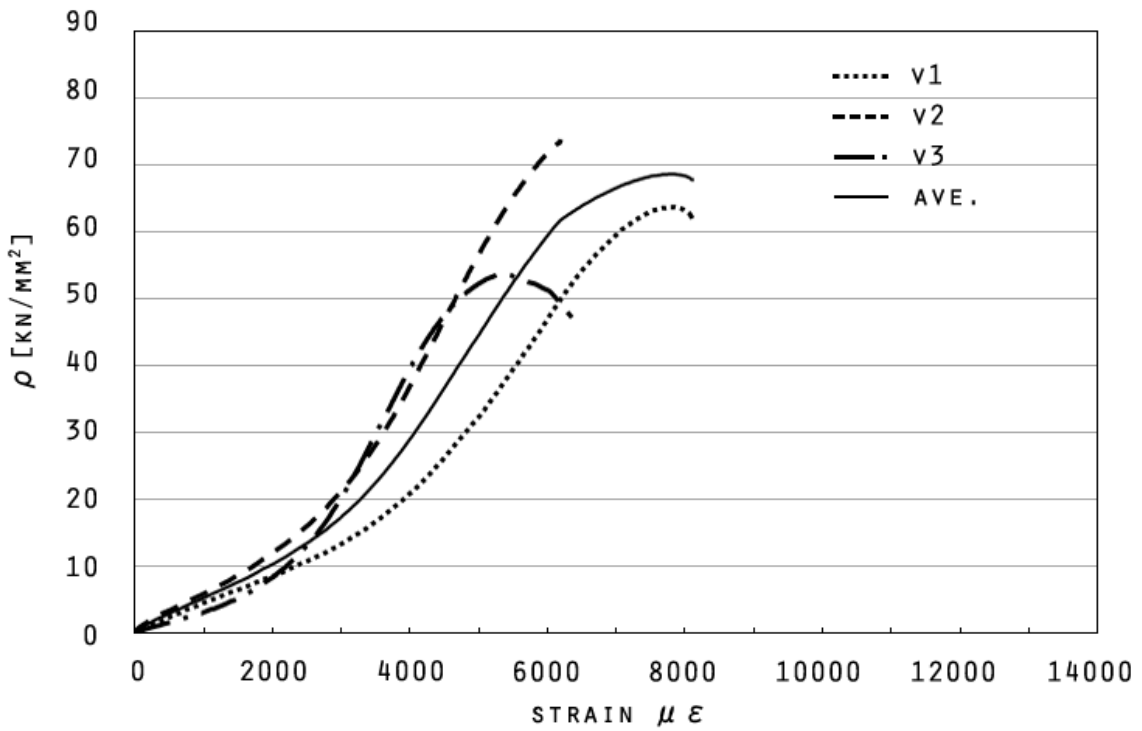


Fig.2-3-10: Stress-strain curve of marbles having vertical crystal direction heated at 400 °C for 2 hours in Case-1

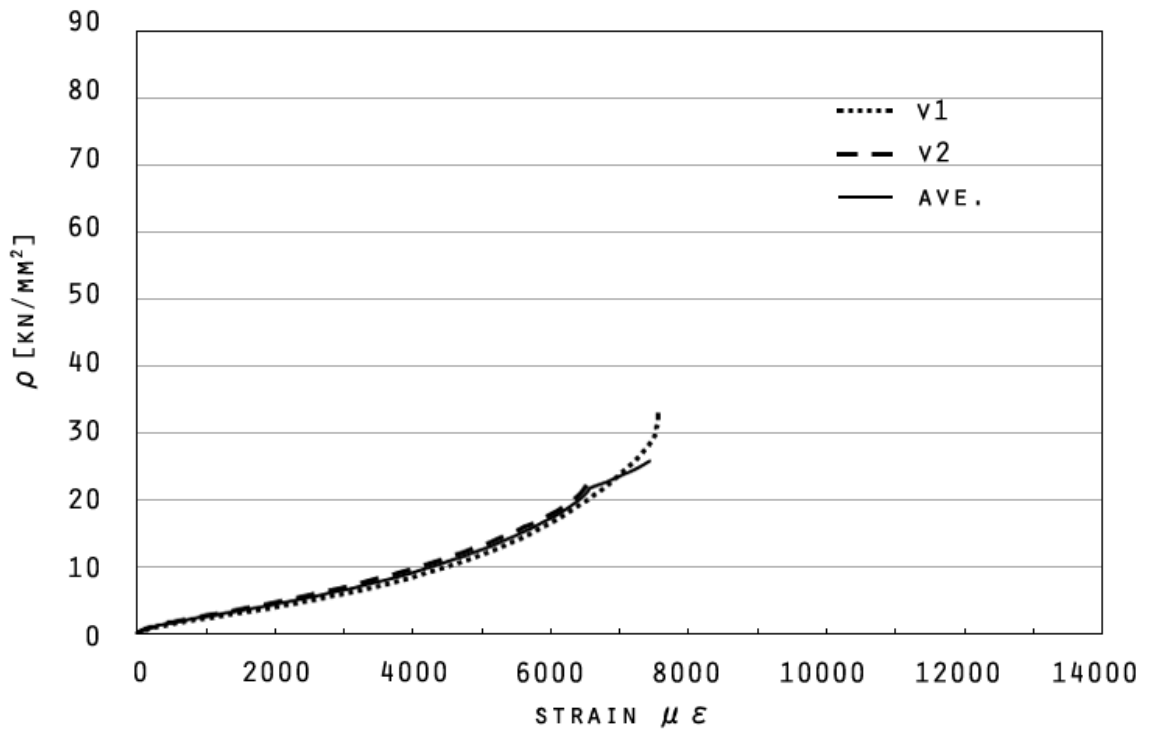


Fig.2-3-11: Stress-strain curve of marbles having vertical crystal direction heated at 600 °C for 1 hour in Case-1

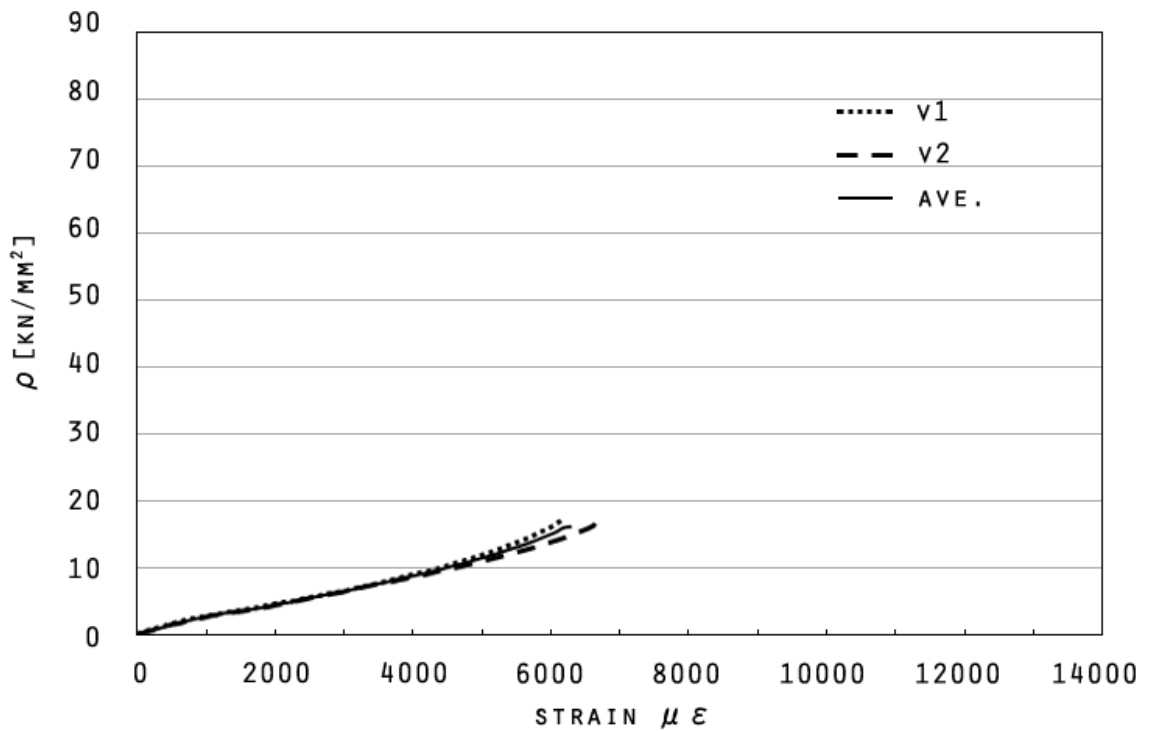


Fig.2-3-12: Stress-strain curve of marbles having vertical crystal direction heated at 600 °C for 2 hours in Case-1

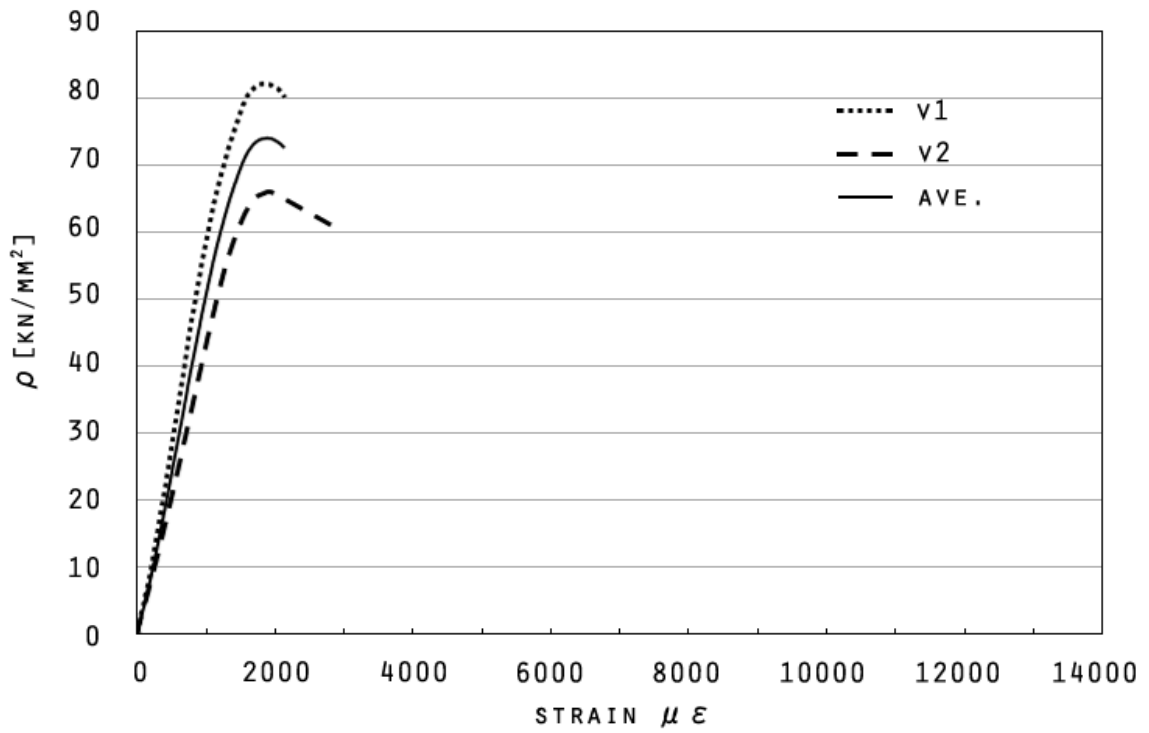


Fig.2-3-13: Stress-strain curve of un-heated marbles having vertical crystal direction in Case-3

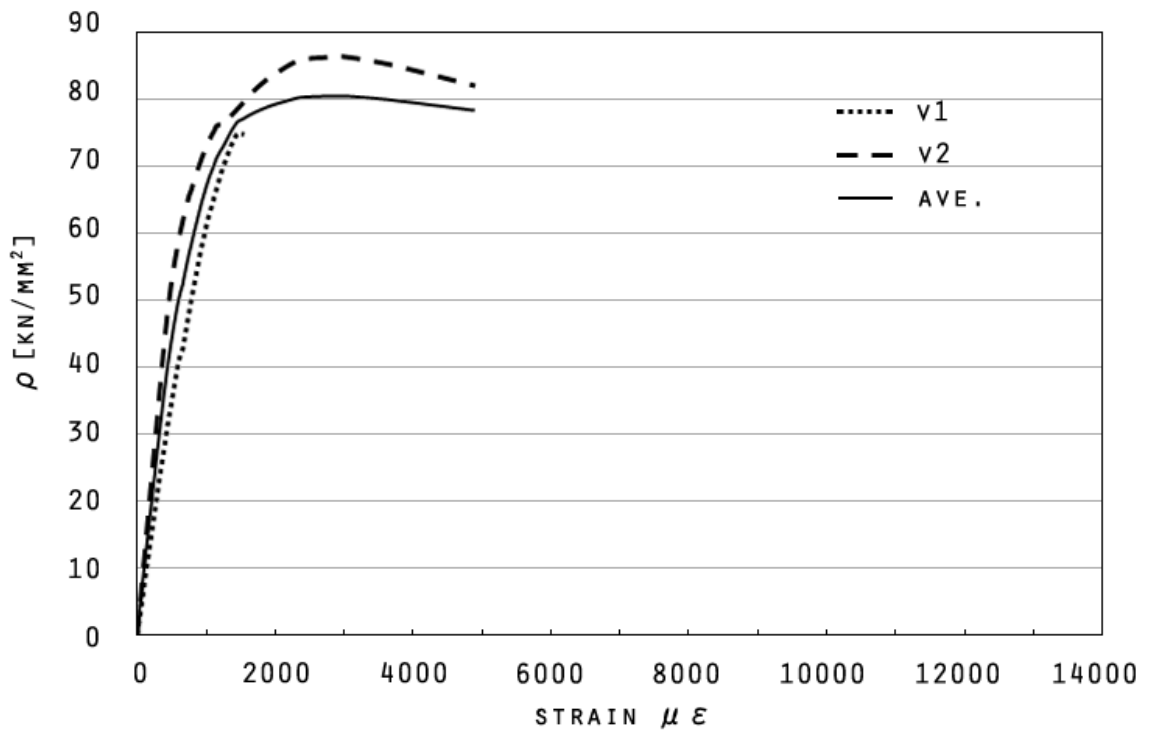


Fig.2-3-14: Stress-strain curve of un-heated marbles having horizontal crystal direction in Case-3

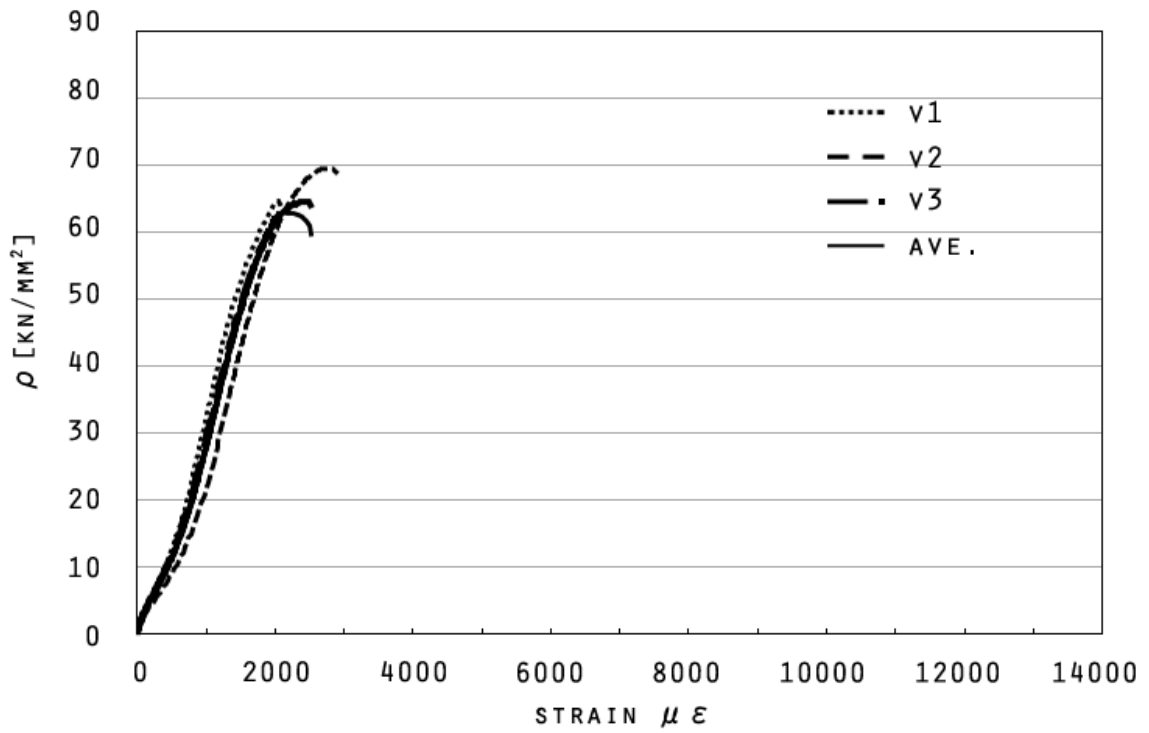


Fig.2-3-15: Stress-strain curve of marbles having vertical crystal direction heated at 200 °C in Case-3

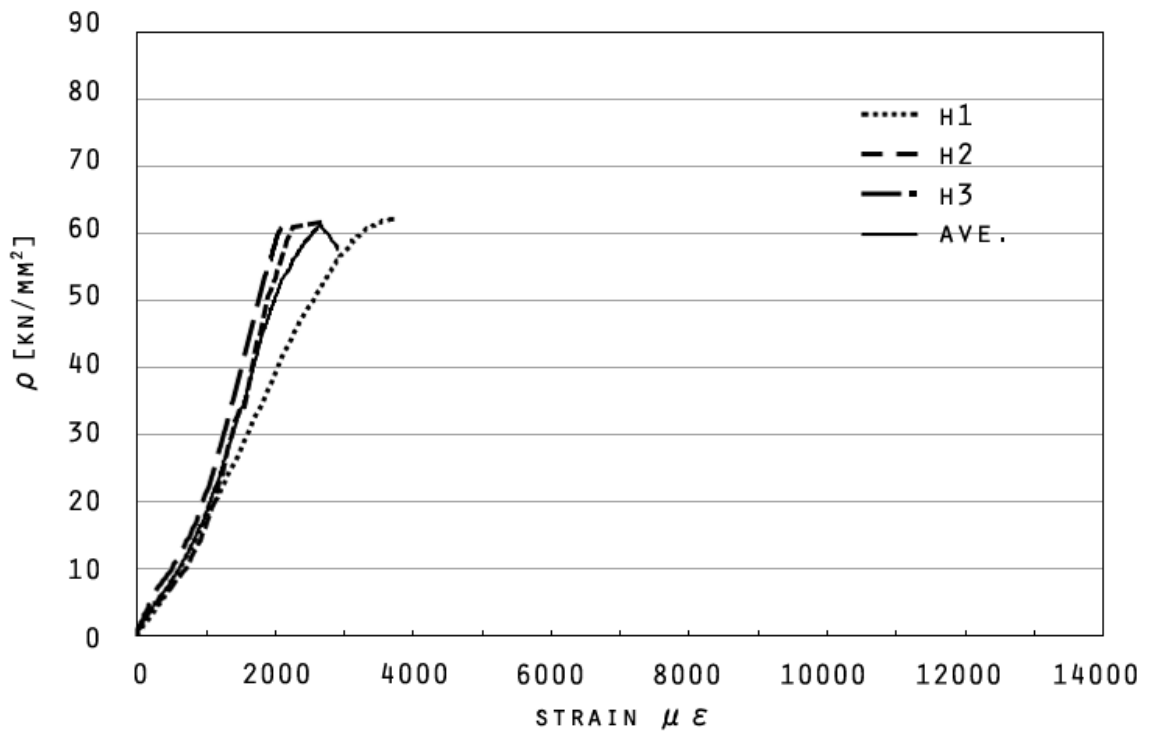


Fig.2-3-16: Stress-strain curve of marbles having horizontal crystal direction heated at 200 °C in Case-3

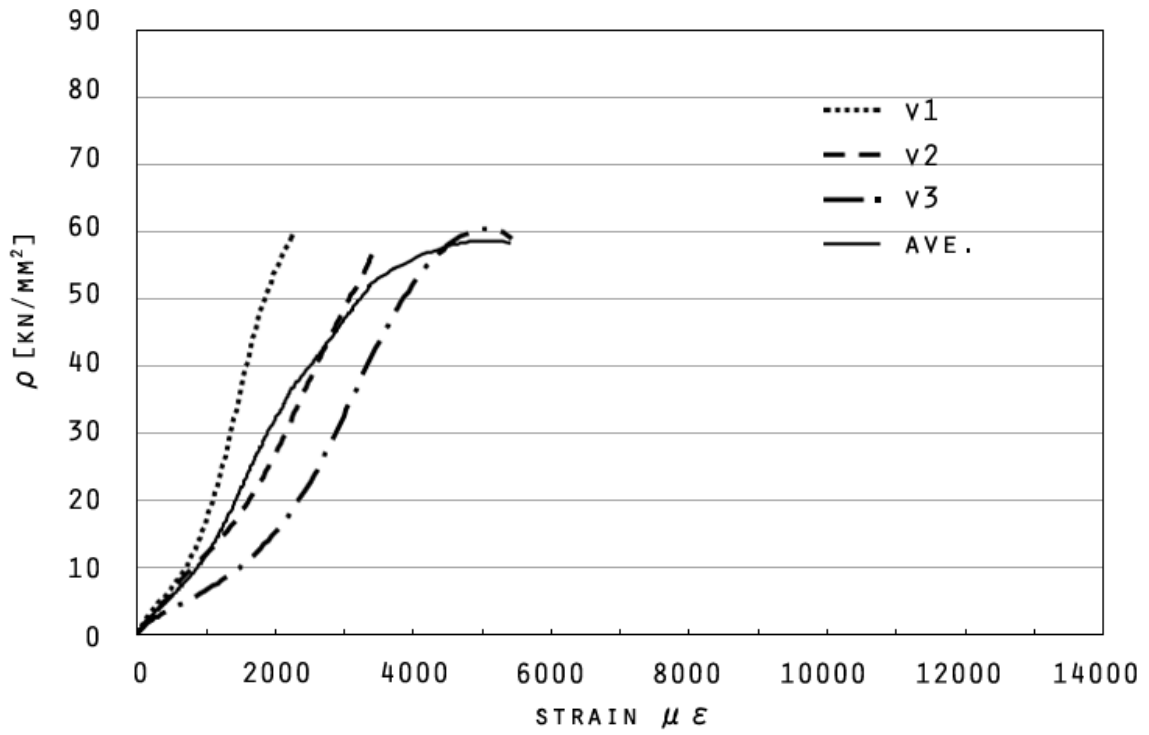


Fig.2-3-17: Stress-strain curve of marbles having vertical crystal direction heated at 400 °C in Case-3

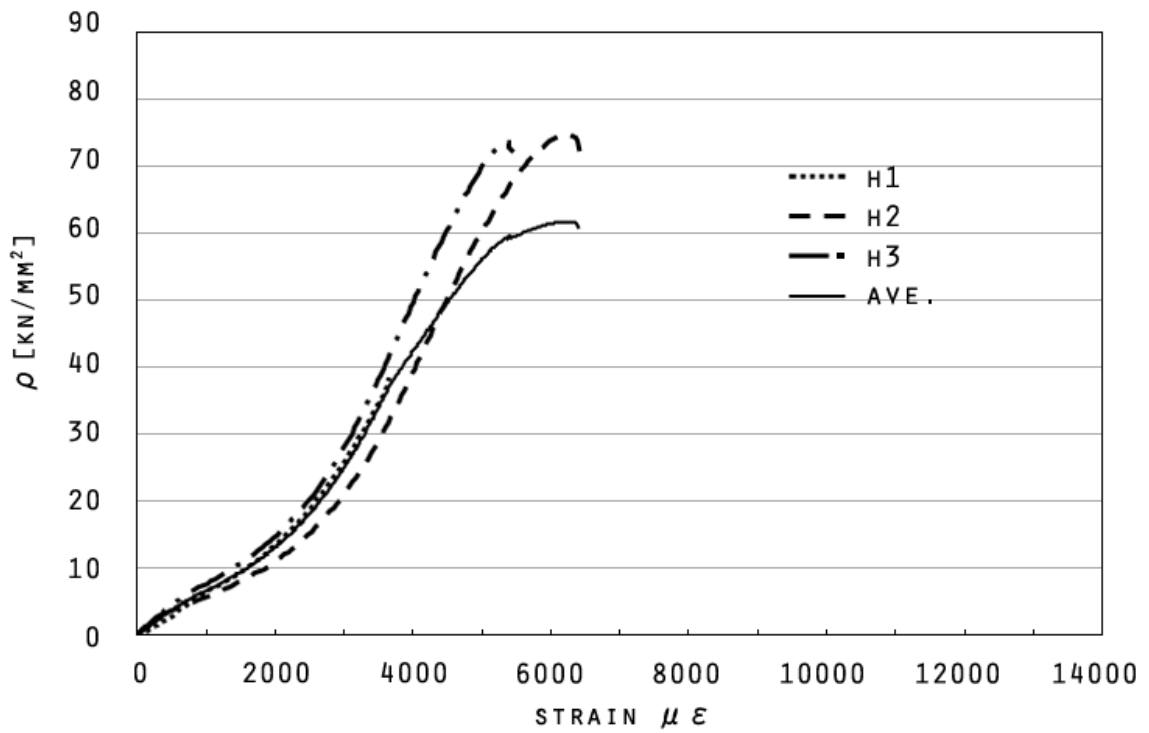


Fig.2-3-18: Stress-strain curve of marbles having horizontal crystal direction heated at 400 °C in Case-3

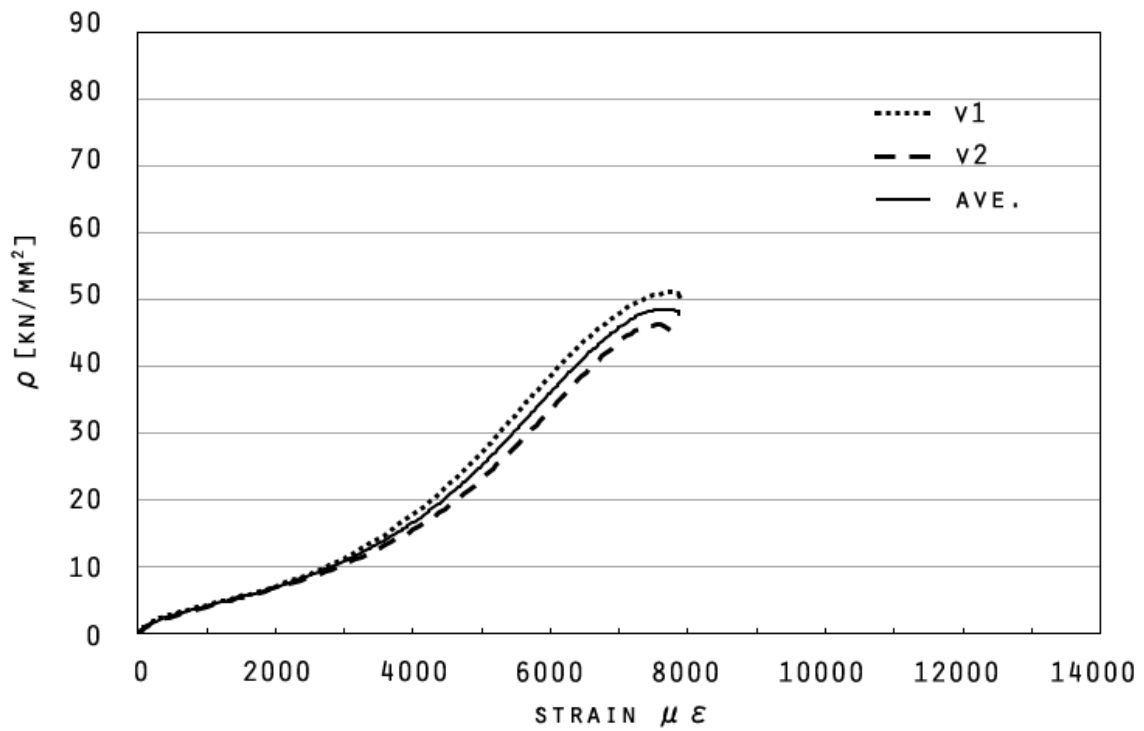


Fig.2-3-19: Stress-strain curve of marbles having vertical crystal direction heated at 600 °C in Case-3

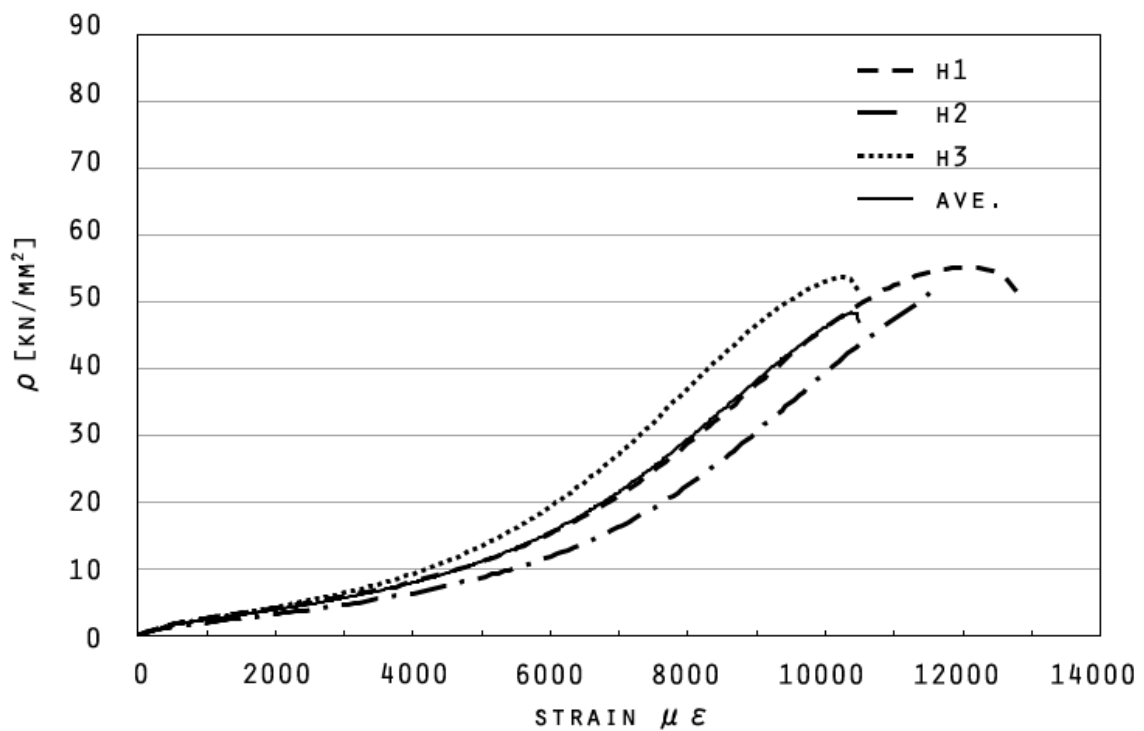


Fig.2-3-20: Stress-strain curve of marbles having horizontal crystal direction heated at 600 °C in Case-3

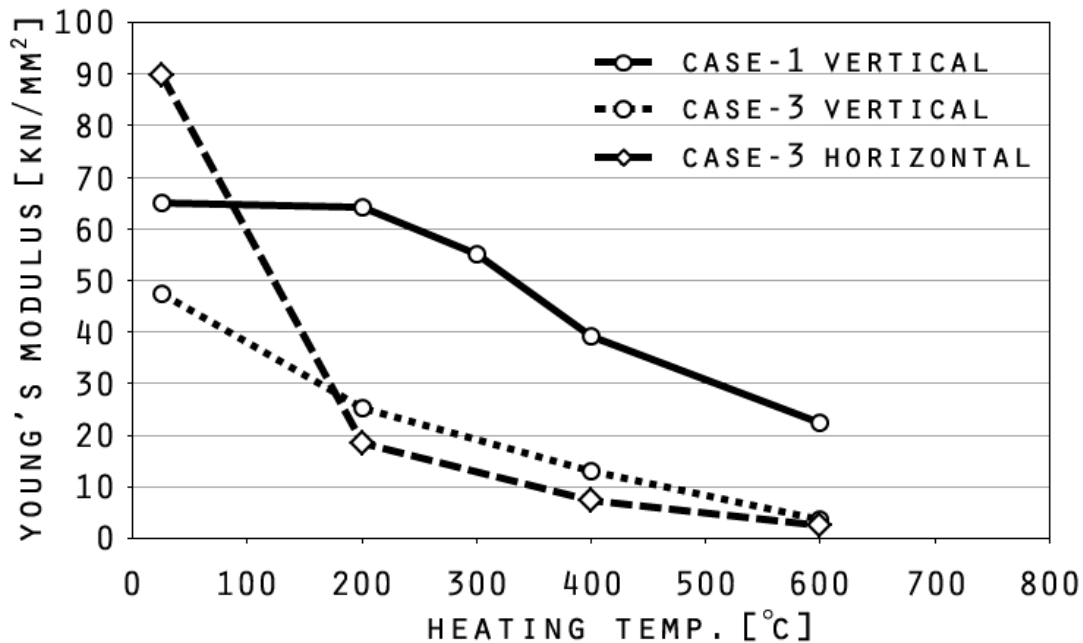


Fig.2-3-21: Rate of variation of Young's modulus in Case-1 and Case-3

IV) Discussions

As shown in Fig.2-3-3, there were the different failure modes between the un-heated specimens and the heated specimens. The un-heated specimens had straight cracks from the center of specimen. It indicated that the specimens were compressed by even loading in the specimen. On the other hand, that of the heated specimens had shear cracks from edge of the specimen, and from this result, it seemed that the heated specimens did not keep parallel between top and bottom in ends because of expanding of the specimen by heating. Hence, the heated specimens were compressed by un-even loading.

Additionally, we hypothesized from the results; if a marble stone deteriorate by heating from the outside, it is included that the specimens of marble stones have the part of the strength different. In addition, the surface of the specimen proceeded deterioration and eventually collapsed, which the strain tends to grow big to the stress. Thus, the transformation of specimens (Chemical change) occurred in the internal specimens which had little deterioration caused by high temperature by the compression, which it is included that the stiffness of the specimens became greater. (See Fig.2-3-7 ~Fig.2-3-20)

In addition, there was difference in compressive strength between vertical crystal direction and horizontal crystal direction about the compressive strength of specimen. However, marble stone has the individual difference because marble stone is natural material. Hence this difference caused by each crystal direction is explained as the individual difference of natural material, and then we concluded that this difference of compressive strength of specimen between both crystal directions can be neglected.

2.4 Measuring the dynamic modulus of elasticity

2.4.1 Non-destructive method

We verified whether this non-destructive method could be suitable for the field survey to the actual buildings with the non-destructive test using by the resonant frequency tester. (See Fig.2-4-1) This tester may determine the longitudinal, torsional and flexural or transverse resonant frequencies of the variation of materials. In the present study, prism marble specimens of $100^L \times 100^W \times 200^H$ mm were examined by the longitudinal mode and the torsional mode. (See Appendix 1) As a side note, the specification complies with ASTM C-215, ASTM C-666, BS 1991, and JISA 1127 standard for testing concrete specimens by the resonant frequency method. It is also meets standards to measure modulus of Elasticity of rocks and other materials.



Fig.2-4-1: Resonant frequency tester (E-Meter Mk II)

As marble stone has crystal direction (See Chapter 2.3.2-II), we checked effects of each crystal direction to the modulus of elasticity and the modulus of rigidity. Fig.2-4-2 described the locations of each point of impact and accelerometer.⁽¹¹⁾

Eq.(3) and Eq.(4) describe the formula for calculation the Young's modulus and the modulus of rigidity and table.2-4-1 shows the measurement parameters used in this test.⁽¹²⁾

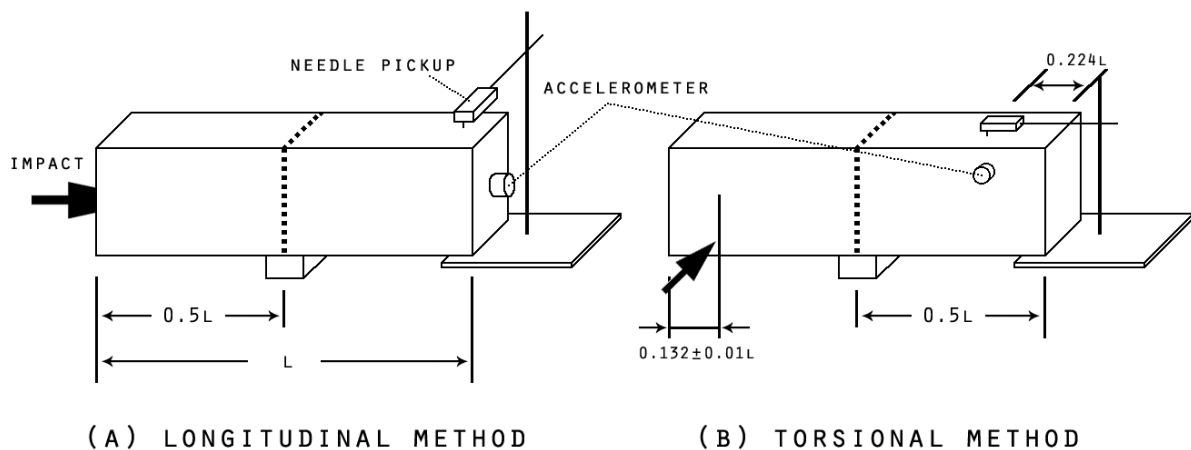


Fig.2-4-2: Locations of driver and impact and accelerometer⁽¹¹⁾

$$E = DM(n')^2 \quad (3)$$

M: Mass of the specimen (kg)

L: Length of the specimen (m)

t,b: Dimensions of cross section of prism (m), $b > t$

$D = 4(L/bt)$ for a prism ($N s^2 / (kg m^2)$)

E: Modulus of Elasticity value (GPa)

(n'): Fundamental longitudinal frequency (Hz)

$$G = BM(n'')^2 \quad (4)$$

G: Modulus of Rigidity value (GPa)

$R = (a/b + b/a) / (4a/b - 2.52(a/b)^2 + 0.21(a/b)^6)$ for a rectangular prism, $b > a$

A: cross-sectional area of test specimen (m^2)

(n''): Fundamental torsional frequency (Hz)

Table.2-4-1: Measurement parameters in the present study

Heating temp.	Sample rate (kHz)	Gain	Sample size	Trigger level
Un-heated	80	10	2048	301
200 °C	80			
400 °C	20			
600 °C	10			
650 °C	Not applicable			

2.4.2 Results and discussions

Fig.2-4-3 described the relation between the modulus of Elasticity obtained by non-destructive method and the compressive strength by NTUA in Athens, Greece. For the detail data of the compressive strength, see Appendix 2. The marble specimen having vertical crystal direction and the compressive strength were correlated on each other, however the specimen having horizontal one didn't have the relation to the compressive strength. From the result, non-destructive method may be suitable to the actual buildings for estimation of the compressive strength as long as the crystal direction is noted.

Fig.2-4-4 and Fig.2-4-5 described the values of modulus of elasticity and modulus of rigidity. Both modulus values have decreased to about 1/2 times caused by heating at 200 °C. Compared to the each modulus value obtained by the compressive tests (See Chapter 2.3), in the result on the specimen having horizontal crystal direction in Case-3, the values of each modulus obtained by non-destructive method is similar to these of each modulus obtained by the compressive tests. In addition, the decrements caused by heating of the modulus of elasticity of the marble specimen having vertical crystal direction obtained by non-destructive method is also similar to these of the modulus of elasticity of the specimen having same crystal direction obtained by the compressive tests. Moreover, the marble specimens having horizontal crystal direction have about 0.4 times lower values of modulus of elasticity than those of the specimens having vertical one. However, we could not find a difference that stood out in the modulus of rigidity value between the specimen having

vertical crystal direction and that having horizontal one. Incidentally, there was also big effect to both modulus values caused by high temperature. The specimens having either crystal direction heated at 650 °C have about 1/5 ~1/10 times lower values of both modulus than un-heated specimens. In a word, both modulus values were confirmed the temperature-dependent.

Fig.2-4-6 shows the each time domain signal of the un-heated marble specimen having vertical crystal direction or horizontal one. The amplitude of the specimen having vertical crystal direction was higher than that of the specimen having horizontal one, however the amplitude of the specimen having horizontal one was hardly attenuated. Moreover, Fig.2-4-7 and Fig.2-4-8 also show the each time domain signal of the specimen having horizontal crystal direction before heating and after heating at 200 °C. In this present study, the sample rate using for the measurement tests by non-destructive method were changed in accordance with heating temperature. Therefore, we compered the results of the specimens heated at 200 °C which were set same conditions of sample rate as un-heated specimens with the results of the un-heated them. Compared with the time domain signal of the specimen heated at 200 °C obtained by longitudinal mode, that of the specimen heated at 200 °C obtained by torsional mode was effected by heating and the amplitude of that was hardly attenuated as well as the un-heated specimen having vertical crystal direction.

Fig.2-4-9 ~Fig.2-4-11 show the Fourier spectrums of un-heated specimen and the specimen heated at 200 °C. In Fig.2-4-7, the frequency obtained by longitudinal mode was about double as the frequency obtained by torsional mode. In addition, the Fourier In addition, in the Fourier spectrum of the specimen heated at 200 °C, each modulus of elasticity and modulus of rigidity was similar as them of the un-heated specimens. However, the Fourier spectrum of the specimen heated at 200 °C obtained by longitudinal mode was about 1/6 times of that of un-heated specimen.

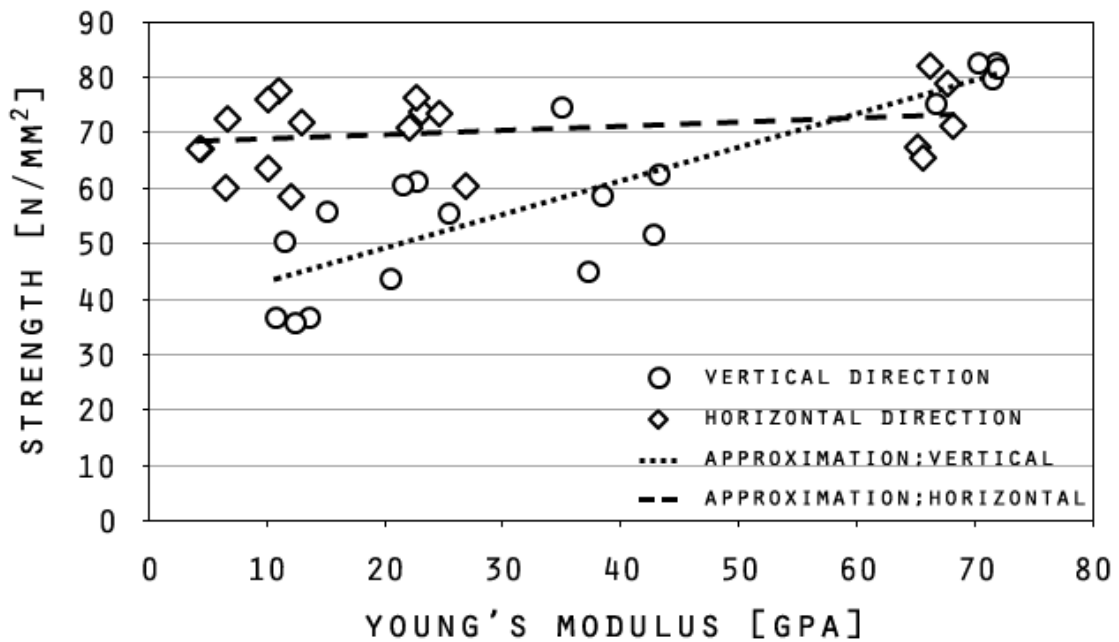


Fig.2-4-3: Relation between Young's modulus and compressive strength

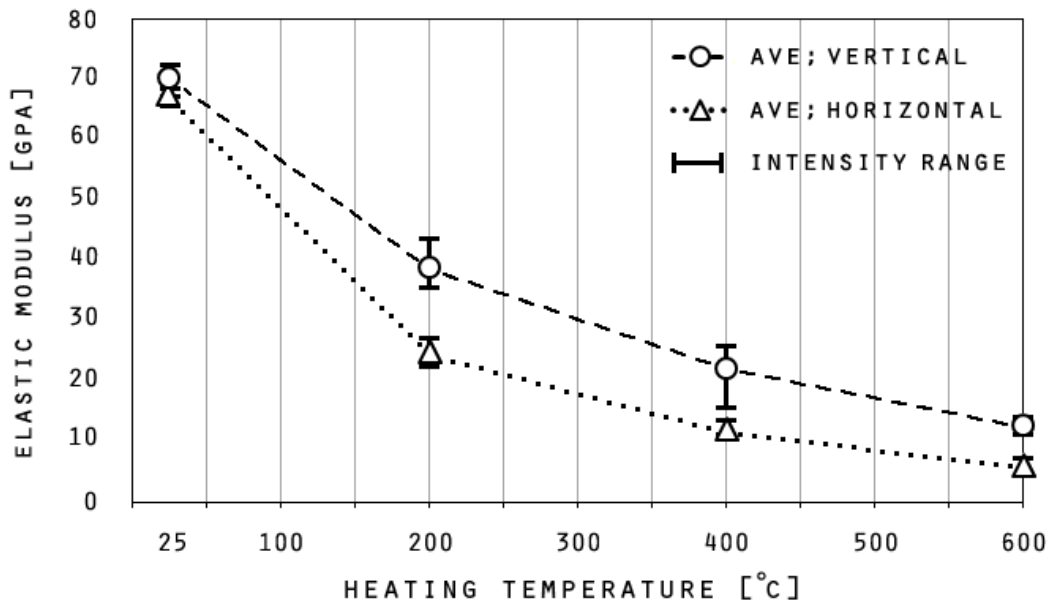


Fig.2-4-4: Elastic modulus of marble in Case-4

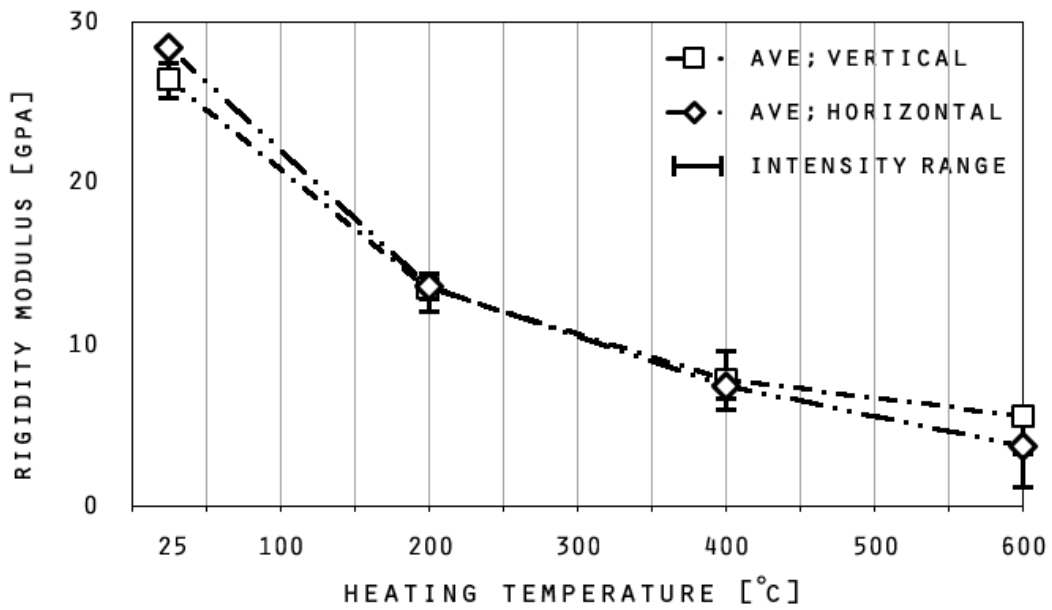


Fig.2-4-5: Rigidity modulus of marble in Case-4

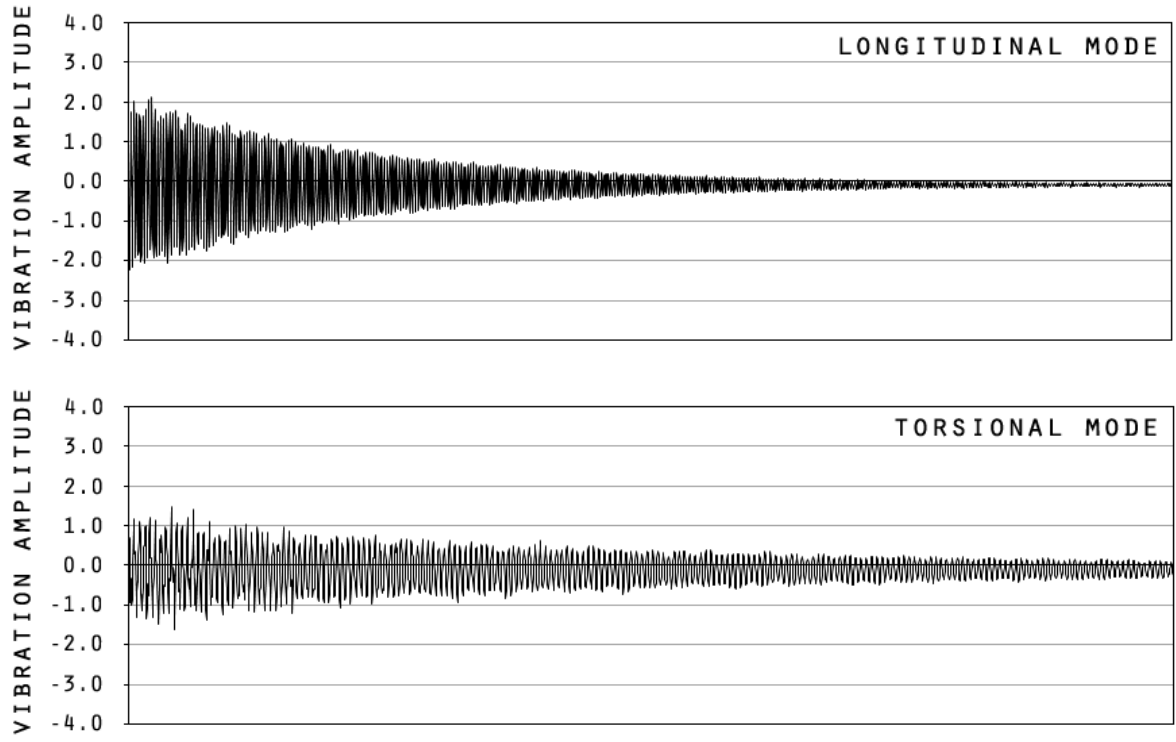


Fig.2-4-6: Time domain signal of the un-heated marble having vertical crystal direction

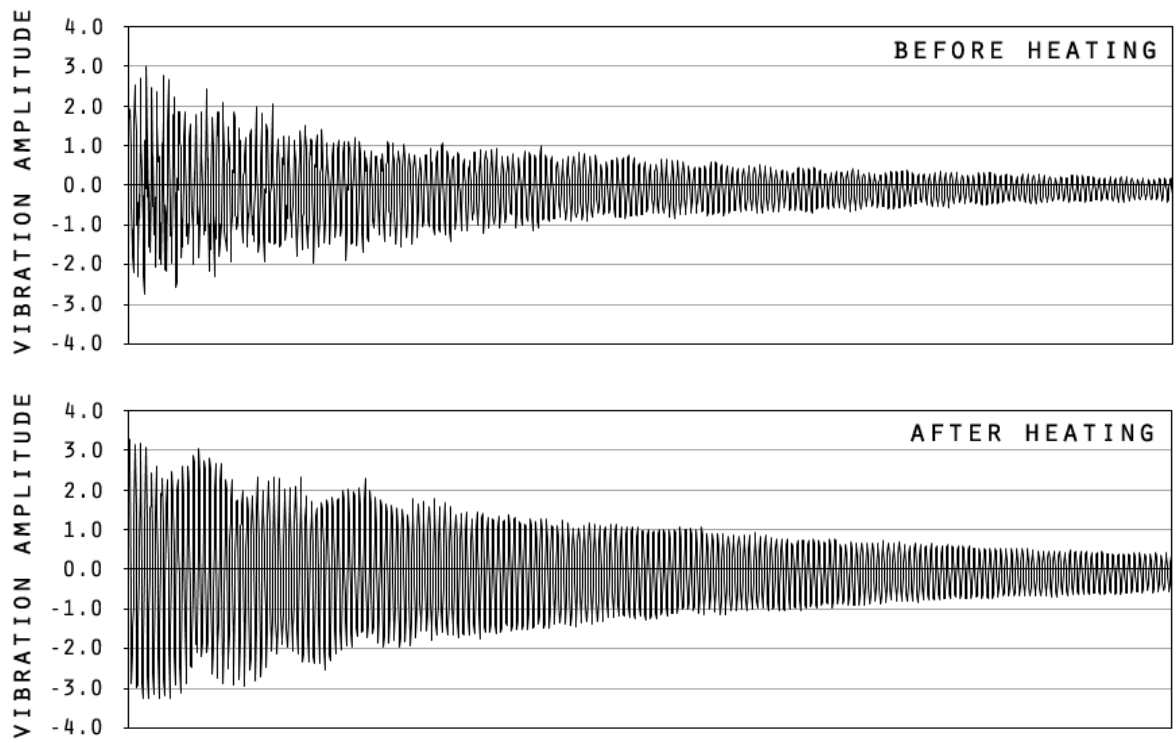


Fig.2-4-7: Time domain signal of the marble heated at 200 °C having horizontal crystal direction by longitudinal mode

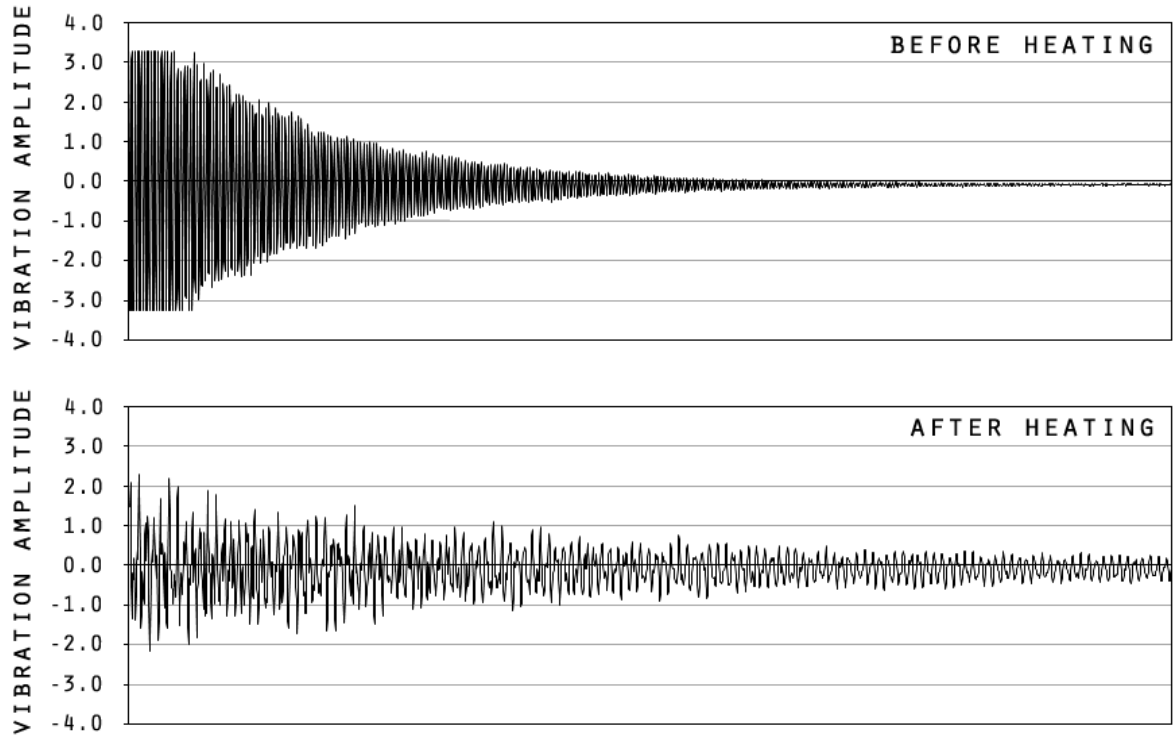


Fig.2-4-8: Time domain signal of the marble heated at 200 °C having horizontal crystal direction by torsional mode

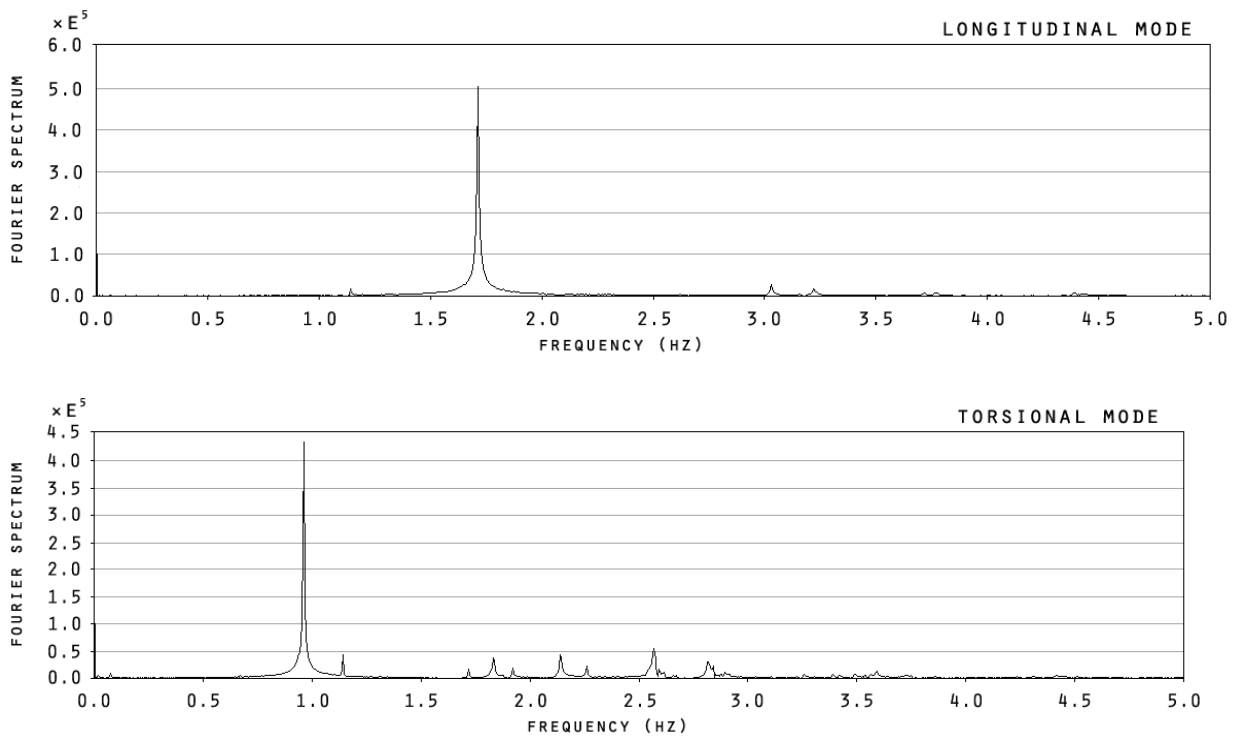


Fig.2-4-9: Fourier spectrum of the un-heated marble having vertical crystal direction

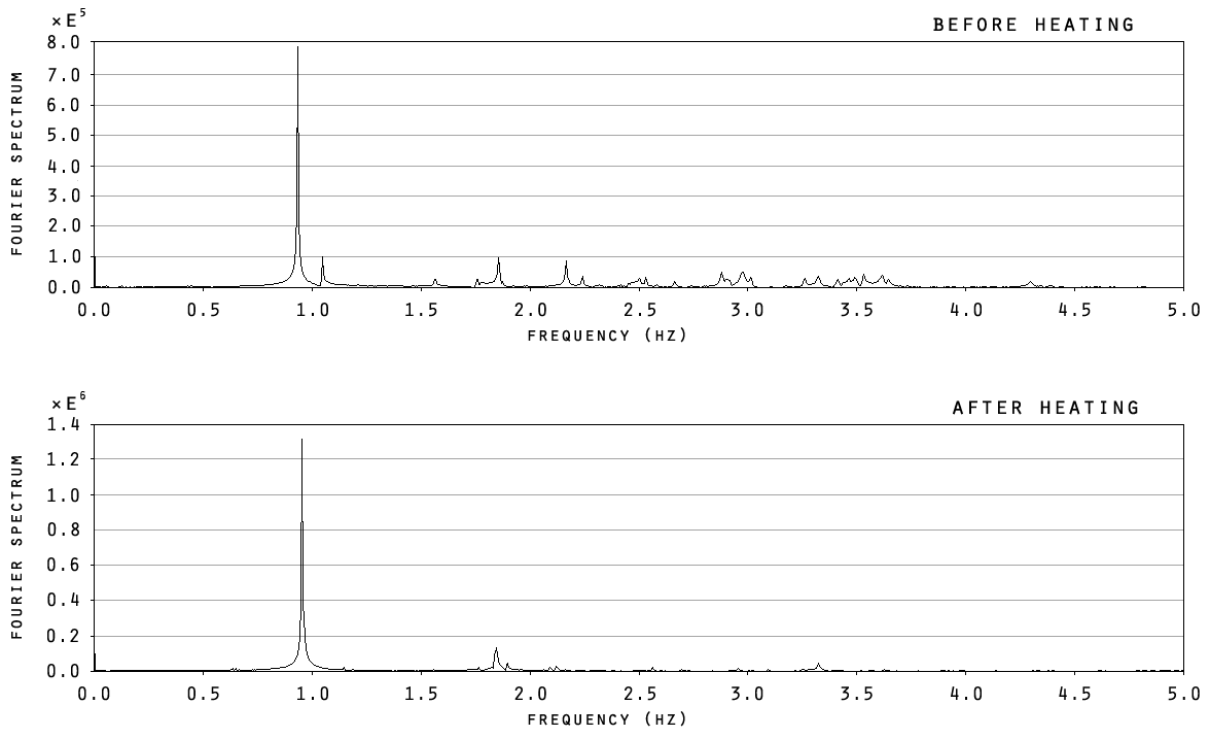


Fig.2-4-10: Fourier spectrum of the marble heated at 200 °C having horizontal crystal direction by longitudinal mode

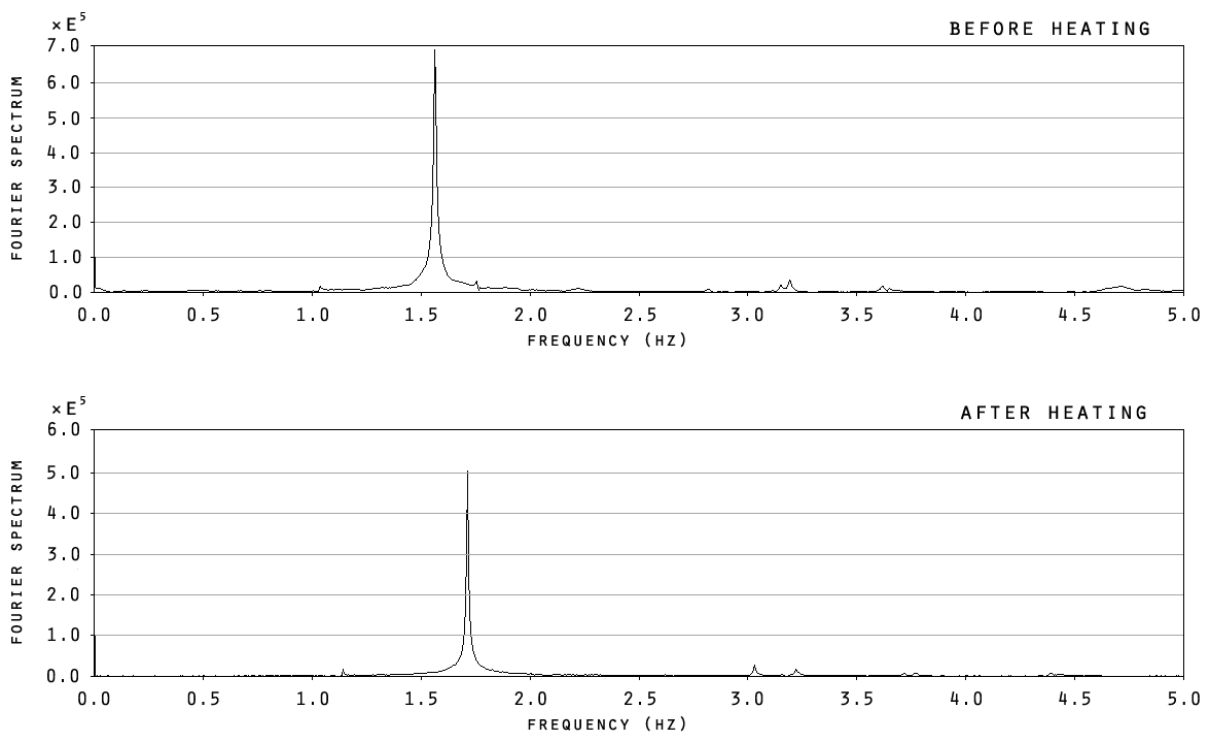


Fig.2-4-11: Fourier spectrum of the marble heated at 200 °C having horizontal crystal direction by torsional mode

CHAPTER 3. THERMAL AND CHEMICAL ANALYSES

3.1 Outlines of thermal analyses

Both un-heated marble specimens and the specimens heated at 800 °C and 1,000 °C were analyzed by Thermal Gravimeter and Differential Thermal Analysis (TG-DTA), X-ray Diffraction and Electron Probe Microanalysis (EPMA) in Mie, Japan. By these analyses, the degree of de-carbonation by high temperature and the compressive strength were evaluated. Moreover, we applied Hot-wire method and Thermal mechanical analysis to the marble specimens for getting the thermal conductivity and thermal expansion rate of marble. In addition, the analyzing about these two tests was consigned to the NIPPON STEEL & SUMIKIN TECHNOLOGY Co., Ltd.

3.1.1 Thermal gravimeter and differential thermal analysis (TG-DTA)

Fig.3-1-1 shows the experimental setup using for TG-DTA. Both un-heated specimens and the specimens heated at 800 °C and 1,000 °C were analyzed by TG-DTA.

Thermal gravimetric is provided for thermal analysis. Changes of physical and chemical properties of materials can be measured as a function of increasing temperature with constant heating rate, or as a function of time with constant temperature and/or constant mass loss.

In this analysis, reference sample was alumina sample.

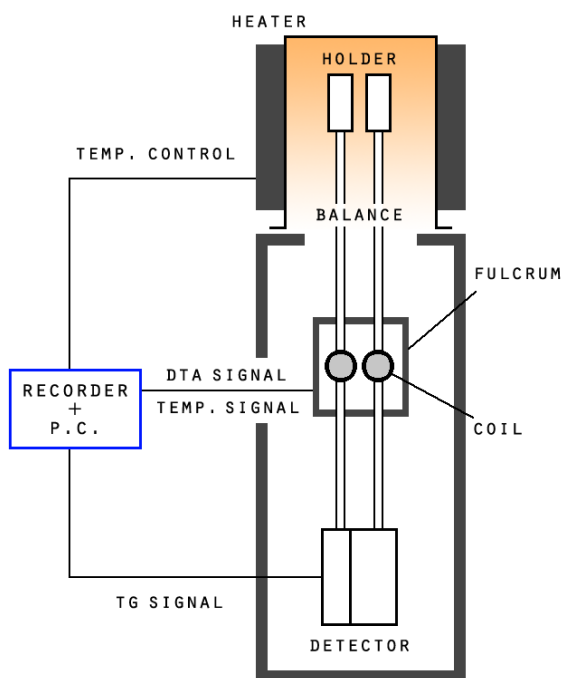


Fig.3-1-1: Experimental setup

3.1.2 X-ray diffraction test

Fig.3-1-2 shows the micro X-ray diffraction detector using this test. X-ray diffraction test is used for identifying the atomic and molecular structure of a crystal, in which the crystalline atoms cause a beam of incident X-rays to diffract into many specific directions. From this electron density, the mean positions of the atoms in the crystal can be determined, as well as their chemical bonds, their disorder and various other information.



Fig.3-1-2: Experimental setup

3.1.3 Election probe microanalysis (EPMA)

Fig.3-1-3 shows the machine used for making color maps of calcium. Electron micro probe analyzer is used for non-destructively test of the chemical composition of small volumes of solid materials. It works similarly to a scanning electron microscope. This test enables us to determine the abundances of elements present within small sample volumes (typically 10-30 cubic micrometers or less).

In this analysis, marble specimens were treated with air purge by using a vacuum pump for 48 hours.



Fig.3-1-3: Experimental setup

3.1.4 Hot-wire method

The hot wire method (JIS R2251-1 or ISO8894-1) is a standard transient dynamic technique based on the measurement of the temperature rise in a defined distance from a linear heat source (heat wire) embedded in the test material. In this method, if flowing a constant current to an infinite thin and long wire inside an infinite long specimen, the radial heat flow around the wire occurs. (See Fig.3-1-4) In addition, the variation of temperature of a wire on surface depends on the thermal conductivity of specimen, and if the variation of temperature of this wire is measured, we can measure thermal conductivity of the specimen.

In the present study, we measured the thermal conductivity of marble at R.T. and 100 °C ~600 °C by using the marble specimen whose size was $230^L \times 110^W \times 37^t$ mm.

As for calculation procedure of the thermal conductivity, if the heat source is assumed to have a constant and uniform output along the length of test sample, the thermal conductivity can be derived directly from the resulting change in the temperature over a known time interval. (See Fig.3-1-5)

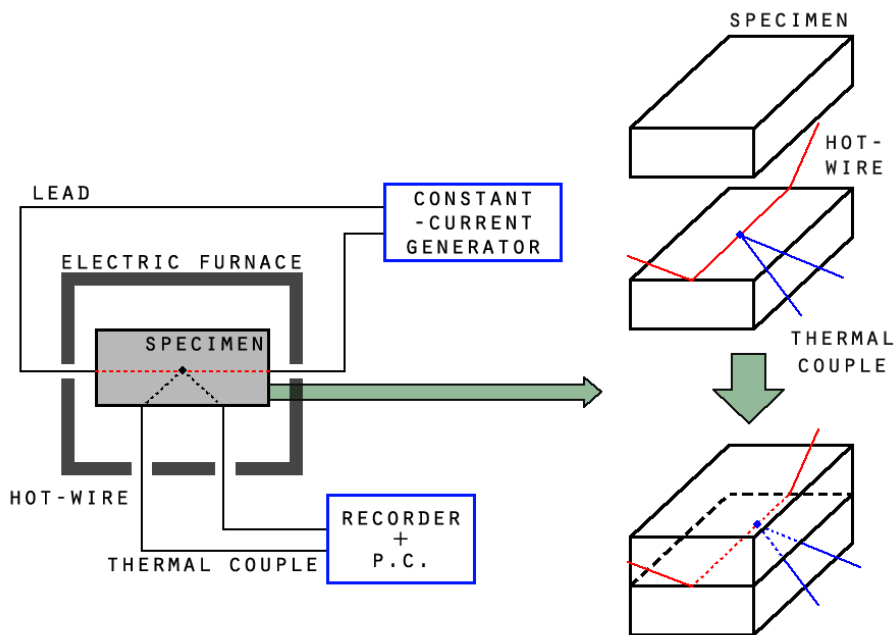


Fig.3-1-4: Experimental setup

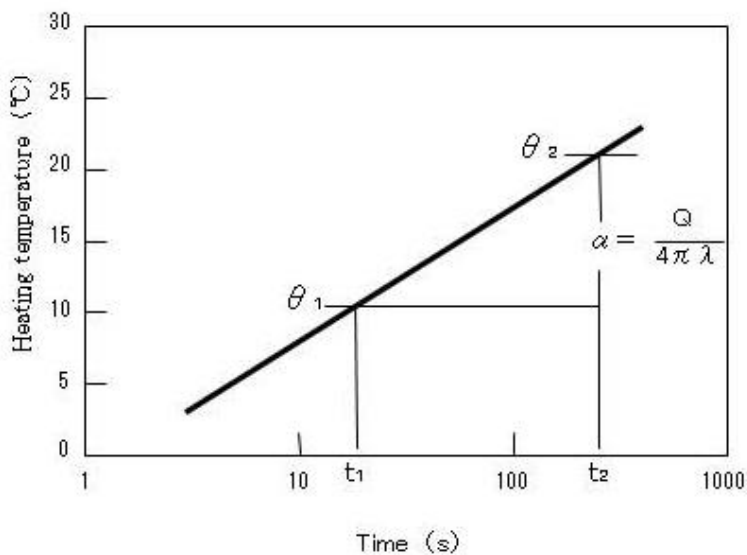


Fig.3-1-5: Temperature rising curve

$$\lambda = \frac{I^2 R}{4 \pi} \cdot \frac{\ln \frac{t_2}{t_1}}{\theta_2 - \theta_1} \quad (\text{W} / (\text{m} \cdot \text{K}))$$

(The formula for thermal conductivity)

λ : Thermal conductivity of sample (W/(m·K))

I: Current value (A)

R: Resistance of heat-wire (Ω/m)

t_1, t_2 : Measured time length (min)

θ_1, θ_2 : Temperature at t_1 and t_2 ($^{\circ}\text{C}$)

3.1.5 Thermal mechanical analysis

TMA (Thermal Mechanical Analysis) is the method for measuring the deformation using by the aperiodic load with changing temperature of material controlled by the program. (See Fig.3-1-6) In general, the result data obtained by TMA is just the rate of change of the dimension of the specimen. Therefore, setting the adequate mode each time lets you to get the numerical analysis data of thermal expansion, thermal shrinkage or mechanical material properties of something related in temperature.

In this analysis, we set the compressive probe mode to the control program, and then measured the thermal expansion rate of marble specimen ($135^L \times 200^W \times 20^t$ mm) between at the temperature of R.T. $\sim 600^{\circ}\text{C} \sim 100^{\circ}\text{C}$. In addition, we set $2.5^{\circ}\text{C}/\text{min}$ to the temperature rising rate of the furnace.

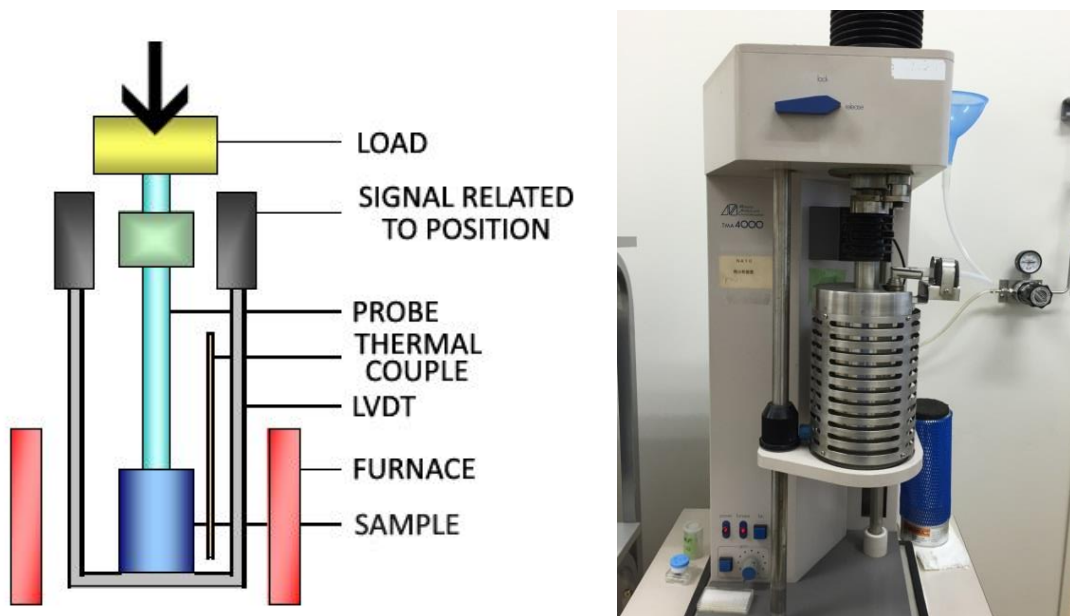


Fig. 3-1-6: Fundamentals and applications of TMA

3.2 Results and discussions

3.2.1 TG-DTA

Fig.3-2-1 shows the results of Thermal gravimeter (TG) and Differential thermal analysis (DTA). In this figure, weight loss indicates CO₂ releasing by decomposition of CaCO₃.

- (A) Un-heated marble specimens have a rapid reduction of TG-curve around 800°C. In the DTA-curve, downward convex curve around 750 °C shows endothermic peak.
- (B) The marble specimens heated at 800 °C have an endothermic peak (-25 %: value of TG) and a dewatering peak of Ca (OH)₂ (-10 %: value of TG). However, the specimens heated at 1,000 °C have not the curve of dewatering reaction.
- (C) The marble specimens heated at 1,000 °C did neither show any thermal gravimetry (TG) variation nor a differential thermal peak (DTA).

Fig.4-2-1 (A) shows releasing of CO₂, when the endothermic reaction occurred at the same time. From the result, the specimens heated at 1,000 °C did not have the thermal reaction of CaCO₃ because such chemical reaction had already completely finished. Moreover, it seemed that the peak of DTA-curve was caused by generation of CaO. In addition, the specimens heated at 800 °C had the curve of dewatering reaction caused by Ca(OH)₂. (See Fig.4-2-1 (B)) However, the specimen heated at 1,000 °C did not show such characterized curve, therefore, it was considered that moisture control by using the desiccators was failed while cooling the marble specimens heated at 800 °C.

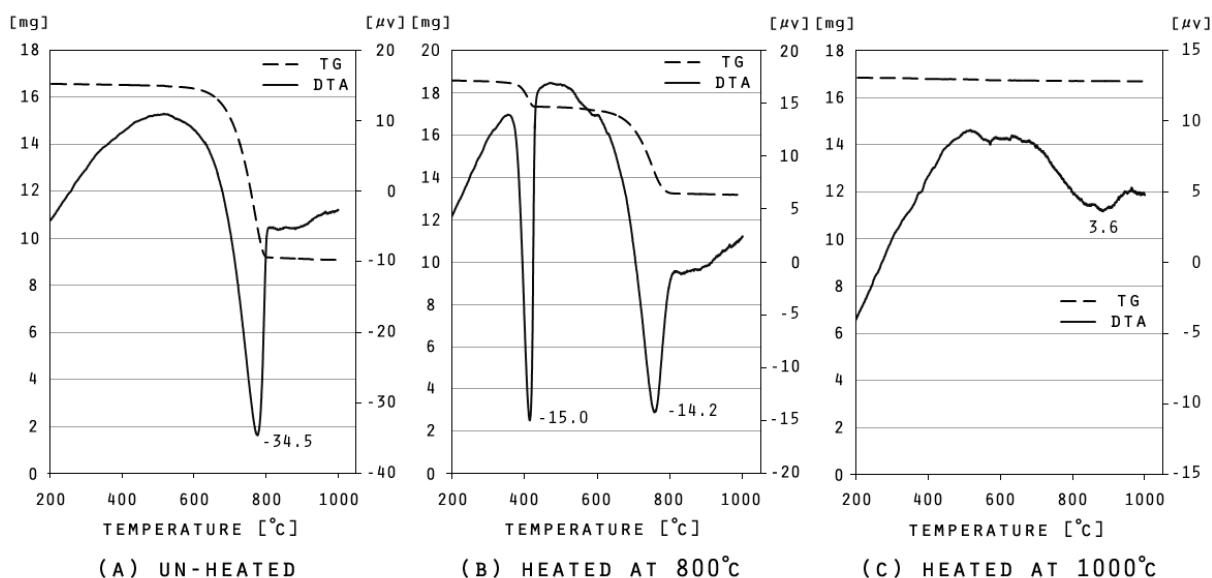


Fig.3-2-1: TG-DTA

3.2.2 X-ray diffraction

Fig 4-2-2 shows the X-ray diffraction in the temperature range between R.T and 1,000 °C. The peak corresponding to CaCO₃ (calcite) can be found along the diffraction angle line of the samples heated at 800 °C and at the temperature lower than 650 °C, indicating that chemical reaction did not occur at the lower temperature than 800 °C. In addition, the samples heated at 800°C had lower diffractive strength and response of CaO. This result shows that samples heated at 800 °C reached to middle of the chemical reaction of CaCO₃. Furthermore, there is no peak of CaCO₃ along the diffraction angle line of the samples heated at 1,000 °C. However, the peak corresponding to CaO can be found along the diffraction angle line at the higher angle.

As a side note, “diffraction intensity” doesn’t mean amount of material.

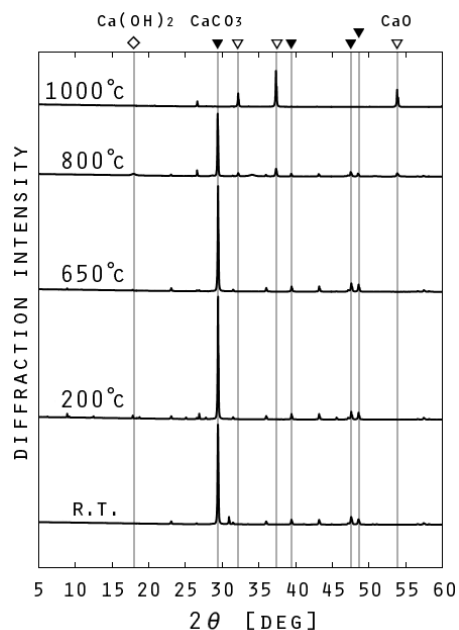


Fig.3-2-2: Results of XRD

3.2.3 EPMA

Fig 4-2-3 shows the carbon color map of a marble specimen heated at 650 °C by mapping analysis of EPMA. In this map, red color zone shows high carbon density and blue color zone shows low carbon density. In this figure, the thermal decomposition occurred by heating at 650 °C. In addition, it can be recognized that inner part of the specimen contained were carbon more than surface of specimen. This result shows the reaction of decarburization. The chemical reaction started from surface of the specimen because it was easier to release CO₂ from surface of specimen than from the inner part of the specimen.

Moreover, the decarburization area (CaO) is very fragile. In the internal of specimen, more progressive thermal reaction might have occurred than on surface of specimen. In other words, there might be more strength difference between surface and internal of marble specimen. Hence, the compressive strength variation might cause the characteristic failure mode as shown in our previous study.⁽¹³⁾

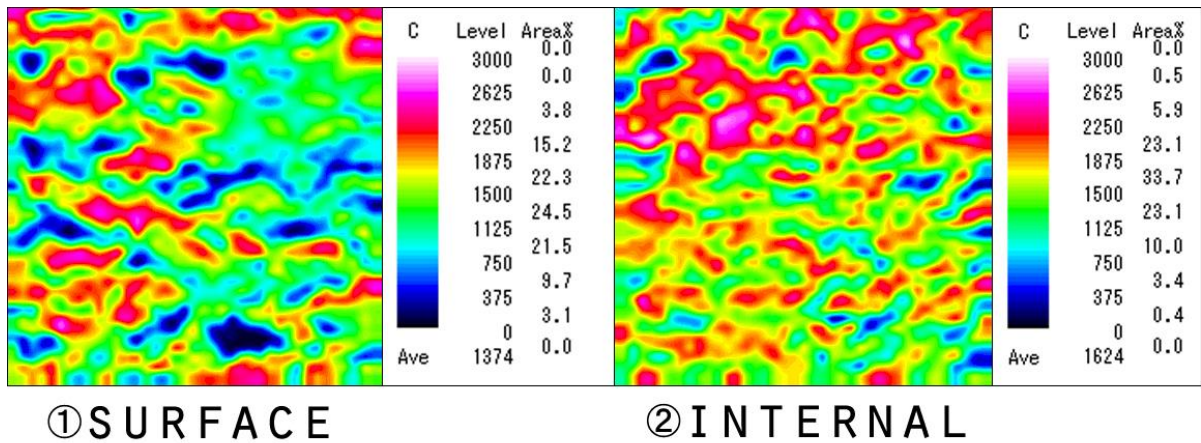


Fig.3-2-3: Carbon color map by EPMA

3.2.4 Thermal conductivity

Fig.3-2-4 and Table.3-2-1 show the result of measurement of thermal conductivity. Fig. 3-2-5 ~Fig. 3-2-25 shows the temperature rising curve used for evaluation.

In these results, the heating temperature and the thermal conductivity of marble have a correlation that the higher heating temperature is, the lower the thermal conductivity of marble become. Moreover, the thermal conductivities of marble heated at less than 200 °C decreased steeply, on the other hand, lowering thermal conductivity rate of marble heated at over 200 °C is slow.

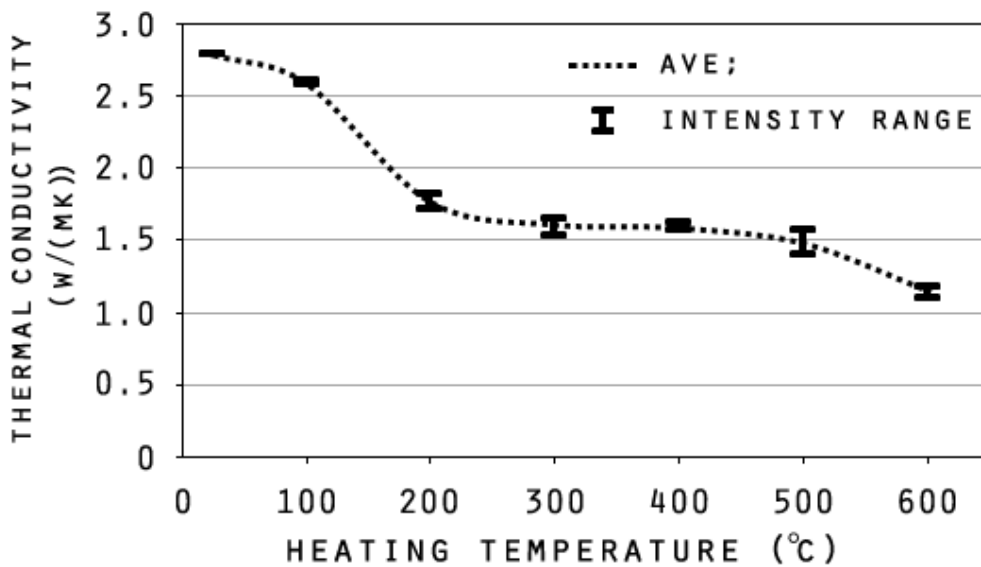


Fig.3-2-4: relation between temperature and thermal conductivity of marble

Table.3-2-1: Thermal conductivity of marble

Measurement Temperature (°C)	Number	Evaluate section (sec)		Temperature (°C)		Average Temperature (°C)	Current value (A)	Resistance (Ω/m)	Thermal conductivity (W/(m · K))	
		t ₁	t ₂	θ_1	θ_2				Result	Ave;
RT	n=1	30	300	35.2	36.3	35.5	2.39	2.93	2.79	2.79
	n=2	30	300	35.2	36.3	35.3	2.39	2.93	2.79	
	n=3	30	300	39.0	40.1	39.5	2.38	2.95	2.79	
100	n=1	30	300	102.0	103.3	102.4	2.38	3.23	2.58	2.59
	n=2	30	300	102.4	103.7	103.0	2.38	3.23	2.58	
	n=3	30	300	104.8	106.1	105.4	2.39	3.24	2.61	
200	n=1	30	300	202.1	204.3	202.8	2.39	3.66	1.74	1.77
	n=2	30	300	200.3	202.5	201.0	2.39	3.66	1.74	
	n=3	30	300	201.1	203.2	202.2	2.39	3.66	1.82	
300	n=1	30	300	303.1	305.9	304.2	2.39	4.09	1.53	1.61
	n=2	30	300	303.4	306.0	304.4	2.39	4.09	1.65	
	n=3	30	300	303.6	306.2	304.6	2.39	4.09	1.65	
400	n=1	30	300	401.1	404.0	402.2	2.39	4.49	1.62	1.59
	n=2	30	300	402.1	405.1	403.5	2.39	4.50	1.57	
	n=3	30	300	403.0	406.0	404.4	2.39	4.50	1.57	
500	n=1	30	300	507.6	511.4	509.7	2.39	4.92	1.40	1.48
	n=2	30	300	508.4	511.9	510.1	2.39	4.92	1.47	
	n=3	30	300	509.1	512.6	510.7	2.39	4.92	1.57	
600	n=1	30	300	604.3	609.3	606.7	2.39	5.29	1.10	1.15
	n=2	30	300	605.8	610.5	608.1	2.39	5.29	1.17	
	n=3	30	300	607.8	612.5	610.4	2.39	5.30	1.18	

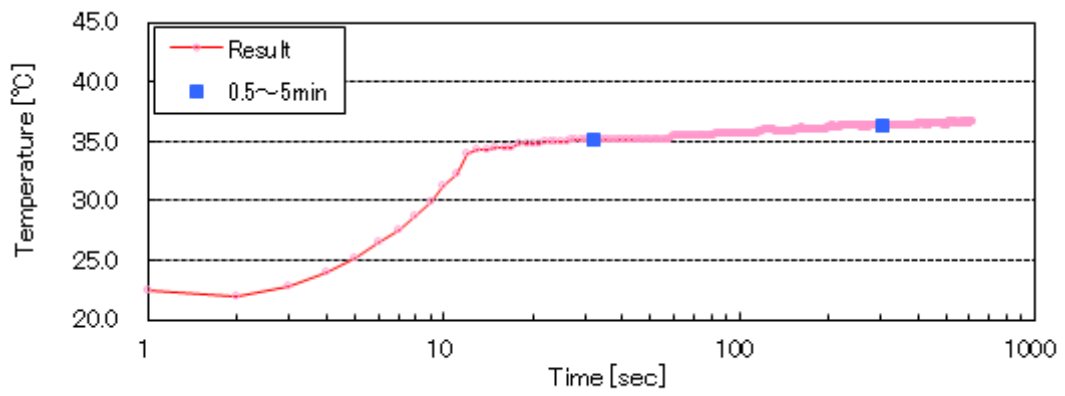


Fig.3-2-5: Temperature rising curve (estimated temp.: R.T.)(n=1)

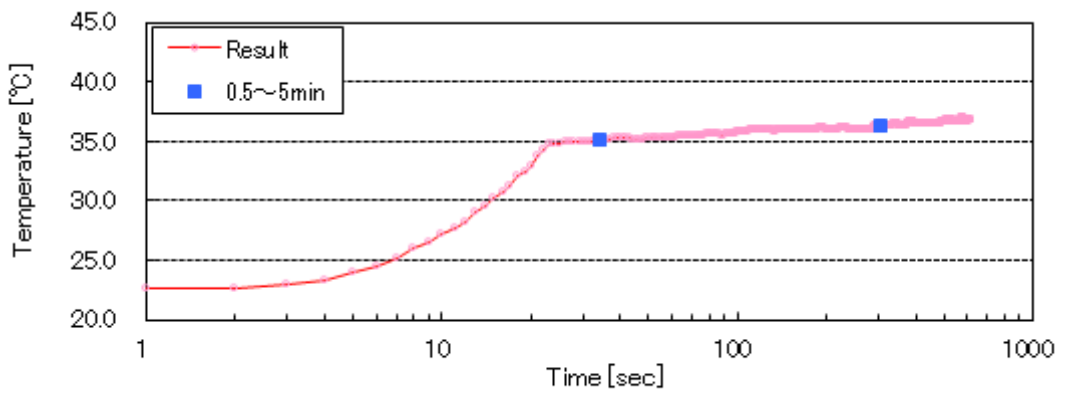


Fig.3-2-6: Temperature rising curve (estimated temp.: R.T.)(n=2)

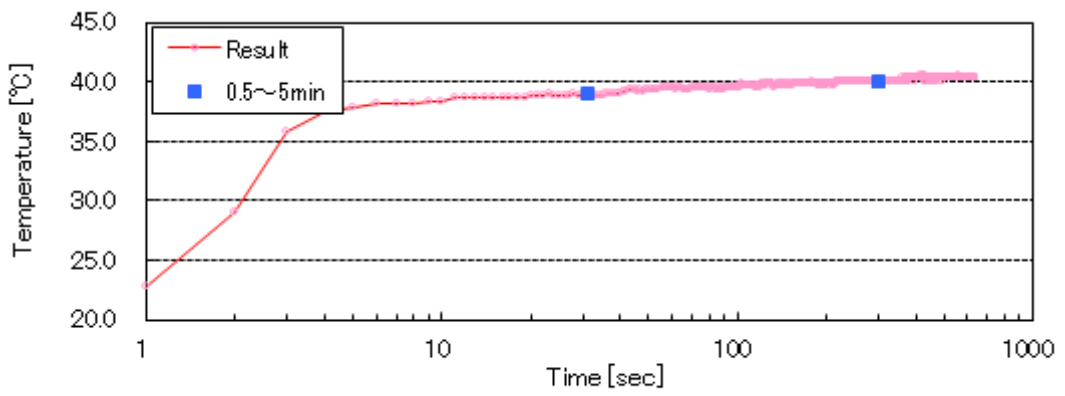


Fig.3-2-7: Temperature rising curve (estimated temp.: R.T.)(n=3)

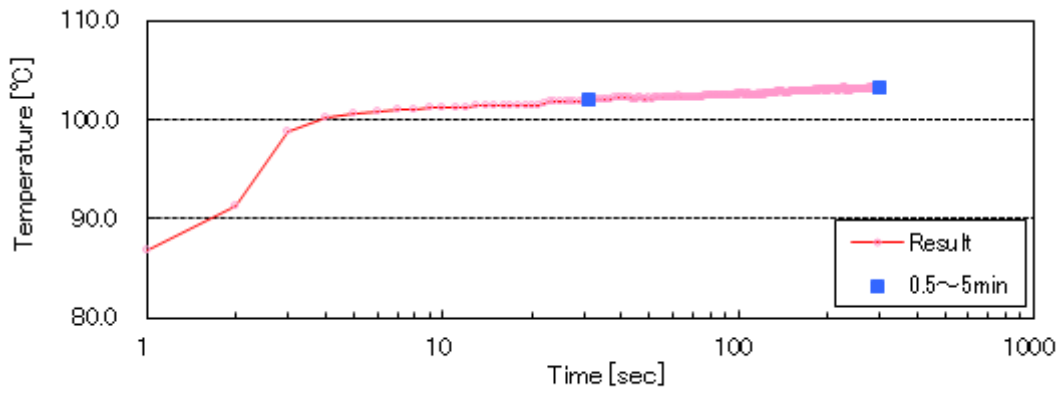


Fig.3-2-8: Temperature rising curve (estimated temp.: 100 °C)(n=1)

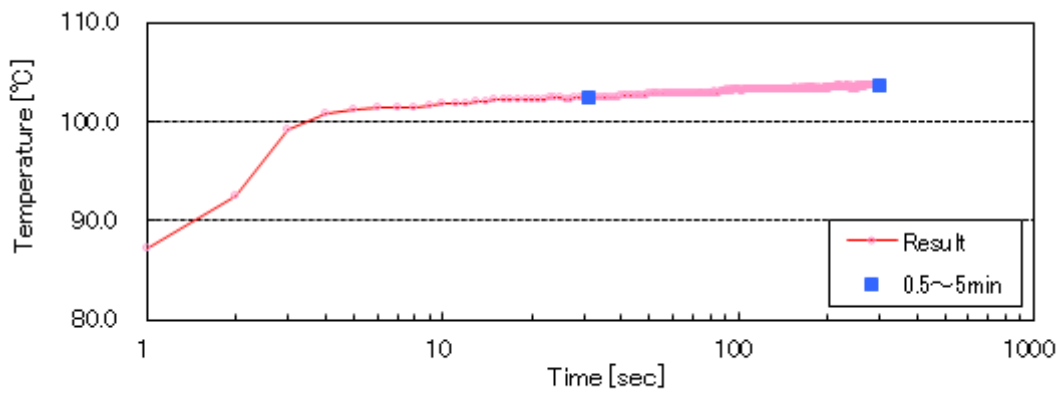


Fig.3-2-9: Temperature rising curve (estimated temp.: 100 °C)(n=2)

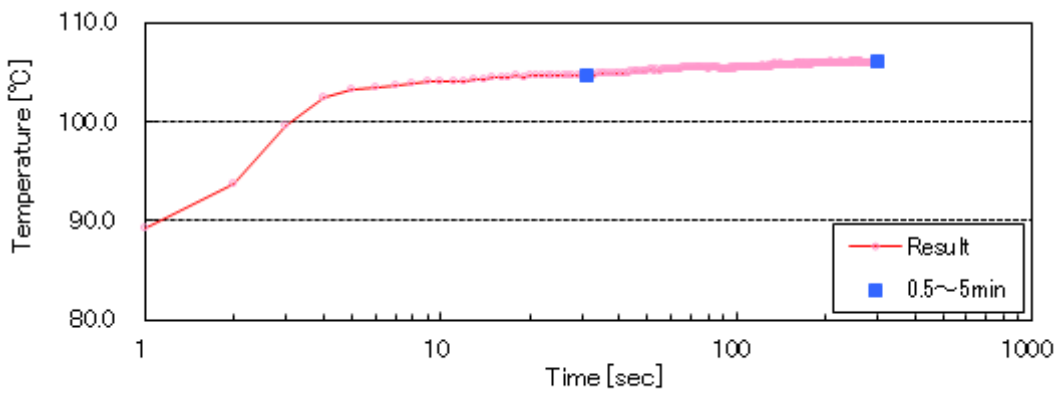


Fig.3-2-10: Temperature rising curve (estimated temp.: 100 °C)(n=3)

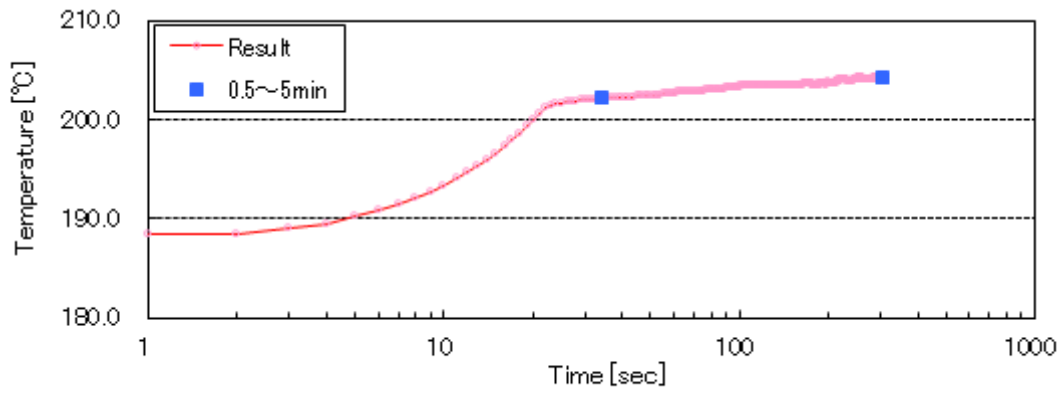


Fig.3-2-11: Temperature rising curve (estimated temp.: 200 °C)(n=1)

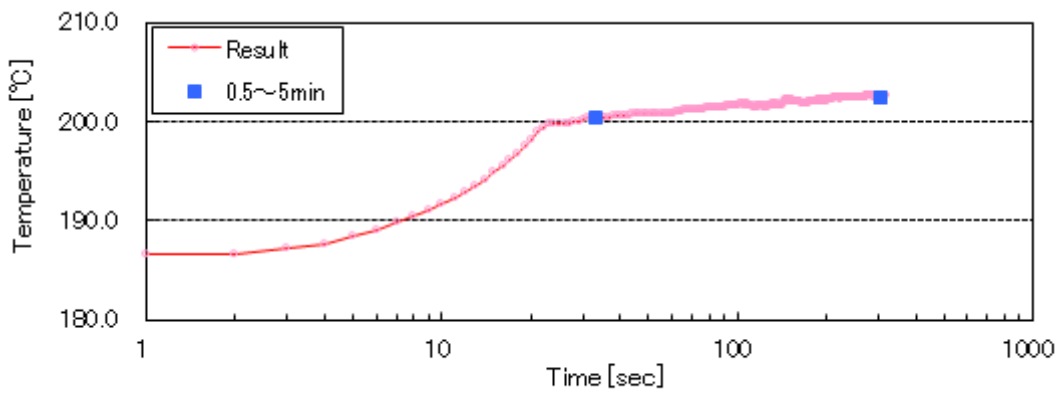


Fig.3-2-12: Temperature rising curve (estimated temp.: 200 °C)(n=2)

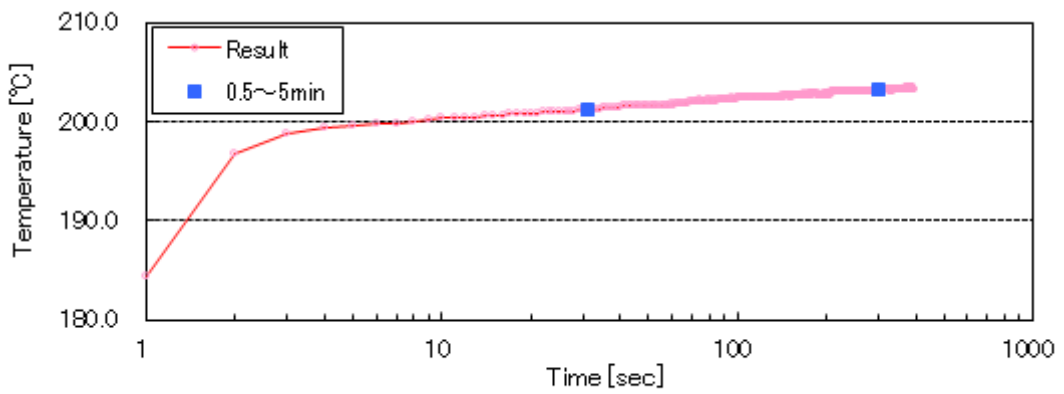


Fig.3-2-13: Temperature rising curve (estimated temp.: 200 °C)(n=3)

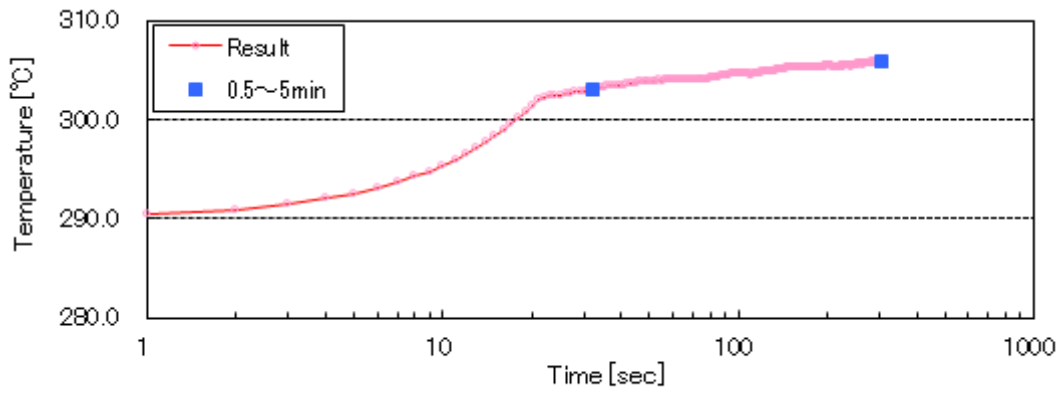


Fig.3-2-14: Temperature rising curve (estimated temp.: 300 °C)(n=1)

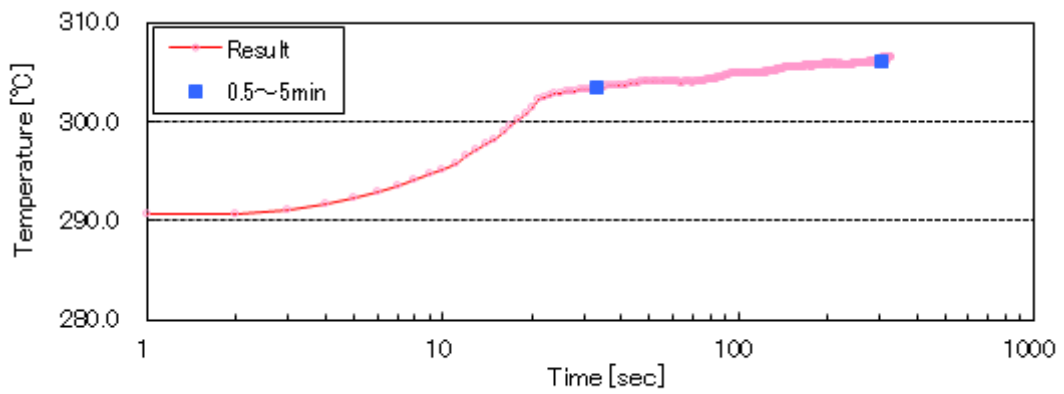


Fig.3-2-15: Temperature rising curve (estimated temp.: 300 °C)(n=2)

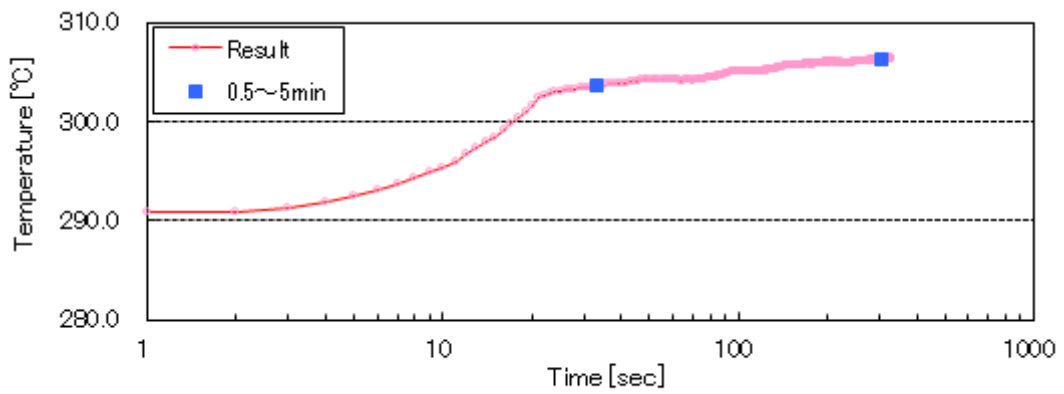


Fig.3-2-16: Temperature rising curve (estimated temp.: 300 °C)(n=3)

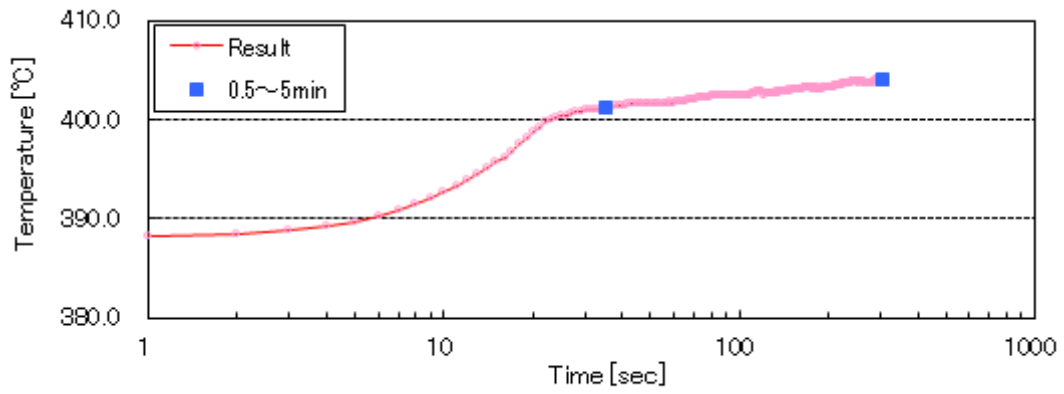


Fig.3-2-17: Temperature rising curve (estimated temp.: 400 °C)(n=1)

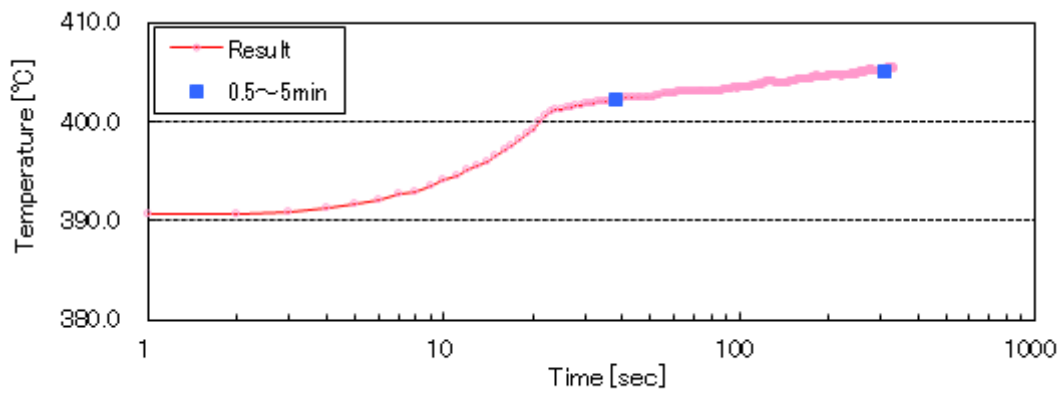


Fig.3-2-18: Temperature rising curve (estimated temp.: 400 °C)(n=2)

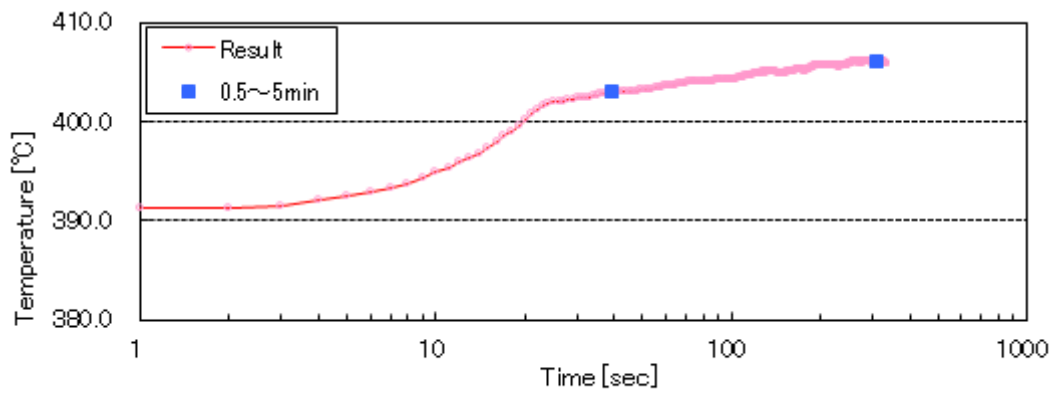


Fig.3-2-19: Temperature rising curve (estimated temp.: 400 °C)(n=3)

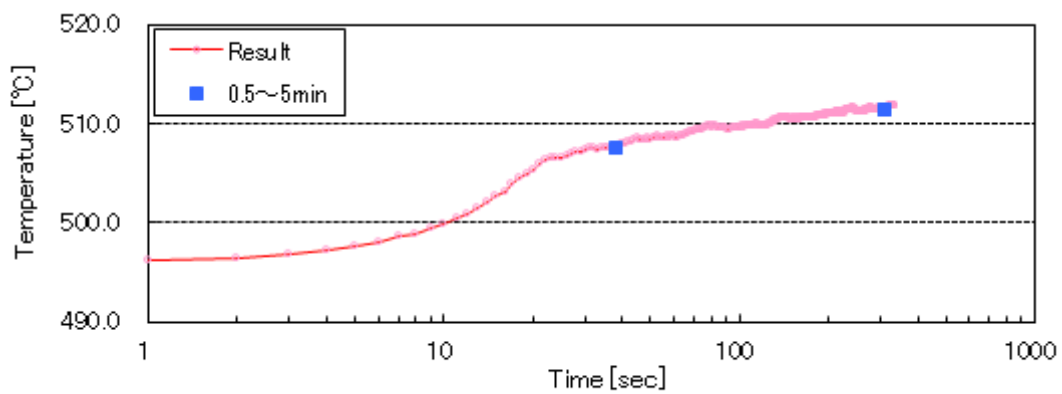


Fig.3-2-20: Temperature rising curve (estimated temp.: 500 °C)(n=1)

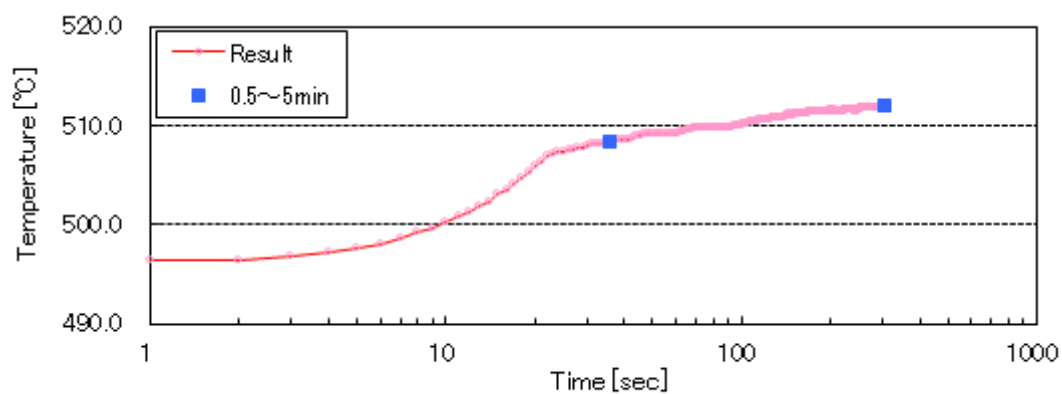


Fig.3-2-21: Temperature rising curve (estimated temp.: 500 °C)(n=2)

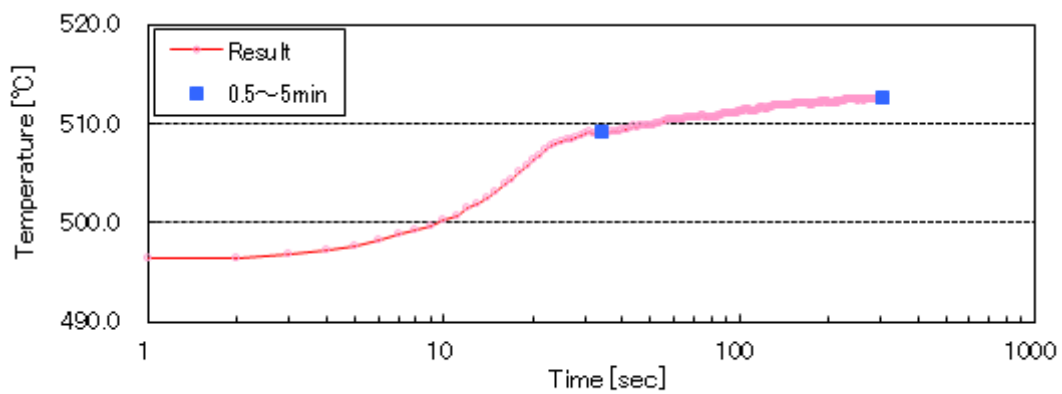


Fig.3-2-22: Temperature rising curve (estimated temp.: 500 °C)(n=3)

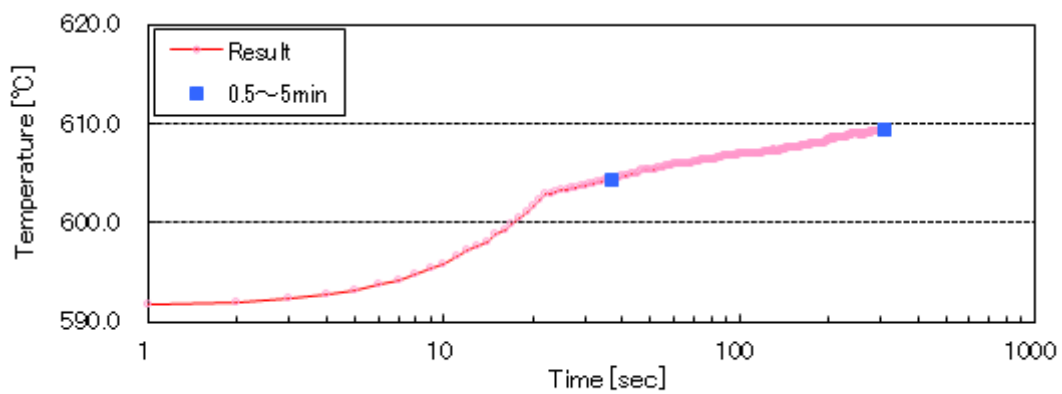


Fig.3-2-23: Temperature rising curve (estimated temp.: 600 °C)(n=1)

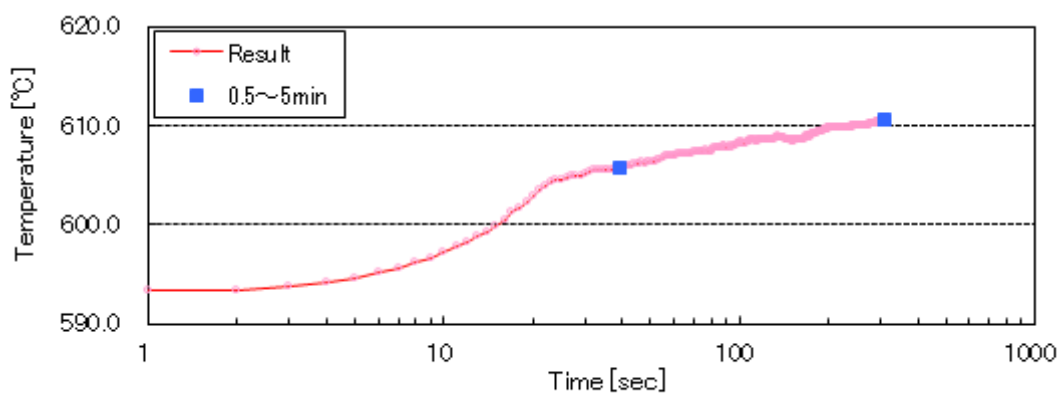


Fig.3-2-24: Temperature rising curve (estimated temp.: 600 °C)(n=2)

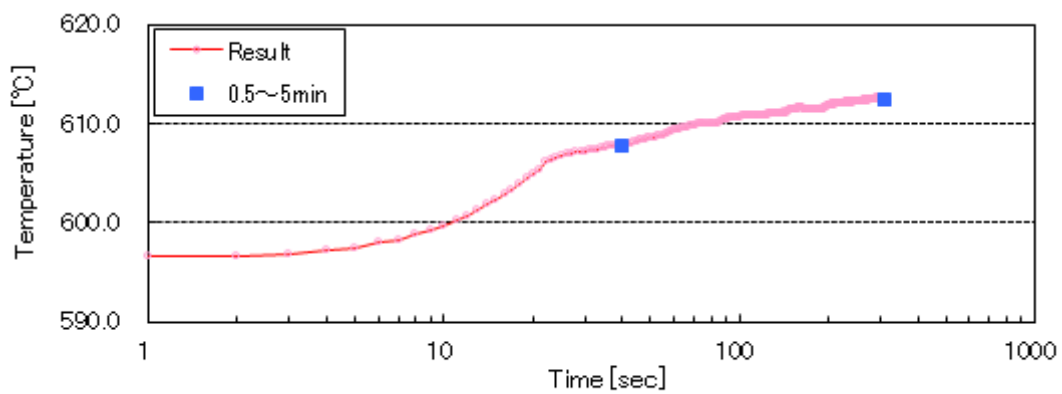


Fig.3-2-25: Temperature rising curve (estimated temp.: 600 °C)(n=3)

3.2.5 Thermal expansion rate

Table. 3-2-2 and Fig. 3-2-26 show the results of the thermal expansion rate and coefficient of marble by TMA.

In these results, thermal expansion rate of marble heated at between 20 °C and 600°C is correlated with heating temperature, as well as thermal conductivity (See 4.2.4). Moreover, it can be confirmed that marble has the irreversibility of thermal expansion. This can happen if CaCO₃ that is the basic content of marble was changing to CaO during heating at the high temperature, because CaCO₃ and CaO are another materials, and in this case, when we need the numerical data of the thermal expansion of marble heated over 600 °C, we should conduct another test by using TMA for marble specimens heated at 600 °C.

Table.3-2-2: Thermal expansion rate and coefficient of marble

Temperature (°C)	Thermal expansion (%)	Expansion coefficient (1/°C)
20	0.000	3.0 E ⁻⁰⁶
100	0.035	5.0 E ⁻⁰⁶
200	0.182	1.07 E ⁻⁰⁵
300	0.365	1.35 E ⁻⁰⁵
400	0.567	1.53 E ⁻⁰⁵
500	0.815	1.73 E ⁻⁰⁵
600	1.094	1.92 E ⁻⁰⁵
500	0.903	1.92 E ⁻⁰⁵
400	0.764	2.07 E ⁻⁰⁵
300	0.686	2.54 E ⁻⁰⁵
200	0.638	3.75 E ⁻⁰⁵
100	0.626	8.94 E ⁻⁰⁵

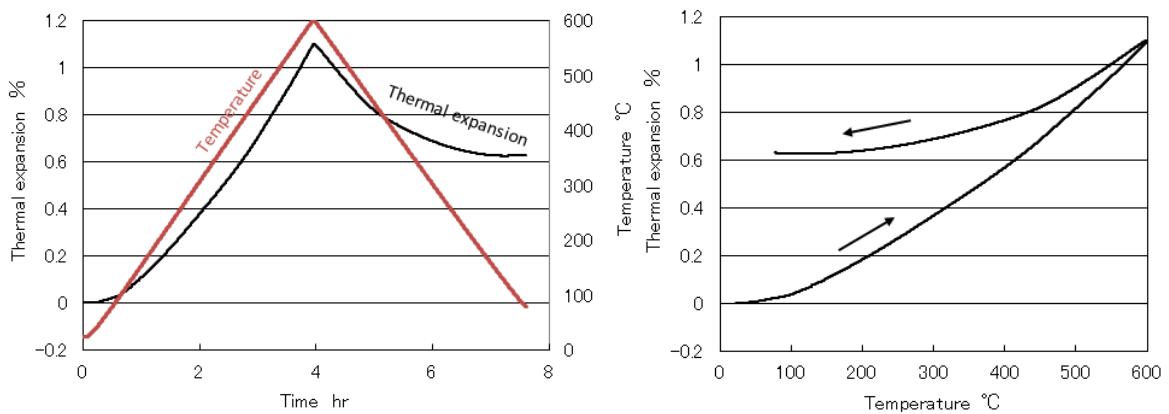


Fig.3-2-26: Thermal expansion of marble

CHAPTER 4. THERMAL ANALYSES

In this chapter, we performed the non-stationary heat conduction analysis and thermal stress analysis by finite element method on the computer utilizing the results presented in the previous chapters as the reference modeling data. The purpose of those analyses was to grasp hourly variation of a marble dram with time history simulation of temperature of whole a multi-dram column. According to the result of heat conduction analysis, we analyzed the thermal stress on the marble multi-dram column. We estimated the axial force variation, maximum stress and the depth of the cracks development of the column caused by fire with the result of thermal stress analysis. Mesh generation method on the modeling influences the accuracy of analysis result in the finite element method. Therefore, we made the simplified modeling for making appropriate mesh on the modeling and lower calculation cost.

The convection coefficient and emissivity rate of marble as input condition using for the heat conduction analysis were set based on the result of fitting analysis (thermal transmitting analysis) using the temperature elevation curve of oven and internal marble specimen obtained by heating tests on Chapter 2.

For the flowchart of thermal analysis, see appendix 4.

4.1 Thermal transmitting analysis

D) Modeling

In the fitting analysis for the convection coefficient and emissivity rate of marble, we made a model as Fig.4-1-1. For the actual dimension data of the structure and the shape of the electric oven, see appendix 5. Moreover, to reproduce the actual experimental conditions on the previous heating tests, we performed the fitting analysis that focused on the temperature elevation curve of the central area in the marble specimen.

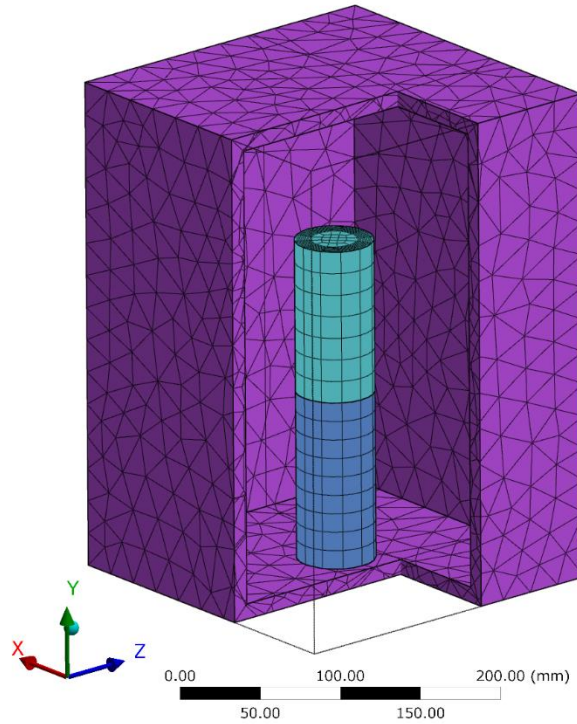


Fig.4-1-1: Model of oven and marble specimen

II) Input conditions of analysis

Nichrome (80Ni-20Cr) was allotted to the oven as the material of the heat source and marble was allotted to the specimens. Table.4-1-1 and Table.4-1-2 show the each physical property value as input conditions. As a side note, See Table.3-2-1 in Chapter 3 for the detail of the thermal conductivity, and See Appendix 6 for the detail of the heat specific. Fig.4-1-2 describes the boundary conditions between models in the fitting analysis. In addition, the temperature rising curve using for the heat source as input condition was the actual temperature rising curve obtained the previous heating test (Case-1) in Chapter 2. (See Fig.4-1-3)

About the emissivity, the radiant heat between marble specimen models was taking into account. Moreover, the correlation of emissivity was set to ‘surface to surface’, and the enclosure type was set to ‘perfect close type’. In the present analysis, we performed the simulations on two temperature cases, 400 °C and 600 °C.

Table.4-1-1: Physical property value as input condition to the heat source⁽¹⁰⁾

Oven			
Temp. (°C)	Thermal conductivity (W/(m °C))	Heat specific (J/(kg °C))	Density (kg/m ³)
0	13	4500	8400
100	14	—	—
300	17	—	—

Table.4-1-2: Physical property value as input condition to the specimen

Marble			
Temp. (°C)	Thermal conductivity (W/(m °C))	Heat specific (J/(kg °C))	Density (kg/m ³)
25	2.79	849.9	2700
100	2.59	945.1	2700
200	1.77	1045.0	2700
300	1.61	1117.4	2700
400	1.59	1159.9	2700
450	—	1182.2	2700
500	1.48	1224.5	2700
550	—	1267.4	2700
600	1.15	1327.6	2600

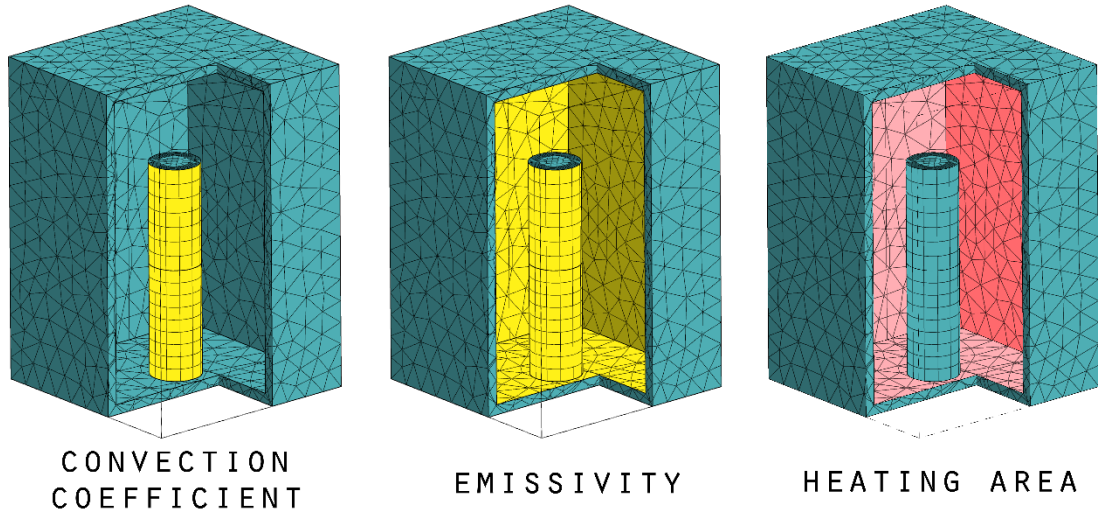


Fig.4-1-2: Boundary conditions for the fitting analysis

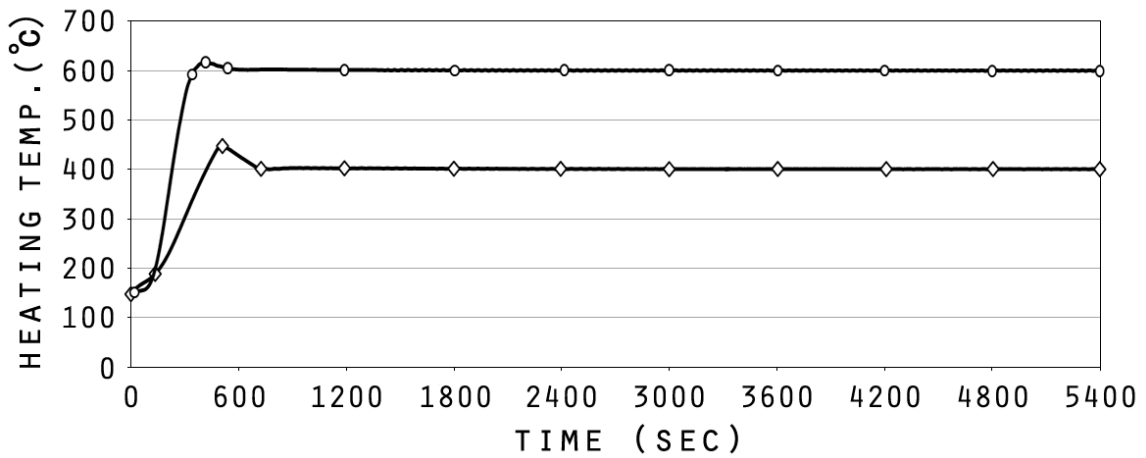


Fig.4-1-3: Temperature rising curve at 400 °C and 600 °C

III) Results and discussions

Fig.4-1-4 describes the point of temperature measurement on the marble specimen model. Fig.4-1-5 and Fig.4-1-6 show the results of the fitting analysis about the convection coefficient at 400 °C, and Fig.4-1-7 and Fig.4-1-8 show the results of that at 600 °C. Temperature rising curves in simulation-C were almost the same value to the experimental value. Moreover, the temperature rising curve at 600 °C was closer to the experimental value than that at 400 °C on the same analysis condition. The numerical values obtained by the fitting analysis are listed Table.4-1-3. From the results of some simulation, the value of emissivity rate affected to the temperature's rising more than the convection coefficient value. Accordingly in the heat conduction analysis for marble dram and multi-dram column, we decided to input those values on the simulation-C obtained by the fitting analysis as the analysis conditions.

Fig.4-1-9 and Fig.4-1-10 indicate images of the heat distributions after 2700 seconds and 5400 seconds from heating start. It can be seen that the model of marble specimen was uniformly heated from the surface. Comparisons of heat distributions after 2700 seconds between at 400 °C and at 600 °C have shown that there was little temperature variation in the heat distribution heated at 600 °C than in that heated at 400 °C.

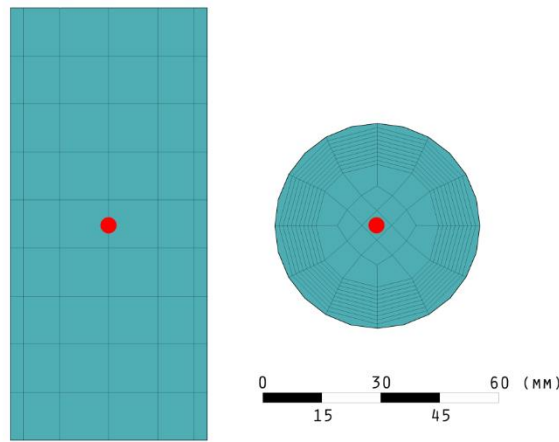


Fig.4-1-4: Measurement point on the modeling of marble specimen

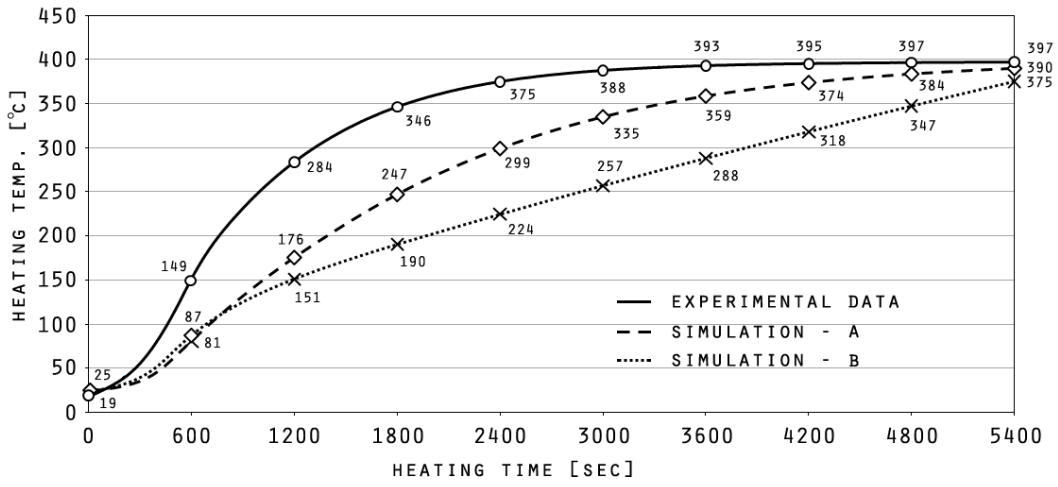


Fig.4-1-5: Temperature rising curve heated at 400 °C in Simulation-A and Simulation-B

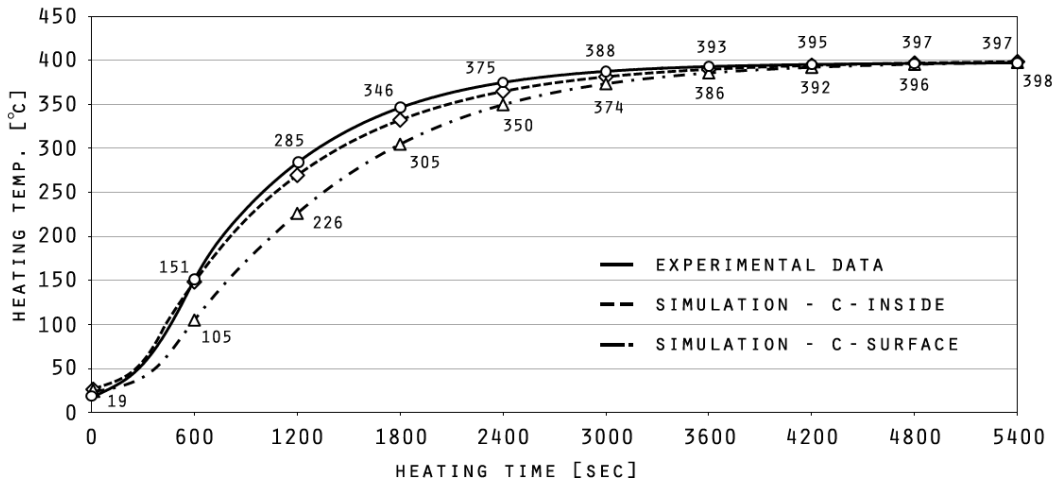


Fig.4-1-6: Temperature rising curve heated at 400 °C in Simulation-C

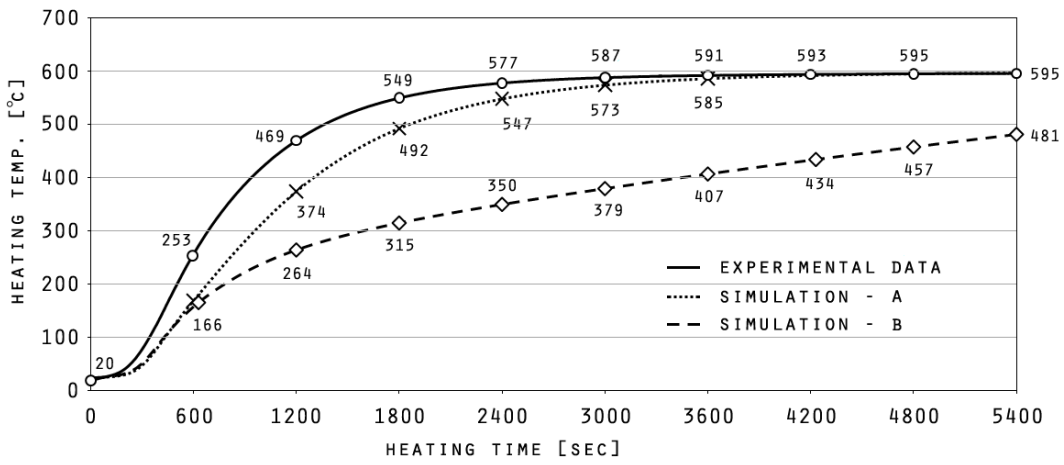


Fig.4-1-7: Temperature rising curve heated at 600 °C in Simulation-A and Simulation-B

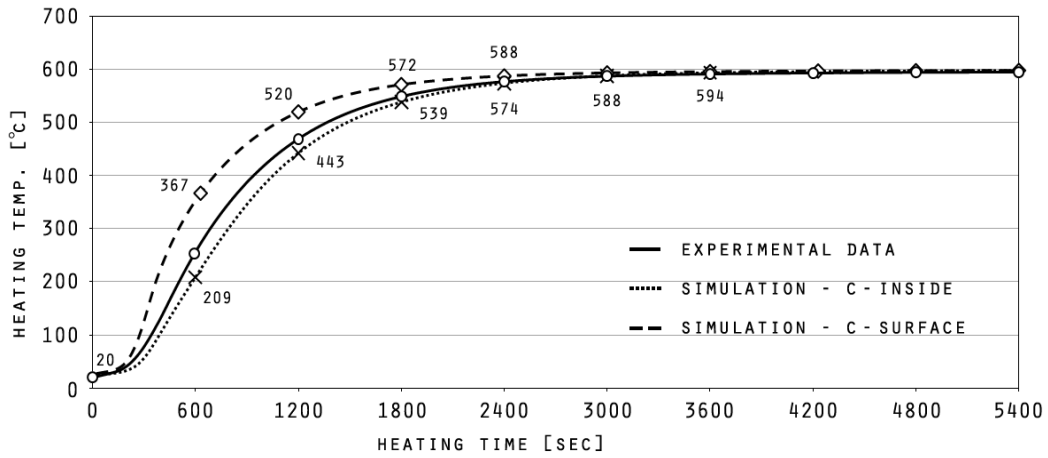


Fig.4-1-8: Temperature rising curve heated at 600 °C in Simulation-C

Table.4-1-3: Results of the condition data by the fitting analysis

Simulation	Convection coefficient (W/(mm ² °C))	Emissivity rate	Max temp. (°C)	
			400 °C	600 °C
A	1.0 E ⁻⁶	0.60	390	596
B	1.0 E ⁻⁴	0.84	375	481
C	1.0 E ⁻⁶	0.84	397	598

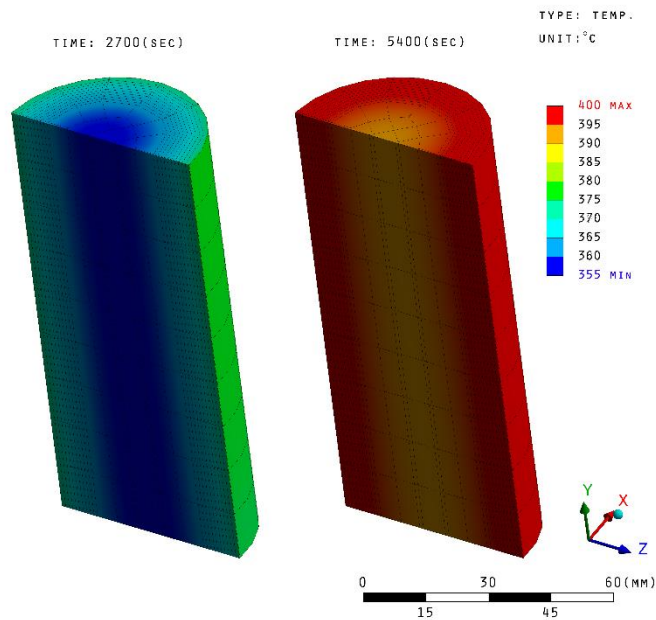


Fig.4-1-9: Distribution maps of temperature heated at 400 °C

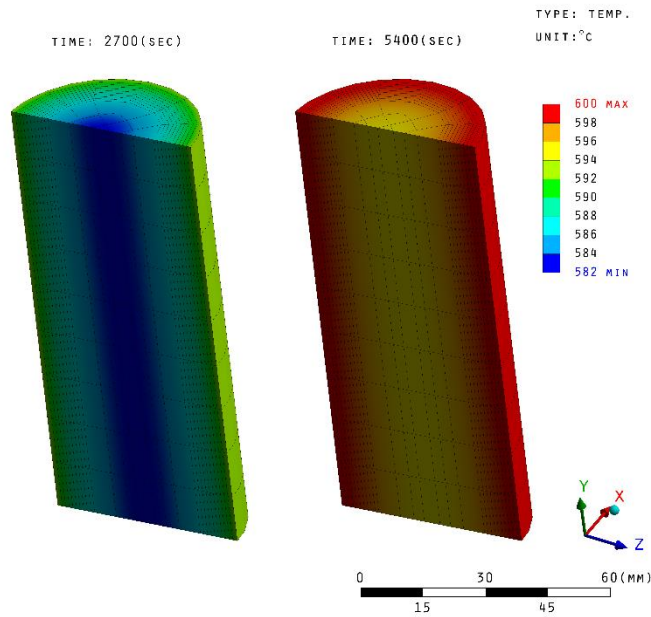


Fig.4-1-10: Distribution maps of temperature heated at 600 °C

4.2 Thermal analysis for a marble drum

4-2-1 Heat conduction analysis

D) Modeling

In the heat conduction analysis, we made a modeling as Fig.4-2-1. The diameter of a drum model with 16 flutes is 1.9 meters and the height of that is 1.2 meters.

As for the heat source on the model, we assumed that the heat source existed concentrically within 4 meters from the center of the drum. As a side note, the distance between columns of the portico in the Parthenon is about 4 meters.

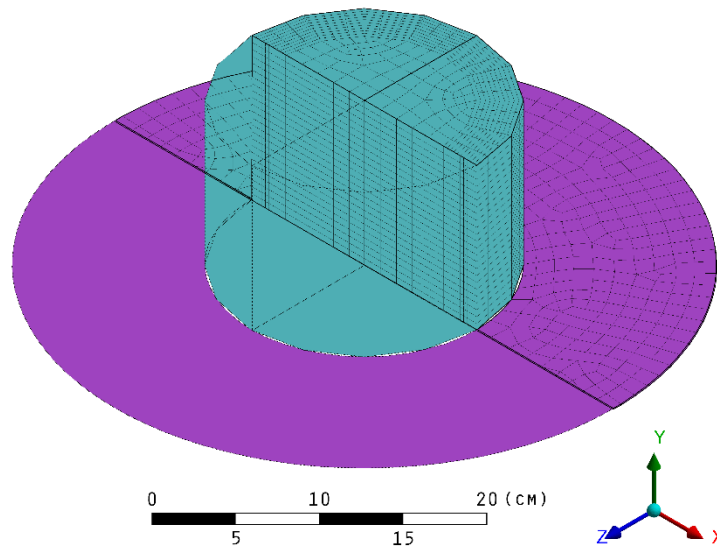


Fig.4-2-1: Model of a marble drum

II) Input conditions of analysis

Wood (Oak) was allotted to the material of the heat source and marble was allotted to the dram. Eq. (5) is the equation for thermal conductivity of wood, and Eq. (6) and Eq. (7) are the equation for heat specific of wood.⁽¹⁴⁾ Moreover, Eq. (8) is the equation for specific gravity of wood.⁽¹⁵⁾ Table.4-2-1 shows the physical property value was calculated by using above equations of wood as input condition. In addition, the heat specific of wood using for this analysis was calculated with the assumption that water content of wood was 15 %. As for the dram, we inputted the same data as those marble value using for the fitting analysis. (See Table.4-1-2)

Fig.4-2-2 describes the each boundary condition between models in the heat conduction analysis. Moreover, the standard fire curves regulated by ISO-834⁽¹⁶⁾ and JIS A 1301⁽¹⁷⁾ (See Fig.4-2-3 and Fig.4-2-4) were inputted to the heating source or the atmosphere around the dram model, and then we designed two assumed heating curves based on the fire curve regulated by JIS A 1301-first grade for input conditions of heating analysis. The renewal fire curves have two types for the heating source and the atmosphere. However the amount of flammable material, for example wooden structure material, using for the Parthenon of the day is vague and obscure. Eq.(9) is the equation of a temperature rising curve.

Moreover, the correlation of emissivity was set to ‘surface to surface’, and the enclosure type was set to ‘open type’. The heating time was set to about 24 hours.

As a side note, we took into account the gravitational acceleration in present analysis.

$$\lambda_2 = \lambda_1 \{1 - 0.012(u_1 - u_2)\} \quad (5)$$

λ_1, λ_2 : Thermal conductivity (kcal/m h °C)
 u_1, u_2 : Water content (%)

$$C_0 = 0.266 + 0.00116t \quad (6)$$

$$C_{av} = 0.266 + 0.00058(t_2 - t_1) \quad (7)$$

C_0 : Heat specific (kcal/kg °C)
 C_{av} : Average of heat specific (kcal/kg °C)
 t, t_1, t_2 : Temperature (°C), $t_2 > t_1$

$$r_u = r_0 \frac{100+u}{100+r_0u} \quad (8)$$

r_u : Air dried specific gravity, (=0.82)⁽¹⁴⁾
 r_0 : Bone dried specific gravity
 u : Water content (%)

Table.4-2-1: Physical property value as input to the heat source

Oak			
Temp. (°C)	Thermal conductivity (W/(m °C))	Heat specific (J/(kg °C))	Density (kg/m ³)
25	0.21	1210.8	820
100		1599.4	
200	0.17	2085.0	798
300		2570.7	
400		3056.4	
450		3299.2	
500		3542.0	
550		3784.9	
600		4027.7	

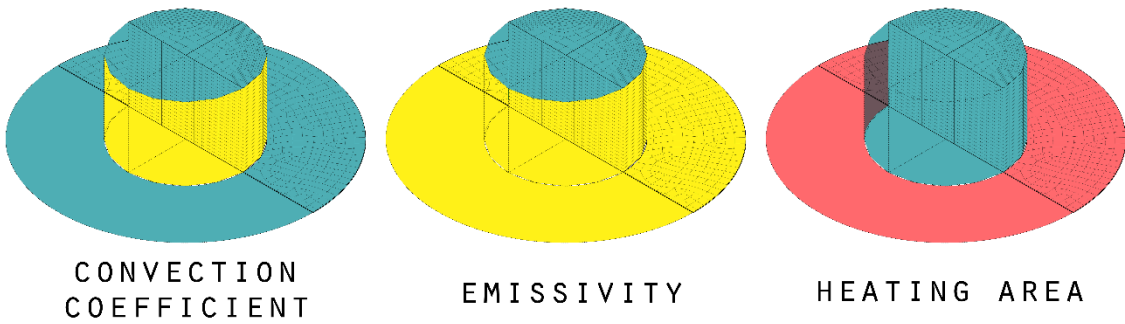


Fig.4-2-2: Boundary conditions

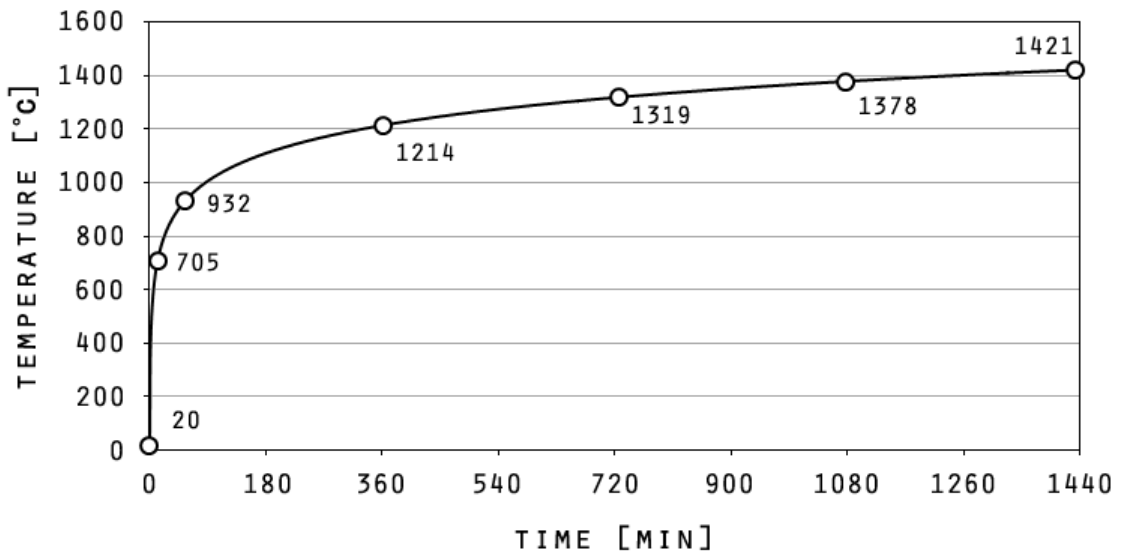


Fig.4-2-3: Standard fire curve (ISO-834)

$$T = 20 + 345 \times \text{Log}(8t + 1) \quad (9)$$

T: Temperature (°C)

t: Time (min)

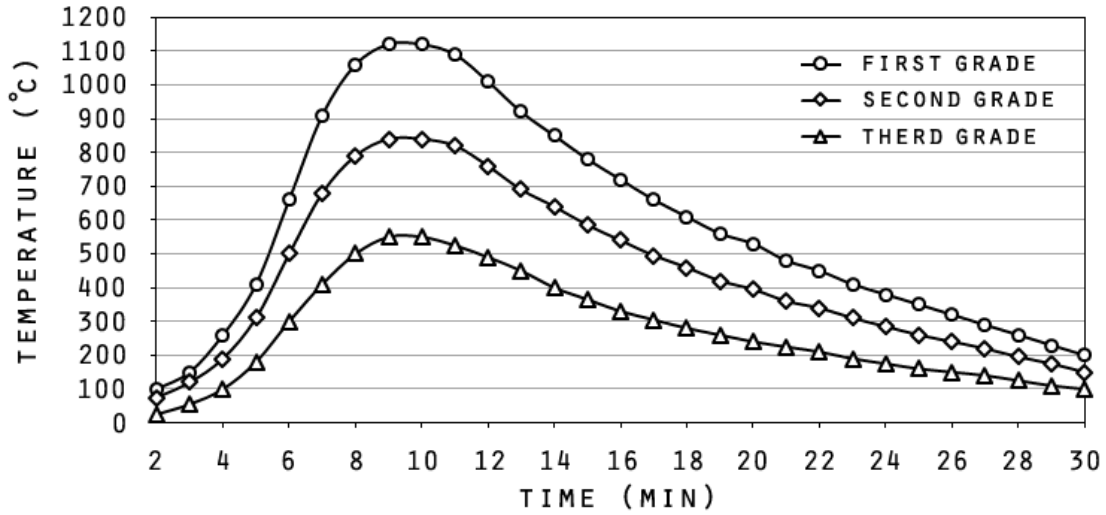


Fig.4-2-4: Standard fire curve (JIS A 1301)

4-2-2 Thermal stress analysis

The analysis models as the objects of thermal stress analysis are marble multi-drum. The heat distribution obtained by the heat conduction analysis above was inputted as thermal load to the thermal stress analysis condition.

Table.4-2-3 shows the physical property value using for thermal stress analysis. Fig.4-2-5 describes the boundary conditions between models in the thermal stress analysis. Two points of the bottom of the model were fixed to prevent from rotating of the model.

Table.4-2-3: Physical property value as input to the heat source ⁽¹⁵⁾

Oak	Young's modulus (MPa)			Poisson's rate			Elastic shear modulus (MPa)		
Temp. (°C)	X	Y	Z	XY	YZ	XZ	XY	YZ	XZ
25	2136	5292	970	0.33	0.5	0.64	390	1294	764

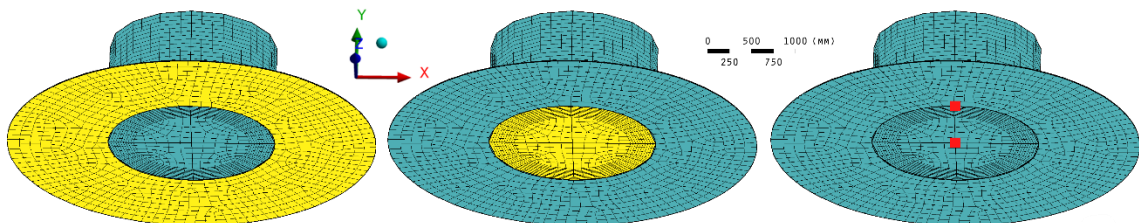


Fig.4-2-5: Restriction condition of models

4-2-3 Results and discussions

Fig.4-2-6 and Fig.4-2-8 show the temperature rising curve of marble dram, and Fig.4-2-7 and Fig.4-2-9 indicate the images of the heat distributions obtained by the heating simulation for 24 hours in the case that the standard fire curve regulated by ISO 834 or the first grade of the standard fire curve regulated by JIS A 1301 were inputted only to the heat source. In addition, the emissivity of marble was taken into account in these cases. In the case of ISO curve, the surface temperature of the model rose slowly as like following the ISO curve. On the other hand, in the case of JIS curve, the surface temperature of the model suddenly rose, and then also suddenly fell after reaching the temperature peak of the JIS curve. Each internal temperature began to climb after the heating point for 8 hours.

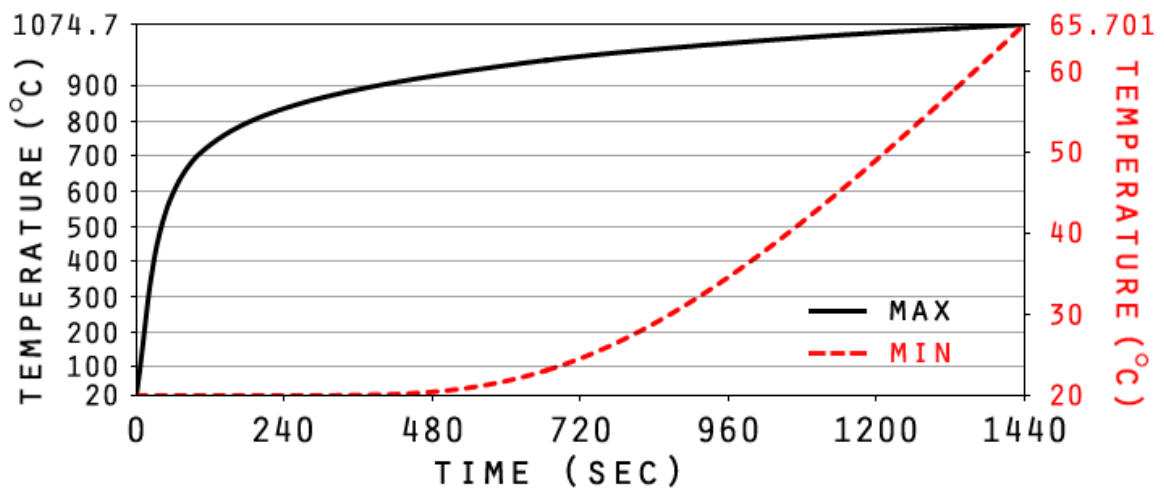


Fig.4-2-6: Thermal rising curve of the dram- ISO version

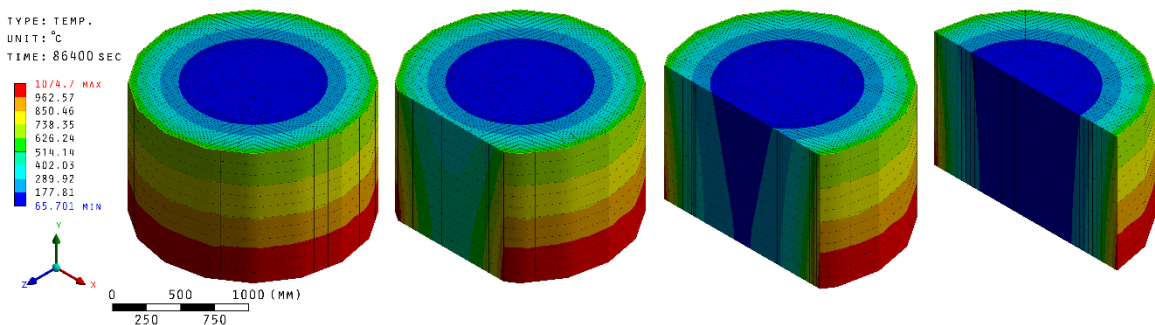


Fig.4-2-7: Distribution images of simulation to the dram- ISO version

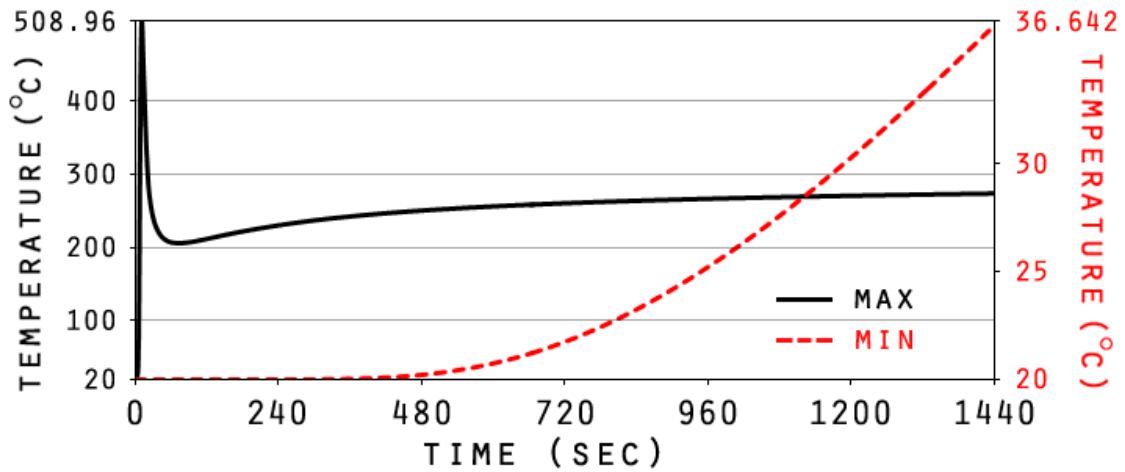


Fig.4-2-8: Thermal rising curve of the dram- JIS version

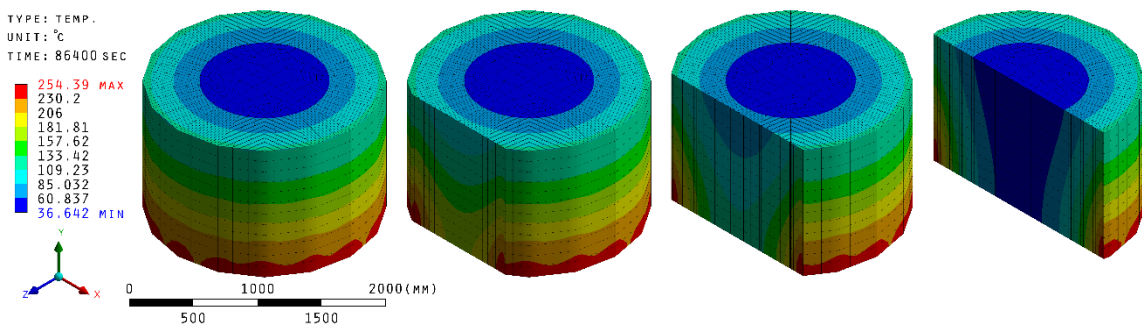


Fig.4-2-9: Distribution images of simulation to the dram- JIS version

Fig.4-2-10 and Fig.4-2-11 describe images of the maximum principal stress obtained by the thermal stress analysis. Fig.4-2-10 is the results in the case the standard fire curve regulated by ISO curve was inputted only to the heat source, and Fig.4-2-11 is the results in the case that curve was inputted only to the atmosphere around the model. In addition, we calculated the critical tensile stress of marble by using the Young's modulus obtained by the compressive tests in Chapter 2 and the split strength of marble obtained by the split cylindrical test in the previous study. For the detail about the split cylindrical test in the previous study, see Appendix 5. We confirmed when the thermal stress exceeds the critical tensile stress from starting heating simulation by comparing these results.

Comparisons of toxicity data between the critical tensile stress and the maximum principal stress obtained by inputting ISO curve only to the heat source have shown that the thermal stress exceeded the critical tensile stress of marble after about 17 minutes from starting heating simulation. Fig.4-2-12 shows the maximum principal stress of model in the case ISO curve was inputted only to the heat source at 17 minutes. Moreover, the temperature at the point of 17 minutes on the ISO curve is about 757 °C, and the maximum temperature on the first grade of JIS A curve (=1120 °C) is higher than that temperature. Besides, it can be assumed that the combustible material was wood and the

size of the section member using for the Parthenon at that time was bigger than the size of that using for a normal house. Therefore, the duration of heating time of maximum temperature is likely to continue at least 30 minutes. From the above, we designed the assumed heating curve for heat source and atmosphere based the first grade of the JIS A 1301. (See Fig.4-2-13)

We performed the thermal stress analysis to the model of marble multi-dram column by the heating simulation for 24 hours with inputting the assumed heating curve to the heat source and atmosphere around model hereafter study.

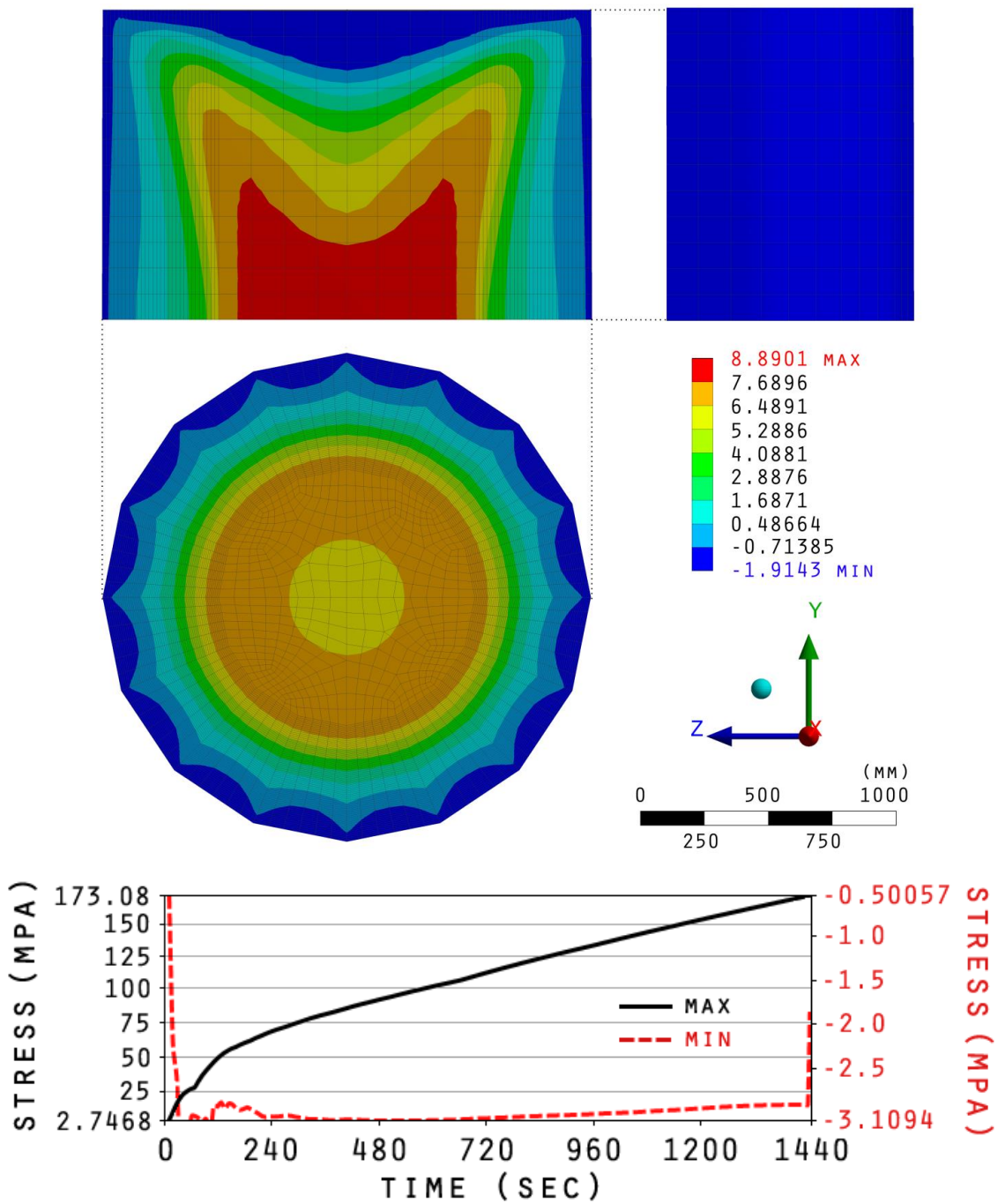


Fig.4-2-10: Maximum principal stress of model (only effect of the emissivity)

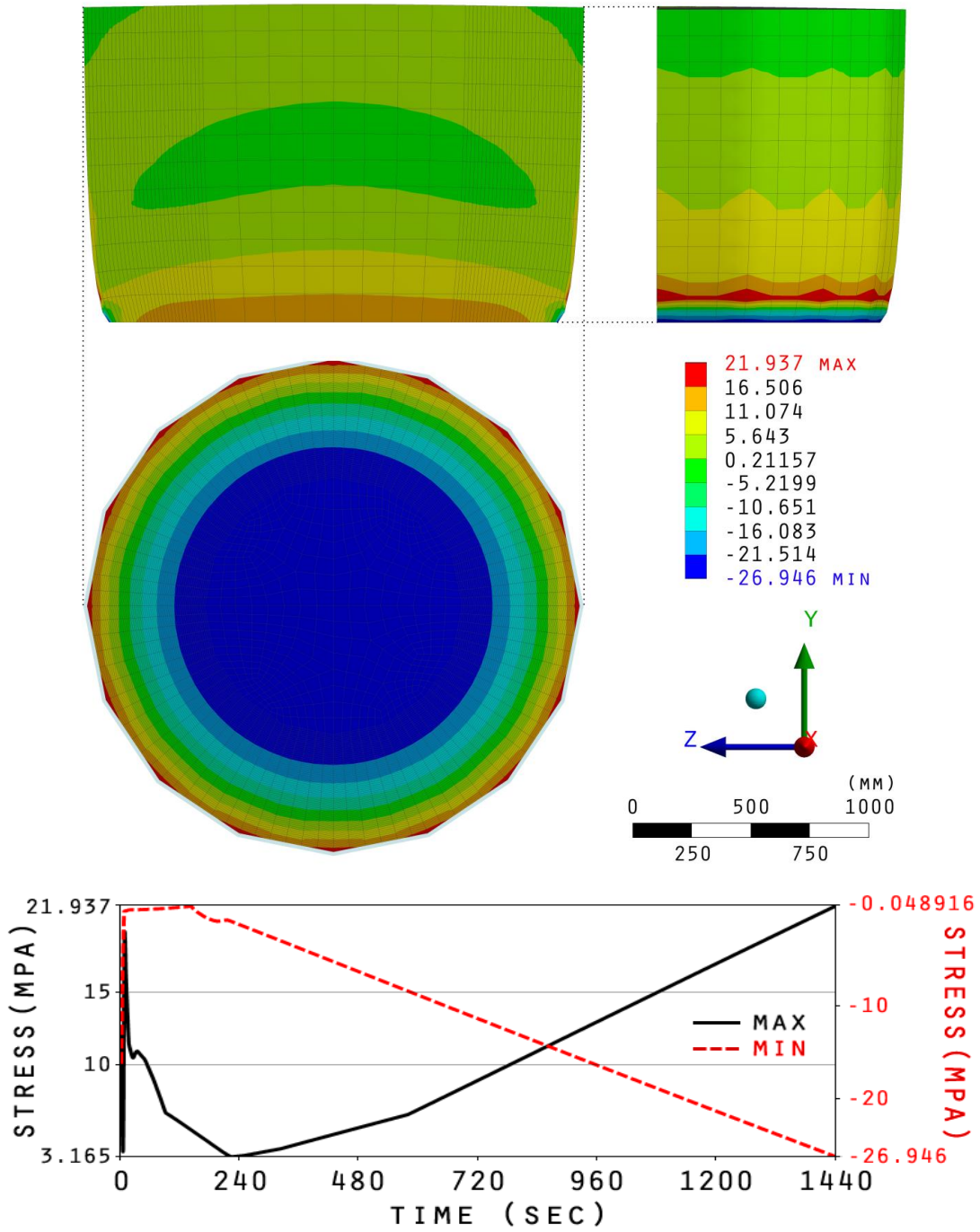


Fig.4-2-11: Maximum principal stress of model (only effect of the convection coefficient)

Table.4-2-4: Results of the split cylindrical test

Temp. (°C)	Split strength (N/mm ²)	Young's modulus (N/mm ²)	Critical strain
25	11	64900	8.78×10^{-5}
200	19	64300	1.54×10^{-4}
650	12	22500	2.80×10^{-4}

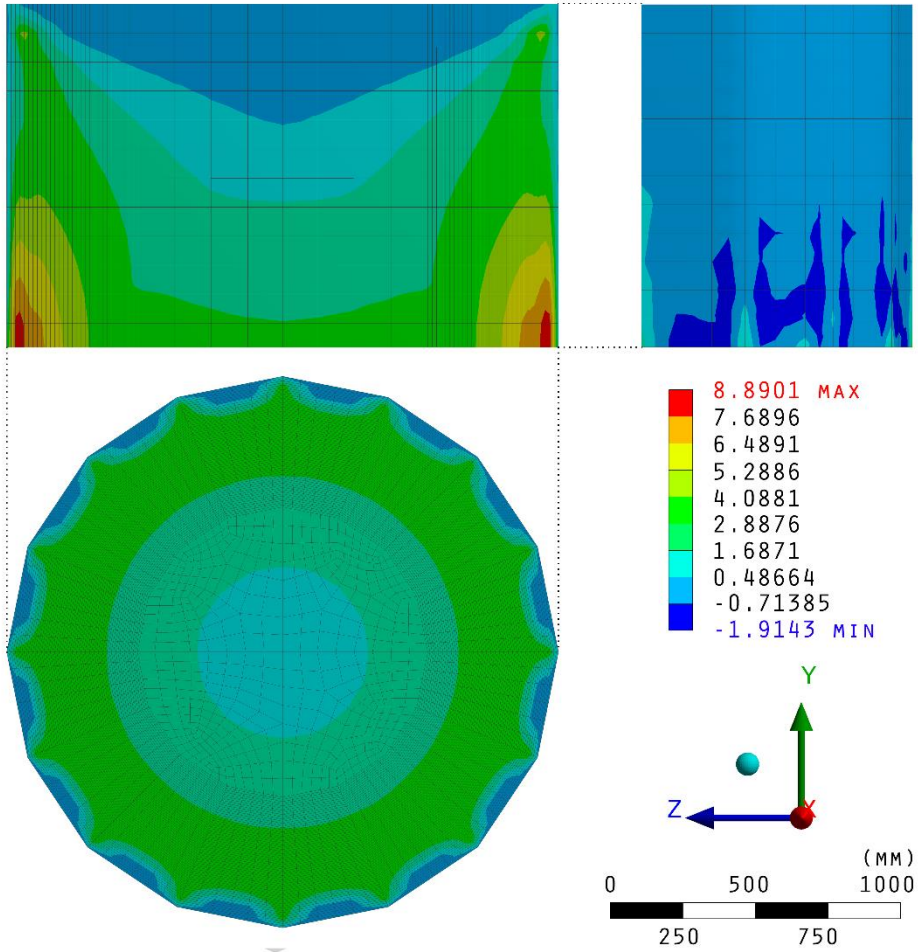


Fig.4-2-12: Maximum principal stress of model at 17 minutes (only effect of the emissivity)

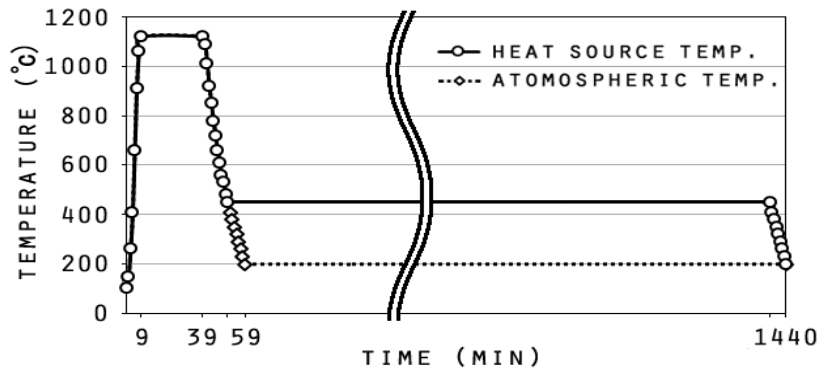


Fig.4-2-13: Assumed heating curve for heat source and atmosphere

Fig.4-2-14 indicates the images of the hat distributions obtained by the heating simulation for 24 hours with inputting the assumed heating curve, and Fig.4-2-15 shows the maximum principal stress of model in the case assumed heating curve was inputted at 17 minutes.

From the cross section images of the model on Fig.4-2-15, the compressive stress was caused along the circumferential direction of the model, and it found that the compressive stress worked as the binding force to the surface of model. Moreover, there were big tensile stress concentration around edges of the model. These stress worked symmetry inside, however the big tensile stress worked to upper edge of the model from around middle of the model. Besides, Fig.4-2-16 described the maximum stress vector on the model. The tensile stress worked from to the depth of around 20 cm from the surface of model. This result was very similar to the failure mode of the specimen heated by high temperature, for example at 800 °C, during cooling after heating test in Chapter 2. Hence, it is highly likely that similar tensile stress was caused on the actual marble dram, and it is seen that micro cracks have occurred within around this area.

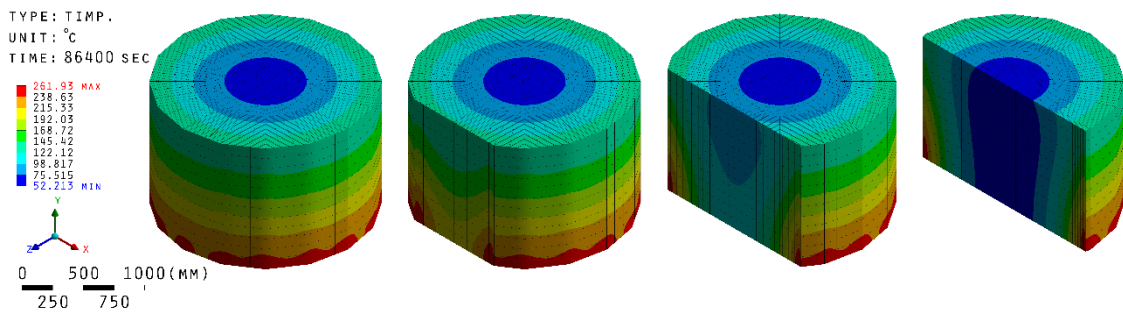


Fig.4-2-14: Distribution images of simulation to the dram- Renewal curve version

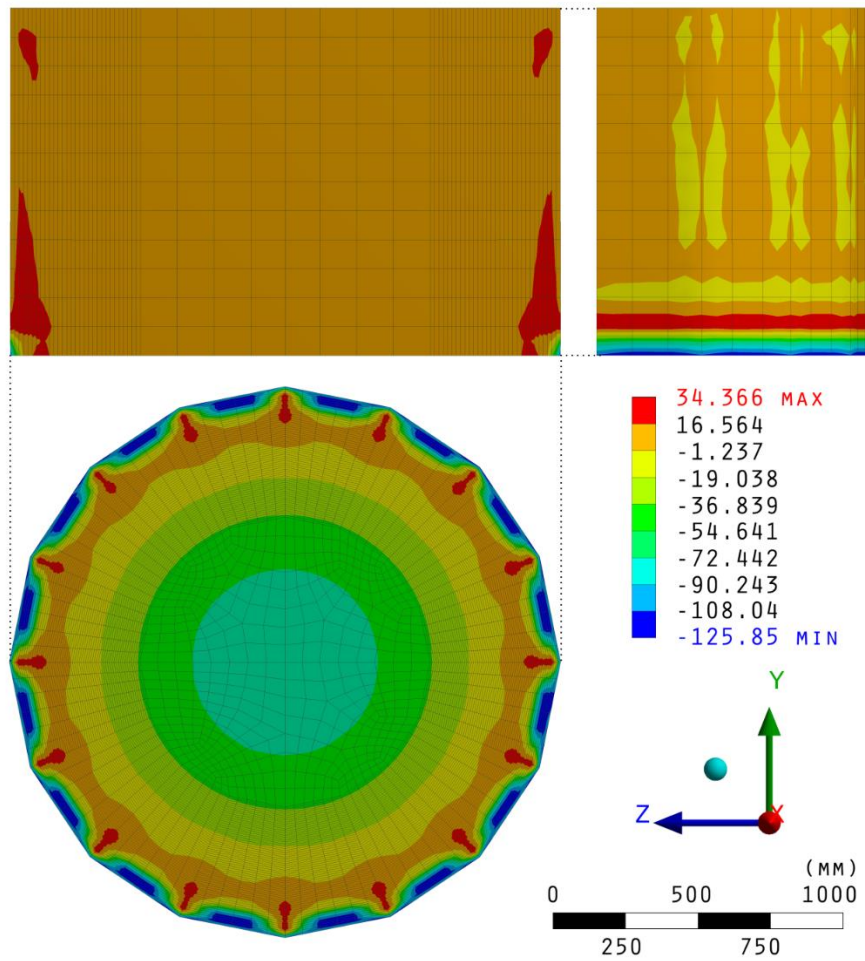


Fig.4-2-15: Maximum principal stress of model at 17 minutes obtained by the assumed heating curve

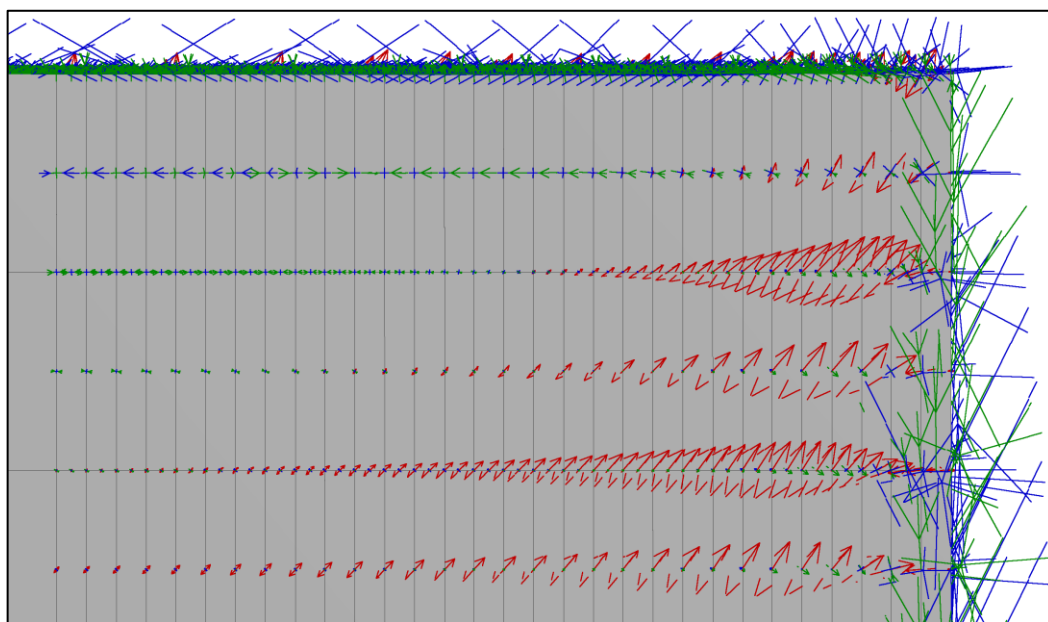


Fig.4-2-16: Maximum stress vector of model at 17 minutes obtained by the assumed heating curve

4-3 Thermal analysis for a marble multi-dram column

4-3-1 Heat conduction analysis

D) Modeling

The model using for the thermal analysis to multi-dram column is designed that the height is 13.2 meters constituted by stacking 11 drams. As for the heat source on the model, we assumed that the heat source existed concentrically within 4 meters from the center of the model as well as the dram model, and the heat source model has 0.5 meters in height.

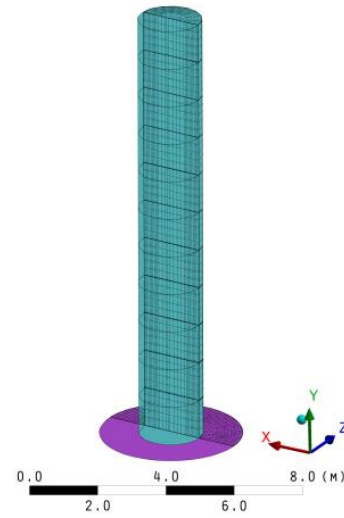


Fig.4-3-1: Multi-dram model

II) Input condition of analysis

Each boundary condition, restriction condition of the multi-dram model and physical property values using for inputting each material have the same condition with the input condition in Chapter 4.2. Moreover, as whole of the actual marble column damaged by fire, the simply heating simulation to whole column was performed by inputting the heating curve not only to the bottom heat source of the model but also to the atmosphere around the model. For the heating curve using for inputting to the heat source and the atmosphere, see Fig.4-2-13.

4-3-2 Thermal stress analysis

The input conditions for thermal stress analysis to multi-dram model are same as the inout conditions using for the thermal analysis to a dram model in Chapter 4-2. About the friction force in the present analysis, the radiant heat between multi-drum models and the ground was not taking into account. Moreover, the radiant heat between multi-dram models was taking into account.

4-3-3 Results and discussions

Fig.4-3-2 describes the image of the heat distributions obtained by the heating simulation, and Fig.4-3-3 shows the thermal rising curve of the multi-dram at the each point. However, we simulated simply whole column was damaged by fire with inputting the heating curve to the heat source and the atmosphere around the model, the maximum temperature of top of the column reached to about 65 °C as shown Fig.4-3-3. From this result, it is found that setting condition on the assumed heating curve that the duration of heating time of maximum temperature continue keeping temperature 30 minutes was too short. Moreover, from the images of the heat distributions obtained by the heating simulation, it is found that there were the significant difference in temperature between surface and internal marble dram. Hence, there were also a difference of thermal expansion coefficients between surface and internal one while marble dram was cooled after heating. Thus, it is seen from the above

result that micro cracks occurred within around this area.

Fig.4-3-4 shows the images of the maximum principal stress after finishing heating simulation, and Fig.4-3-5 shows the images of that at 17 minutes from starting simulation. The thermal stress which exceeded the critical tensile stress occurred to the depth of about 20 cm from surface of the model and to the height of about 3 meters from the ground in Fig.4-3-4. From this results, it is also seen that micro cracks have occurred within around this area as well as the result of the analysis to a dram. In addition, as shown Fig.4-3-2 and Fig.4-3-3, however the top of the column was conducted not enough heat, there were tensile stress which did not exceed the critical tensile stress on the images of the distribution of thermal stress.

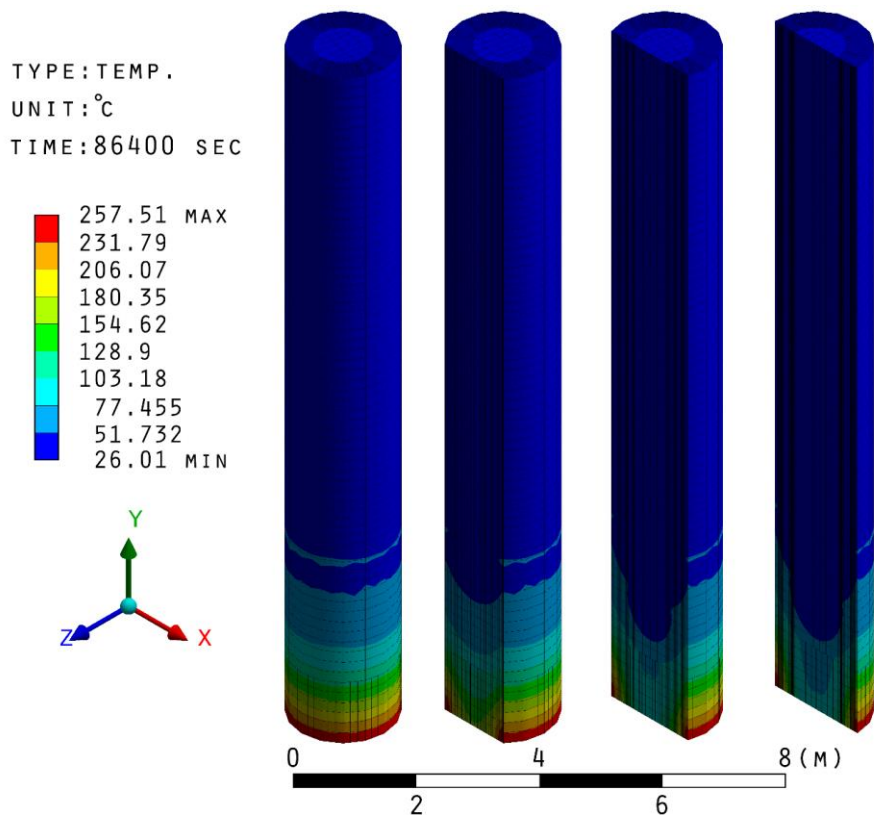


Fig.4-3-2: Distribution images of simulation to the multi-drum

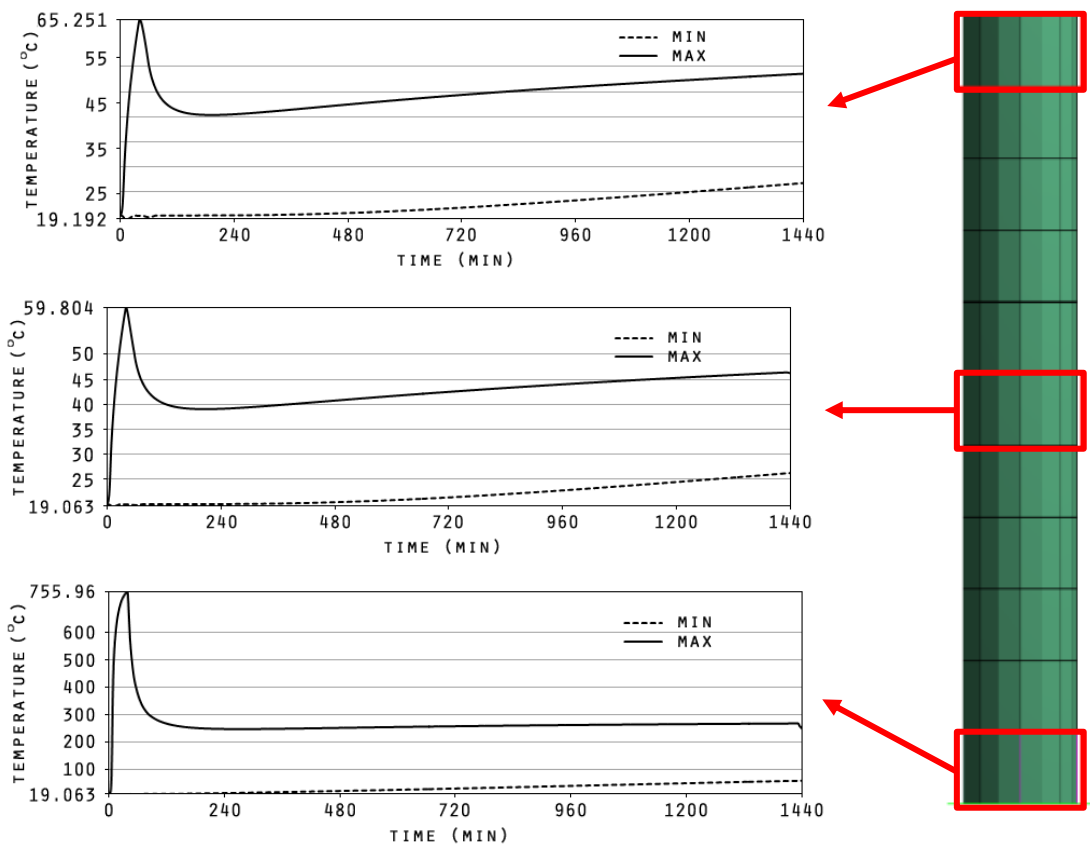


Fig.4-3-3: Thermal rising curve of the multi-drum at the each point

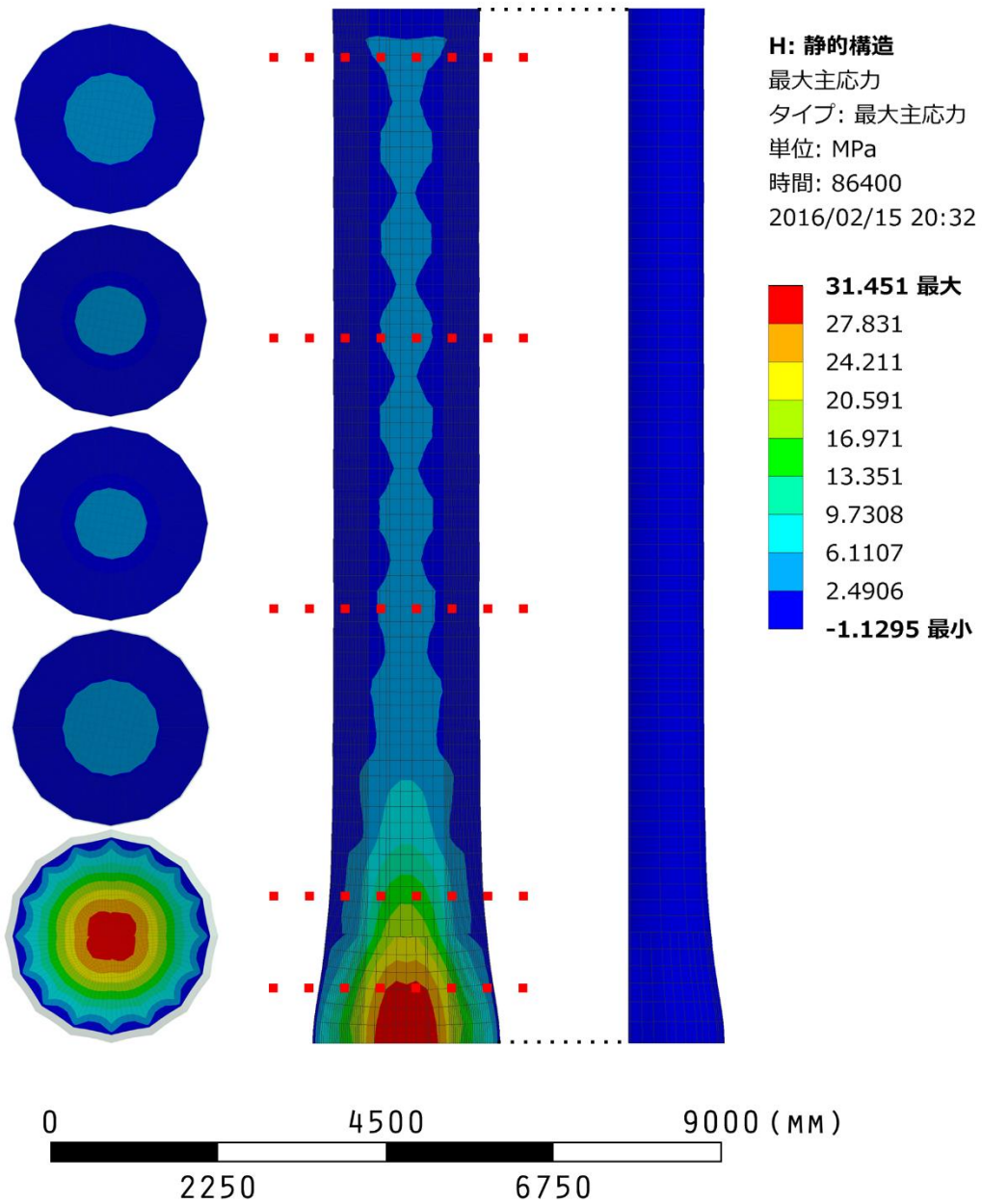


Fig.4-3-4: Maximum principal stress of model at 24 hours

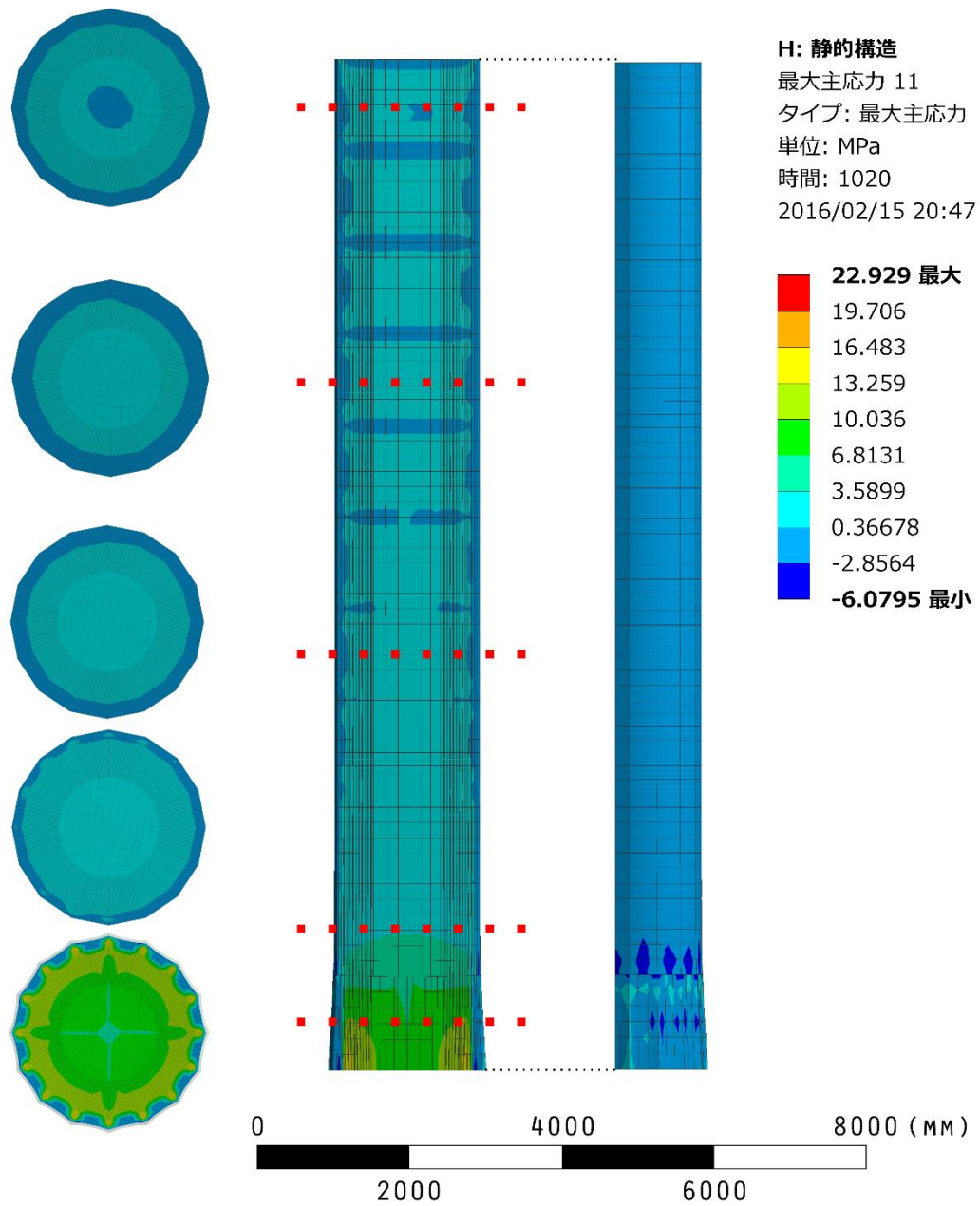


Fig.4-3-5: Maximum principal stress of model at 17 minutes

CHAPTER 5. CONCLUDING REMARKS

5.1 Conclusions

As results of the experimental study, the compressive strength of marble specimen began to decrease at the temperature of 300 °C and the specimen heated at over 750 °C collapsed naturally while cooling. In addition, the weight of all of the specimens heated at 800 °C increased with time by moisture absorbing, and deterioration of the specimens significantly proceeded. Accordingly moisture absorption affected deterioration process of marble. Moreover, cooling speed after end of the heating also affected crack occurrence on marble. The rapid temperature change gave the specimens big shock, hence occurring cracks on marble depended on the thermal shock caused by quickly cooling than heating temperature.

About crystal directions of marble, there was the significant difference between vertical crystal direction and horizontal crystal direction about the compressive strength of specimen. However, marble stone has the individual variation because marble stone is natural material. Hence such difference in mechanical properties caused by each crystal direction is explained as the individual variation of natural material, and then we concluded that this difference of compressive strength of specimen between both crystal directions can be neglected.

In sonic tests by non-destructive method, the marble specimen having vertical crystal direction and the compressive strength were interdependent on each other, however the specimen having horizontal one didn't have the relation to the compressive strength. From the result, non-destructive method may be suitable to the actual buildings for estimation of the compressive strength as long as the crystal direction is noted.

In the fitting analysis for the convection coefficient and emissivity rate of marble, the convection coefficient of marble was evaluated to be $1.0 \text{ E}^{-6} \text{ (W/(mm}^2 \text{ °C))}$ and the emissivity rate was 0.84. From the results of some simulation, the value of emissivity rate affected the temperature's rising more than the convection coefficient value.

Moreover, in the result of thermal stress analysis by ANSYS code, the compressive stress was caused along the circumferential direction of the marble multi-dram. This result was very similar to the failure mode of the heated marble specimen. Hence, it is highly likely that similar compressive stress was caused on the actual marble multi-dram. In addition, the tensile stress was also caused along the radial direction at about 30 cm from the surface. Moreover, from the result image of the heat distributions obtained by the heating simulation, it is found that there were the significant difference in temperature between surface and internal marble dram. Hence, there were also a difference of thermal expansion coefficients between surface and internal one while marble dram was cooled after heating. Thus, it is seen from the above result that micro cracks occurred within around this area.

5.2 Future study

The amount of flammable material, for example wooden structure material, using for the Parthenon of the day is vague and obscure. Therefore, it requires more comparative study with other alternatives about amount and position of heat source, duration of heating time, input conditions or modeling.

Moreover, we took thermal expansion of marble into account when we performed thermal analysis to marble dram and multi-dram. However, it is assumed that cracks occurred on marble dram while marble was cooled after heating, we should take not only thermal expansion but also thermal shrinking of marble into account in the future study.

ACKNOWLEDGEMENTS

The author sincerely thanks to Prof. T. Hanazato for guiding my study with many useful data and helpful advices. The author also is deeply grateful to Dr. J. Suzuki from the Building Research Institute and Mr. R. Taniguchi from the Cybernet Systems CO., LTD. and Dr. Y. Hasemi from Waseda University for taking the time to give me valuable and detailed advices. At the field survey, the author was supported by Dr. H. P. Mouzakis from the National Technical University of Athens and the Acropolis Restoration Services.

Lastly, the seniors of the Hanazato Lab. and my contemporaries at the Mie University gave me their kind help and encouraged me. The author would like give a special thanks to them.

REFERENCE

- (1) P. Tournikiotis: The Parthenon and its impact in modern times, trans. Cox and Solman, pp59-61, pp64-65, pp143, 1994
- (2) N.Theofanopoulos, T. Hanazato, and M. Watabe: Seismic Response Analysis of Parthenon Columns, Proc. of STREMAH 89, pp339-348, 1989
- (3) N. Theofanopoulos, T. Hanazato and M. Watabe: Probabilistic Approach to Generate the Reference Motion for the Protection of Historical Monuments Against Earthquakes, Proc. Of the 1st International Conference on Structural Repair and Maintenance of Historical Buildings (STREMAH 89), pp289-298, 1989
- (4) N. Oyaizu: Seismic Structural Monitoring of World Heritage Masonry Monuments in Earthquake-prone Countries, Master thesis, Department of Architecture, Faculty of Engineering, Mie University, 2013
- (5) H. P. Mouzakis, I. N. Psycharis, D. Y. Papastamatiou, P. G. Carydis, C. Papantonopoulos and C. Zambas: Experimental investigation of the earthquake response of a model of a marble classical column, Earthquake engineering and Structural Dynamics, 2002; 31: 1981-1698
- (6) C. Papantonopoulos, I. N. Psycharis, D. Y. Papastamatiou, J. V. Lemos and H. P. Mouzakis: Numerical prediction of the earthquake response of classical columns using the distinct element method, Earthquake engineering and Structural Dynamics, pp1699-1717, 2002
- (7) N. Sakai: Mechanical Behaviours of Heated Rocks under Uniaxial Compression, 応用地質 第28巻 第1号, 28-1, p19-24, 1987

- (8) 関隆司: 都市と文化財 アテネと大阪 : 大阪市立大学国際学術シンポジウム, 東信堂, pp26-28, pp31-32, p102-105, p111-113, 1998
- (9) 社会法人 日本セラミックス協会: セラミック工学ハンドブック 第2版, 技報堂出版, 2002
- (10) 自然科学研究機構 国立天文台: 理科年表 平成 25 年, pp415, p672-p674, 2012
- (11) American Society of Testing Materials: Standard C215-02 Standard Test Method of Fundamental Transverse, Longitudinal and Torsional Frequencies of Concrete Specimens
- (12) James Instruments INC.: E-Meter Mk II Resonant Frequency Tester User's Manual, pp15, pp18, 2010
- (13) 山田眞生、鈴木淳一、花里利一: 海外の世界遺産組積造建築物に用いられる大理石材料に関する研究 - パルテノン神殿に用いられる大理石材料の耐火性能, 日本建築学会大会, pp237-238, 2014
- (14) 梶田茂: 木材工学, pp250-251, pp254-255, 1961,
- (15) 林業試験場: 木材工業ハンドブック, pp102-103, pp128-131, 1982
- (16) International Organization for Standardization: ISO 384-1 Fire-resistance tests –Elements of building construction, 1999
- (17) 日本工業規格: JIS A 1301 Method of fire test for wooden structural parts of buildings, 1994
- (18) 土木学会 岩盤力学委員会: 熱環境下の岩盤施設の開発をめざして - 熱物性と解析 -, 2006
- (19) 武井吉一, 中山實: 石と建築 -材料と工法”, 鹿島出版会, pp35-49, 1992
- (20) 山口梅太郎, 宮崎道雄: 熱による岩石の強度の変化あるいは破壊について, 日本鉱業会誌, pp346-350, 1970
- (21) T. Matsukawa: ギリシア・パルテノン神殿のエンタシス石柱の動的挙動解析, 東京都立大学工学部建築工学科 渡部研究室, 1984

Appendix 1: List of the dimensions of marble specimens using for non-destructive method

Specimen No.	Mass (kg)	Length (cm)	Dimensions of cross section		Area (cm ²)	
			b (cm)	t (cm)		
V1	5.46	20.00	11.20	10.00	112.00	
V2	5.46	20.00	11.20	10.00	112.00	
V3	5.48	20.00	11.40	9.95	113.43	
V4	5.48	20.00	11.60	10.00	116.00	
V5	5.50	20.00	11.40	10.25	116.85	
V6	5.48	20.00	11.65	9.95	115.92	
V7	Before	5.48	20.00	11.80	9.85	116.23
	After	5.48	20.00	11.80	10.00	118.00
V8	Before	5.46	20.00	11.00	9.90	108.90
	After	5.48	20.00	11.05	10.00	110.50
V9	Before	5.46	20.00	11.15	9.95	110.94
	After	5.46	20.00	11.05	10.05	110.55
V10	Before	5.48	20.00	11.40	9.95	113.43
	After	5.47	20.00	11.40	10.00	114.00
V11	Before	5.47	20.00	10.95	10.10	110.60
	After	5.46	20.00	11.20	10.10	113.12
V12	Before	5.48	20.00	11.20	9.80	109.76
	After	5.46	20.00	11.50	9.80	112.70
V13	Before	5.47	19.99	11.35	10.00	113.50
	After	5.43	20.20	12.45	11.20	139.44
V14	Before	5.48	20.00	11.25	10.20	114.75
	After	5.42	20.10	12.70	11.25	142.88
V15	Before	5.42	20.00	10.55	9.70	102.34
	After	5.40	20.10	11.85	10.80	127.98
V16	Before	5.49	20.00	11.35	10.25	116.34
	After	5.46	20.10	12.60	11.20	141.12
V17	Before	5.42	20.00	10.70	9.40	100.58
	After	5.40	20.10	11.80	10.35	122.13
V18	Before	5.47	20.00	11.20	10.20	114.24
	After	5.46	20.0	12.40	11.10	137.64

Appendix 1: List of the dimensions of marble specimens using for non-destructive method

Specimen No.		Mass (kg)	Length (cm)	Dimensions of cross section		Area (cm ²)
				b (cm)	t (cm)	
V19	Before	5.48	20.00	11.40	10.05	114.57
	After	5.47	20.00	11.45	10.30	117.94
V20	Before	5.48	20.00	11.35	10.10	114.64
	After	5.48	20.00	11.85	10.60	125.61
V21	Before	5.42	20.00	10.50	9.65	101.33
	After	5.42	20.00	11.10	10.00	111.00
V22	Before	5.42	20.00	10.70	9.70	103.79
	After	5.42	20.00	11.10	10.00	111.00
V23	Before	5.46	20.00	11.15	9.50	105.93
	After	5.46	20.00	11.20	10.25	114.80
V24	Before	5.47	20.00	11.40	9.95	113.43
	After	5.46	20.00	11.75	10.15	119.26
V25	Before	5.45	20.00	10.10	10.02	101.20
	After	5.44	20.10	10.21	10.10	103.12
V26	Before	5.46	20.00	10.10	9.95	100.50
	After	5.44	20.10	10.21	10.08	102.92
V27	Before	5.46	20.00	10.11	9.70	98.07
	After	5.44	20.10	10.24	10.06	103.01
V28	Before	5.48	20.00	10.13	10.01	101.40
	After	5.45	20.00	10.24	10.09	103.32

Appendix 1: List of the dimensions of marble specimens using for non-destructive method

Specimen No.	Mass (kg)	Length (mm)	Dimensions of cross section		Area (cm ²)	
			b (mm)	t (mm)		
H1	5.36	19.80	10.10	10.00	101.00	
H2	5.34	19.80	9.95	9.50	94.53	
H3	5.36	19.80	10.00	9.85	98.50	
H4	5.36	19.80	10.00	9.90	99.00	
H5	5.34	19.80	9.90	9.80	97.02	
H6	5.34	19.80	9.80	9.80	96.04	
H7	Before	5.34	19.80	10.25	9.75	99.94
	After	5.34	19.80	10.35	10.00	103.50
H8	Before	5.36	19.80	10.10	9.80	98.98
	After	5.36	19.80	10.15	9.90	100.49
H9	Before	5.34	19.80	9.95	9.80	97.51
	After	5.33	19.80	10.00	9.80	98.00
H10	Before	5.38	19.80	10.30	10.10	104.03
	After	5.38	19.80	10.40	10.20	106.08
H11	Before	5.34	19.80	9.95	9.85	98.01
	After	5.34	19.80	10.00	9.85	98.50
H12	Before	5.34	19.80	9.95	9.80	97.51
	After	5.34	19.80	9.95	9.90	98.51
H13	Before	5.34	19.80	10.05	9.55	95.98
	After	5.32	20.10	10.95	10.60	116.07
H14	Before	5.34	19.80	9.80	9.80	96.04
	After	5.31	20.10	10.75	10.60	113.95
H15	Before	5.36	19.80	10.20	10.10	103.02
	After	5.34	20.10	11.00	10.90	119.90
H16	Before	5.34	19.80	10.10	9.60	96.96
	After	5.30	20.10	10.90	10.55	115.00
H17	Before	5.34	19.80	9.90	9.70	96.03
	After	5.30	20.20	10.85	10.50	113.93
H18	Before	5.34	19.80	9.80	9.80	96.04
	After	5.30	20.10	10.70	10.70	114.49

Appendix 1: List of the dimensions of marble specimens using for non-destructive method

Specimen No.		Mass (kg)	Length (mm)	Dimensions of cross section		Area (cm ²)
				b (mm)	t (mm)	
H19	Before	5.34	19.80	9.95	9.65	96.02
	After	5.34	19.80	10.20	9.80	99.96
H20	Before	5.34	19.80	10.40	9.70	100.88
	After	5.35	19.80	10.45	10.35	108.16
H21	Before	5.32	19.80	9.90	9.60	95.04
	After	5.32	19.80	10.25	9.90	101.48
H22	Before	5.36	19.80	10.35	9.85	101.95
	After	5.35	19.80	10.35	10.00	103.50
H23	Before	5.36	19.80	10.40	10.10	105.04
	After	5.36	19.90	10.50	10.20	107.10
H24	Before	5.34	19.80	9.80	9.60	94.08
	After	5.34	19.80	10.00	9.80	98.00
H25	Before	5.36	19.80	10.25	9.85	100.96
	After	5.34	20.00	10.08	10.07	101.51
H26	Before	5.36	19.80	10.55	9.90	104.45
	After	5.35	20.00	10.11	10.06	101.71
H27	Before					
	After	5.34	20.00	10.09	10.06	101.51
H28	Before					
	After	5.37	19.95	10.10	10.04	101.40
H29	Before					
	After	5.34	20.00	10.04	10.04	100.80

Appendix 2: Value of Modulus of Elasticity and Rigidity obtained by non-destructive method

Specimen No.		Modulus of Elasticity (GPa)	Modulus of Rigidity (GPa)	Max stress (kN)
V1		71.4	27.0	894.60
V2		71.7	26.6	927.05
V3		71.8	27.4	927.04
V4		70.2	26.8	959.41
V5		66.6	25.4	880.00
V6		67.2	26.1	—
V7	Before	70.1	27.1	—
	After	35.2	12.8	
V8	Before	72.6	25.4	691.61
	After	43.1	13.5	
V9	Before	71.8	26.9	498.30
	After	37.2	13.7	
V10	Before	71.8	27.1	670.00
	After	38.4	14.2	
V11	Before	70.8	25.8	584.67
	After	42.7	14.1	
V12	Before	70.4	27.0	841.69
	After	35.0	13.1	
V13	Before	69.4	26.2	—
	After	5.8	1.7	
V14	Before	65.9	24.2	—
	After	5.0	1.4	
V15	Before	77.3	29.2	—
	After	6.6	8.9	
V16	Before	67.7	25.6	—
	After	6.7	2.3	
V17	Before	77.6	29.3	—
	After	10.2	3.4	
V18	Before	72.1	26.8	—
	After	9.1	3.1	

Appendix 2: Value of Modulus of Elasticity and Rigidity obtained by non-destructive method

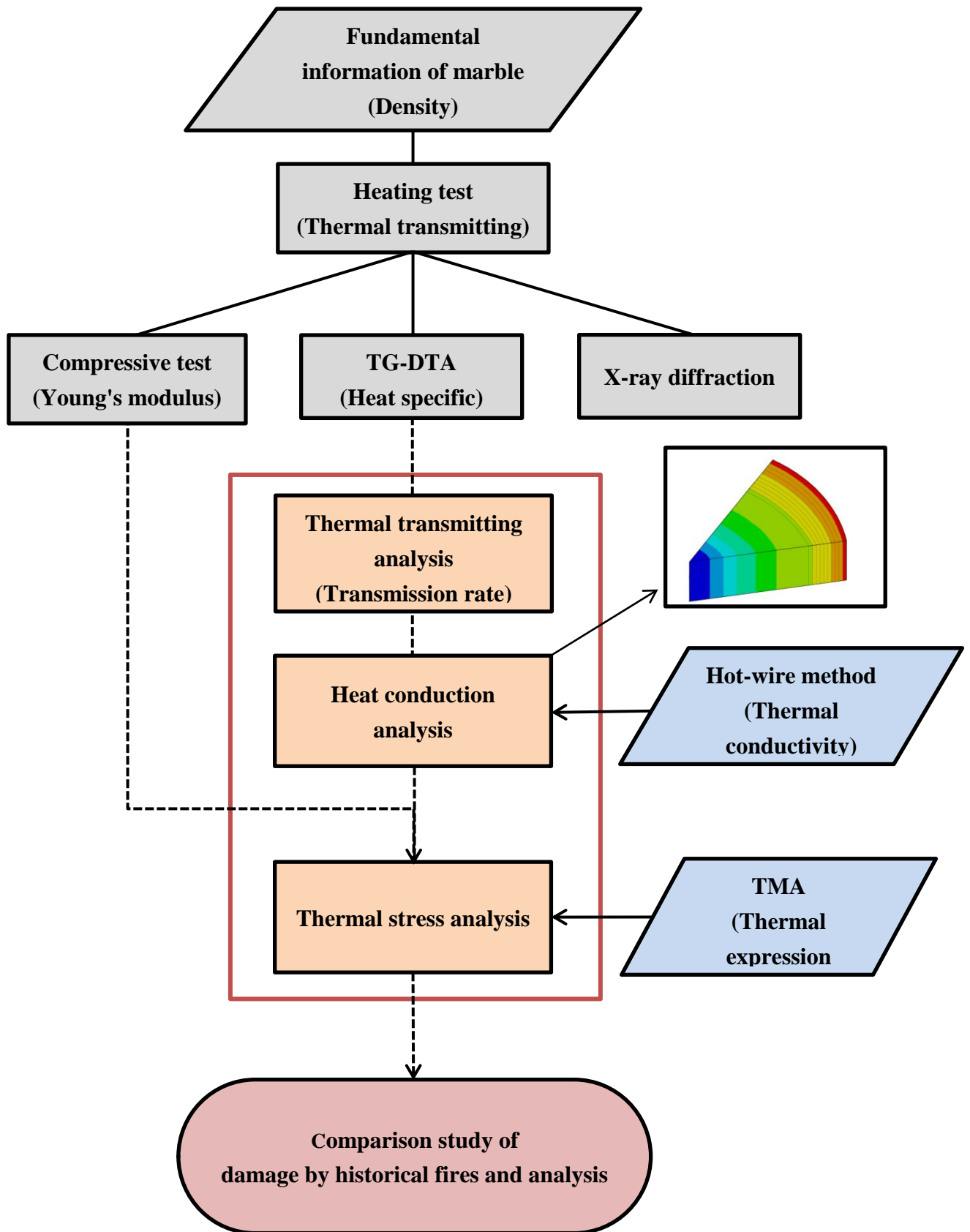
Specimen No.		Modulus of Elasticity (GPa)	Modulus of Rigidity (GPa)	Max Stress (kN)
V19	Before	69.9	26.2	659.23
	After	24.7	8.2	
V20	Before	65.9	25.2	552.30
	After	15.1	5.9	
V21	Before	78.5	29.4	680.80
	After	20.4	7.4	
V22	Before	76.5	29.0	—
	After	22.7	8.8	
V23	Before	72.7	27.5	637.60
	After	25.4	9.6	
V24	Before	70.6	26.6	723.97
	After	21.5	7.3	
V25	Before	72.1	25.4	380.62
	After	13.6	11.2	
V26	Before	72.7	26.8	369.83
	After	12.4	3.8	
V27	Before	74.3	28.5	519.93
	After	11.5	4.0	
V28	Before	67.3	25.3	380.62
	After	10.8	3.3	
V29	Before	68.8	26.2	560.00
	After	—	—	

Appendix 2: Value of Modulus of Elasticity and Rigidity obtained by non-destructive method

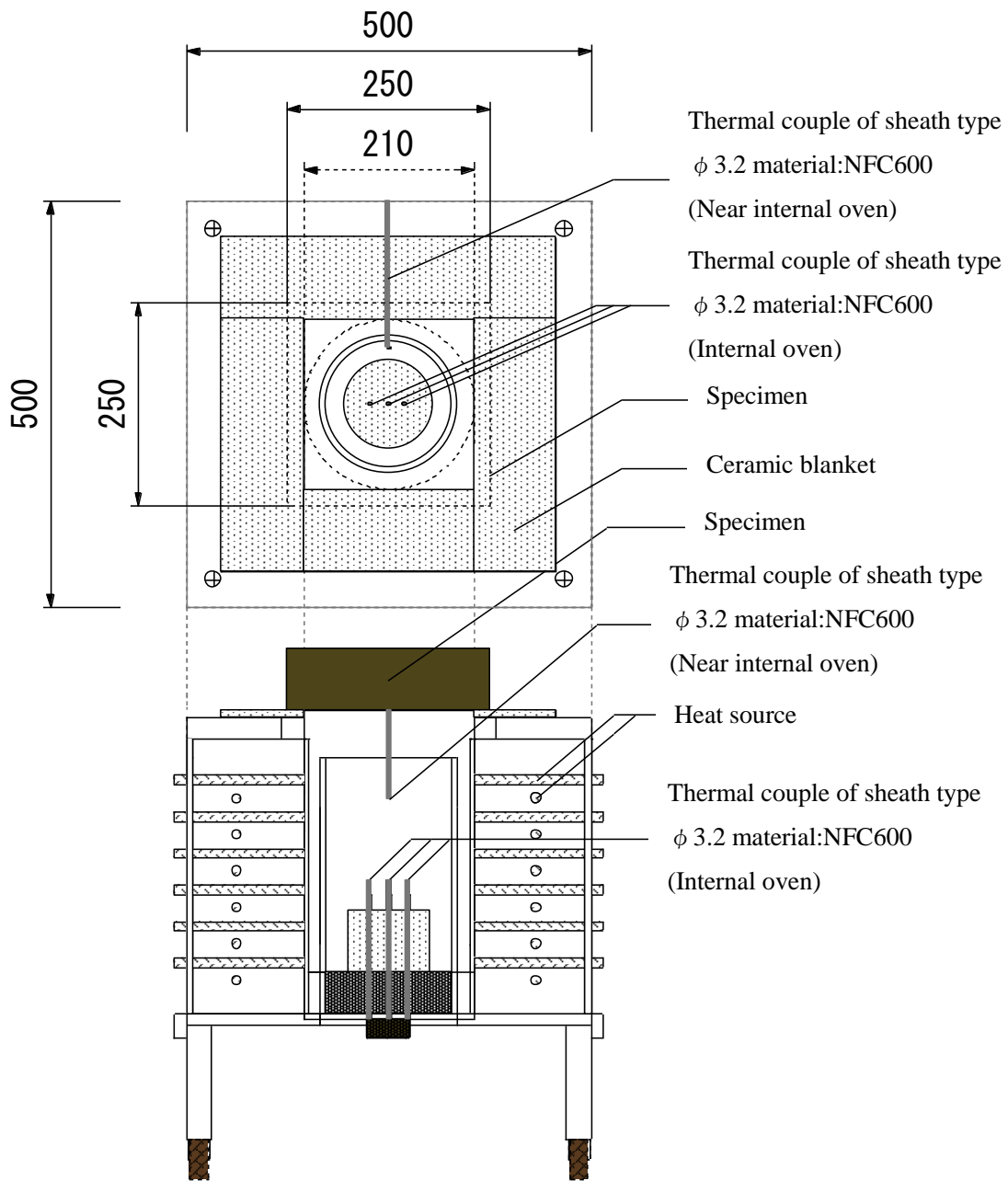
Specimen No.		Modulus of Elasticity (GPa)	Modulus of Rigidity (GPa)	Max stress (kN)
H1		65.1	27.9	680.80
H2		66.1	28.7	776.95
H3		67.6	28.5	776.95
H4		65.5	27.9	648.44
H5		68.1	28.8	691.6
H6		67.5	28.5	—
H7	Before	66.3	28.2	734.77
	After	22.1	12.1	
H8	Before	68.5	29.2	—
	After	25.2	14.4	
H9	Before	69.1	29.2	723.98
	After	23.2	13.1	
H10	Before	58.9	26.6	809.33
	After	22.7	13.5	
H11	Before	66.8	28.3	595.47
	After	26.8	14.3	
H12	Before	66.2	28.3	723.91
	After	24.7	14.1	
H13	Before	64.8	28.4	—
	After	11.7	1.9	
H14	Before	69.7	29.7	—
	After	3.2	2.3	
H15	Before	65.4	27.7	—
	After	2.7	2.0	
H16	Before	69.9	29.6	—
	After	2.8	2.0	
H17	Before	53.9	28.3	—
	After	10.8	1.8	
H18	Before	65.0	28.5	—
	After	2.2	1.8	

Appendix 2: Value of Modulus of Elasticity and Rigidity obtained by non-destructive method

Specimen No.		Modulus of Elasticity (GPa)	Modulus of Rigidity (GPa)	Max stress (kN)
H19	Before	45.8	27.4	776.90
	After	—	—	
H20	Before	65.5	28.2	776.95
	After	11.1	7.5	
H21	Before	71.3	30.1	—
	After	12.9	8.1	
H22	Before	64.6	27.6	787.43
	After	10.1	6.7	
H23	Before	63.3	26.9	680.80
	After	10.2	6.8	
H24	Before	67.2	29.2	573.88
	After	12.1	8.2	
H25	Before	62.1	27.8	680.80
	After	4.5	3.5	
H26	Before	—	25.9	—
	After	—	—	
H27	Before	64.5	28.7	680.80
	After	4.3	1.2	
H28	Before	63.9	28.0	734.77
	After	6.7	4.8	
H29	Before	66.3	29.4	606.25
	After	6.5	5.1	



Appendix 4: Actual dimension data of the structure and the shape of the electric oven



Appendix 5: Result of the split-cylinder tests

Table.1: dimensions of specimens and results

Temp. (°c)	Dimensions (mm)	Weight (g)	Density (g/cm ³)	Area (mm ²)	Max stress (kN)	Split strength (N/mm ²)
25	$\phi 49.50 \times 100.55^H$	516.7	2.67	1924.42	11	5.7
200	$\phi 49.35 \times 100.50^H$	515.2	2.68	1912.78	19	9.9
650	$\phi 49.40 \times 100.65^H$	519.2	2.69	1916.65	12	6.3

Ave; 7.3

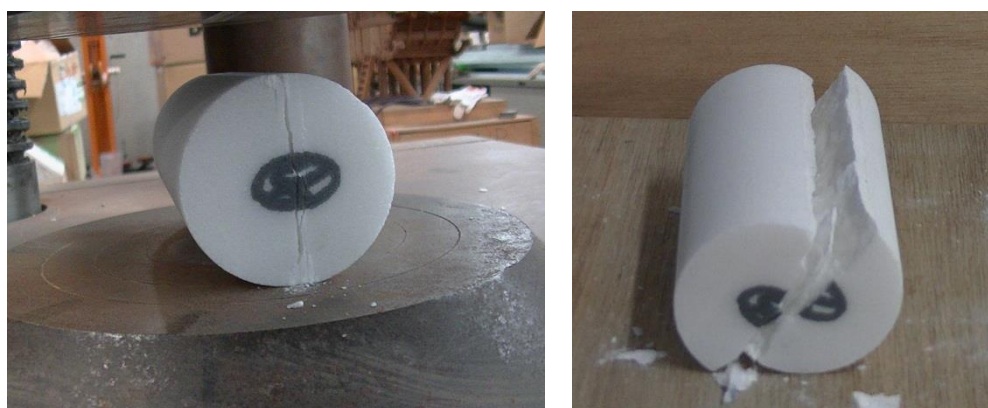
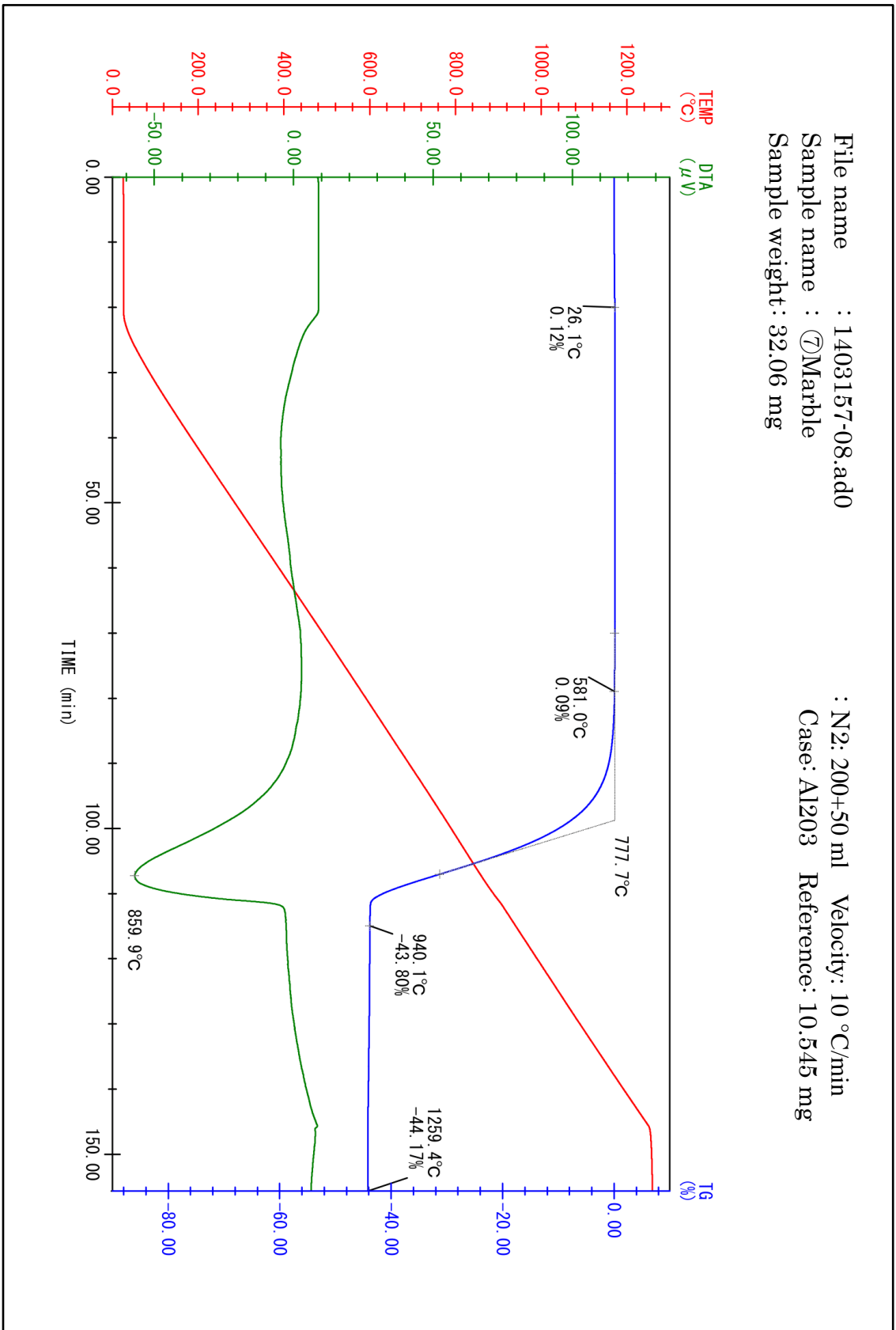
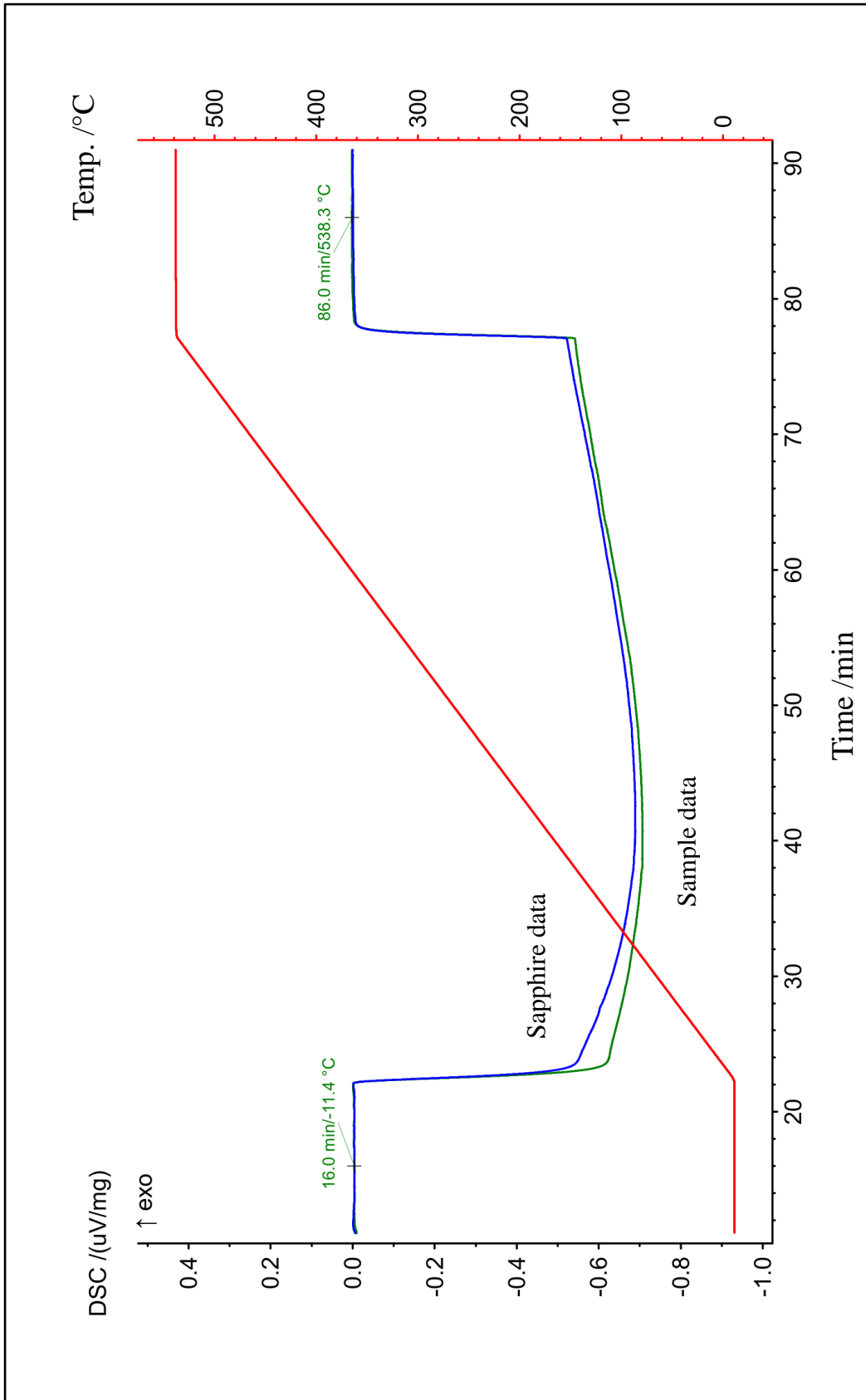


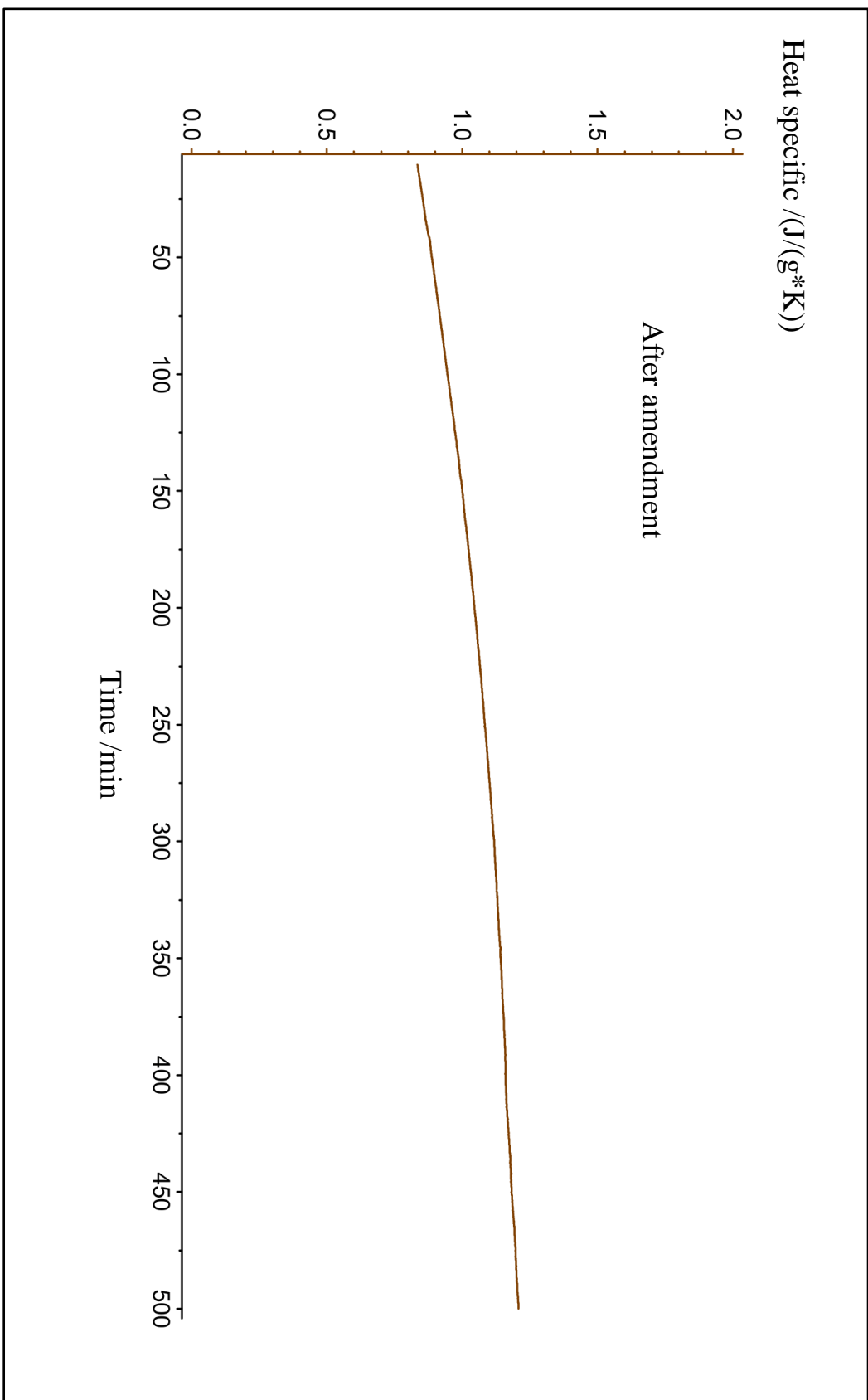
Fig.1: Marble specimen after compression

Appendix 6: Heat specific of marble stone



Appendix 6: Heat specific of marble stone





Appendix 6: Heat specific of marble stone

